

# Adversarially Robust Detection of Harmful Online Content: A Computational Design Science Approach

1<sup>st</sup> Yidong Chai  
Hefei University of  
Technology  
chaiyd@hfut.edu.cn

2<sup>nd</sup> Yi Liu  
Hefei University of  
Technology  
yiliu@mail.hfut.edu.cn

3<sup>rd</sup> Mohammadreza  
Ebrahimi  
University of South  
Florida  
ebrahimim@usf.edu

4<sup>th</sup> Weifeng Li  
University of  
Georgia  
weifeng.li@uga.edu

5<sup>th</sup> Balaji  
Padmanabhan  
University of  
Maryland  
bpadmana@umd.edu

## Abstract

Social media platforms are plagued by harmful content such as hate speech, misinformation, and extremist rhetoric. Machine learning (ML) models are widely adopted to detect such content; however, they remain highly vulnerable to adversarial attacks, wherein malicious users subtly modify text to evade detection. Enhancing adversarial robustness is therefore essential, requiring detectors that can defend against diverse attacks (generalizability) while maintaining high overall accuracy. However, simultaneously achieving both optimal generalizability and accuracy is challenging. Following the computational design science paradigm, this study takes a sequential approach that first proposes a novel framework (Large Language Model-based Sample Generation and Aggregation, LLM-SGA) by identifying the key invariances of textual adversarial attacks and leveraging them to ensure that a detector instantiated within the framework has strong generalizability. Second, we instantiate our detector (Adversarially Robust Harmful Online Content Detector, ARHOCD) with three novel design components to improve detection accuracy: (1) an ensemble of multiple base detectors that exploits their complementary strengths; (2) a novel weight assignment method that dynamically adjusts weights based on each sample's predictability and each base detector's capability, with weights initialized using domain knowledge and updated via Bayesian inference; and (3) a novel adversarial training strategy that iteratively optimizes both the base detectors and the weight assignor. We addressed several limitations of existing adversarial robustness enhancement research and empirically evaluated ARHOCD across three datasets spanning hate speech, rumor, and extremist content. Results show that ARHOCD offers strong generalizability and improves detection accuracy under adversarial conditions. Our study contributes to IS research at the intersection of social media management, AI security, and computational design science, and offers practical implications for users, platforms, and regulators.

**Keywords:** Harmful Online Content Detection, Adversarial Robustness, Ensemble Learning, Bayesian Learning, AI Security, Computational Design Science

## 1. Introduction

Social media platforms enable people to share experiences and ideas, playing a key role in information dissemination and public discourse. However, they are also inundated with harmful content, including hate speech, misinformation, and extremist rhetoric. Such content disrupts users' lives, fuels social polarization, and threatens societal stability. Reports note that "social media allows extremist ideologies, conspiracies, dis- and misinformation to be shared at an unprecedented scale and speed", becoming "the world's most potent incubator of extremism"<sup>1</sup>. Detecting such harmful content is therefore essential. Given the massive volume of online content and the strengths of Machine Learning (ML) models in text analysis, ML models have been widely adopted for automated harmful content detection (Etudo and Yoon 2024, Wei et al. 2022).

Harmful content is often crafted by users with goals such as spreading misinformation, promoting extremism, or inciting hatred. To achieve their goals, these users are motivated to evade detection. This challenge is exacerbated by the vulnerabilities of ML models. Although ML models can achieve high accuracy, they are vulnerable to adversarial manipulation. In harmful content detection, once a harmful text is flagged, a user can slightly modify its wording without altering its meaning, to create a new version that deceives the detector into misclassifying it as non-harmful. The modified text is an *adversarial sample*, and the initial text is a *clean sample*. The process where a detector initially detects harmful content but fails after subtle wording modifications is known as an *adversarial attack*. Adversarial attacks have been shown to fool various detectors. For instance, Oak and Berkeley (2019) showed that the statement "go back to where you came from these fu\*\*ing immigrants are destroying America" is correctly detected as hate, but when "fu\*\*ing immigrants" is changed to "fuking immgrants," the classifier misclassifies it as non-hate, even though the edits are superficial and the meaning remains unchanged. Hence, there is a pressing need to enhance detectors' ability to withstand such attacks. Such ability is *adversarial robustness*. Enhancing adversarial robustness involves two key requirements. First, since many attack methods already exist and

---

<sup>1</sup> <https://www.theguardian.com/australia-news/2024/oct/11/australias-spy-chief-warns-ai-will-accelerate-online-radicalisation>

new ones continue to emerge, a detector must handle a broad range of attacks, including new ones, to ensure strong worst-case performance, which we refer to as *high generalizability*. Second, because real-world attacks can vary widely, detectors must also maintain strong average performance, which is *high accuracy*. Robust detectors must therefore perform well in both worst-case scenarios and typical real-world settings.

Adversarial attacks affect not only text-based ML models but also models in other fields, such as computer vision. Many methods have been proposed to enhance adversarial robustness across these fields. However, these enhancement methods still have major drawbacks that limit both the generalizability and accuracy of the detectors they enhance. A key challenge arises from the multi-tiered hierarchy of text, where characters form words and words form sentences. This hierarchical structure leads to diverse textual adversarial attacks, occurring at the character, word, or sentence level. However, existing methods typically focus on defending against attacks at only a specific level, failing to account for attacks at other levels. Consequently, detectors enhanced by these methods may perform well against certain attacks (e.g., achieving 90% accuracy) but poorly against others (e.g., only 10% accuracy). Moreover, adversarial attacks evolve continuously, creating an ongoing arms race between attackers and defenders. The hierarchical nature of text compounds this problem: not only can attacks take various known forms, but new ones can also emerge at any level. As a result, detectors robust to known attacks may still be misled by new ones. This means that detectors robustified by existing methods exhibit *limited generalizability* across both known and new attacks. In addition, the existing robustness enhancement methods also struggle to deliver high accuracy for the detectors they enhance (i.e., *limited accuracy*, will be discussed in later content).

Achieving both optimal generalizability and accuracy is challenging because (1) each detector is a discrete ML model, leading to a discrete search space that is difficult to optimize, (2) potential attacks are vast and potentially unbounded, particularly due to the hierarchical nature of text, and (3) the two objectives may conflict (e.g., overfitting to common attacks may improve accuracy but reduce generalizability). To address the first challenge, we adopt the computational design science paradigm. Rather than directly optimizing the discrete search space, we focus on designing a novel detector that overcomes the limitations of existing methods. Since the ideal detector would achieve optimal performance, the observed

improvements indicate that our design moves closer to the ideal detector and better addresses the underlying optimization problem. To tackle the second and third challenges, we employ a sequential approach where we first propose a novel framework that ensures high generalizability for detectors instantiated within it, and then instantiate a detector with multiple novel design components to further improve overall accuracy.

Specifically, we first propose a Large Language Model-based Sample Generation and Aggregation (LLM-SGA) framework. The core idea is that, while textual adversarial attacks vary in form and occur at multiple levels, they share two key invariances: an adversarial sample and its initial clean sample convey the same meaning (*Invariance 1*), and the detector under attack has correctly detected the initial clean sample and generally performs well on diverse samples (*Invariance 2*). These invariances arise not only from the definition of adversarial attacks but also from the attacker’s practical constraints. For Invariance 1, altering the meaning renders the attack ineffective, as the functional intent of the attack will be lost. For example, modifying “go back to where you came from these fu\*\*ing immigrants are destroying America” to “It’s okay” would evade detection, but it no longer conveys the initial intent, so attackers would avoid such modifications. For Invariance 2, ML-based detectors typically perform quite well across diverse inputs. Moreover, if a clean sample is already misclassified as non-harmful, attackers have no incentive to modify it further, since the clean sample already achieves their goal. Based on the two invariances, our LLM-SGA proceeds in three steps. In Step 1, given an input sample, we prompt an LLM to generate multiple samples that preserve its meaning. In Step 2, the detector predicts both the input and the generated samples, yielding a predictive probability of harmfulness for each. In Step 3, these probabilities are aggregated, specifically averaged, to determine whether the input is harmful. Our LLM-SGA is generalizable for the following reason. If the input is adversarial, the generated samples will preserve its meaning, and thus also that of the clean sample (Invariance 1). Since the detector has correctly classified the clean sample and performs well on diverse samples (Invariance 2), it is expected to correctly classify the generated samples. While a detector can be misled by a single sample (e.g., adversarial one), incorporating multiple samples dilutes the effect of any adversarial one, thereby increasing the probability of correct detection. We also theoretically prove that this probability is lower-bounded, and the bound rises with the number of generated samples.

LLM-SGA is a generalizable framework that allows any instantiated detector to defend against various known and newly emerging adversarial attacks. However, the detection accuracy still depends on the specific detector instantiated within the framework. Designing such an accurate detector presents three key challenges, which motivate the three novel design components we introduce next to address them.

First, prior studies show that relying solely on one detector leaves detection systems vulnerable, as its weaknesses can be easily exploited to craft targeted attacks. To address this *single-detector challenge*, we adopt an ensemble approach, combining multiple detectors, each serving as a *base detector*, to leverage their complementary strengths. For each sample (initial input or generated ones), we obtain the predictive probability from each base detector. These probabilities form a two-dimensional matrix, which is then aggregated to produce the final result. We refer to this design component as the *two-dimensional ensemble* (Design Component 1). The novelty is that, unlike prior studies that aggregate along only one dimension, either samples or base models, we aggregate both, creating a novel two-dimensional ensemble structure.

Second, even among the samples that convey the same meaning, a detector’s predictive probabilities may vary, making the probability of each sample being correctly detected differ. A prediction more likely to be correct is viewed as a *more accurate prediction*, and should receive a higher weight during aggregation. Since our first design component introduces multiple base detectors, the resulting two-dimensional probability matrix introduces additional complexity. Predictions vary not only across samples but also across base detectors. Assigning appropriate weights to each prediction, which we refer to as the *weighting challenge*, is therefore essential. To address this challenge, we propose a *Bayesian two-dimensional weight assignment method* (Design Component 2) to determine the weight of each prediction in the matrix. Since a prediction’s accuracy depends on both samples and models (i.e., base detectors), we decompose it into a *sample’s predictability* and a *model’s capability*. We theoretically show that a sample’s predictability is negatively correlated with the variance of its predictions across models, while a model’s capability is negatively correlated with the variance of its predictions across samples. Based on these insights (as domain knowledge), we design novel variance-based priors for the weights to be assigned to each prediction, and then propose an attention-based neural network to infer the posterior weights. Since the posterior determines

the final weights, we refer to this neural network as the *weight assignor*. The novelty lies in our Bayesian two-dimensional weighting mechanism, which integrates theoretically grounded variance-based priors with an attention-based network to derive posterior weights for each element in the two-dimensional matrix.

Third, unlike a single model whose parameters can be directly optimized by adversarial training (AT), our setting involves base detectors and a weight assignor that jointly determine detection outcomes, making it necessary to learn robust parameters for both. The data used to train the weight assignor should accurately capture the robustness of the base detectors. Using the same dataset for both base detectors and the weight assignor risks overfitting, causing the weight assignor to misallocate weights. Thus, the base detectors and the weight assignor need to be adversarially trained jointly but on separate datasets, known as the *learning challenge*. To address this, we propose an *iterative adversarial training strategy* (Design Component 3). We emulate attackers to generate adversarial samples, and then alternately train the base detectors with the weight assignor fixed, and train the weight assignor with the base detectors fixed. This alternating procedure enables the base detectors and the weight assignor to adapt to adversarial conditions while maintaining the required independence between their training data. The key novelty is an AT tailored for ensemble learning: unlike prior work that uses AT only to enhance base models, our strategy captures the interaction between the base models and the weight assignor, adversarially training both to enhance the ensemble’s robustness.

We instantiate the three design components in the LLM-SGA framework, yielding our instantiated Adversarially Robust Harmful Online Content Detector (ARHOCD). We evaluated ARHOCD on three datasets covering hate speech, rumor, and extremist content. Two sets of experiments were conducted: the first evaluated generalizability, and the second evaluated accuracy against both known and new attacks. We further validated ARHOCD’s advantages in broader settings, including cases where the base detectors are fixed and in an image classification task. We also conducted a case study to examine its advantages.

Our study contributes to interdisciplinary research on social media management, AI security, and computational design science. Detecting harmful content is crucial for a healthy social media environment and is a key topic in the IS field. This study highlights the security threats posed by adversarial attacks and focuses on strengthening the robustness of harmful content detection systems. To this end, we develop a

general framework (LLM-SGA), a novel IT artifact that defends against diverse textual adversarial attacks by leveraging their underlying invariances. We instantiate this framework through three novel design components to develop ARHOCD, a situated implementation of an adversarially robust detector for harmful content detection. Beyond advancing harmful content detection, our study also informs broader AI security challenges, such as privacy protection, and provides a principled approach for enhancing adversarial robustness in other IS applications, including detecting hacker assets and identifying phishing attacks.

## 2. Research Background

### 2.1 Harmful Online Content Detection and Adversarial Attacks

The growing threat of harmful online content makes its detection imperative. As ML can learn the patterns pertaining to harmful content, it is commonly used for detection, with major studies shown in Appendix A. A major security threat to these detectors is adversarial attacks. According to Kurakin et al. (2017), an adversarial attack is defined as follows: given a clean sample  $x^C$  with ground truth  $y^C$  and a model  $F$ , the goal is to craft an adversarial sample  $x^A$  that is perceptually indistinguishable from  $x^C$  but causes  $F$  to mispredict, despite  $F$  correctly predicts the initial input  $x^C$ . Formally,  $F(x^C) = y^C, F(x^A) \neq y^C$ , and  $x^C \sim x^A$ , where we use  $\sim$  to denote perceptual indistinguishability. For example, in computer vision where adversarial attacks were first observed, slight pixel perturbations to a panda image keep it perceptually unchanged, yet GoogLeNet shifts from correctly classifying it as a panda (57.7% predictive probability) to incorrectly classifying it as a gibbon (99.3% predictive probability) (Goodfellow et al. 2015).

Later studies showed that adversarial attacks also threaten models handling text, known as *textual adversarial attacks* (Papernot et al. 2016, Qiu et al. 2022). Text's multi-tiered hierarchy, where characters form words and words form sentences, complicates adversarial attacks and distinguishes them by enabling attacks at the character, word, or sentence level. Character-level attacks perturb text by inserting, flipping, swapping, or removing characters. For instance, in Table 1, attackers replace the characters s, a, and h in the word "trash" with s (Cyrillic letter Dze), a (Latin letter Alpha), and h (Cherokee letter Ni). While these changes preserve the initial meaning and appear perceptually identical to humans, they cause the detector

to misclassify the hate speech as non-hate. Word-level attacks modify text by inserting, replacing, or removing words. In Table 1, replacing the word “bitches” with “knuckleheads” causes the model to incorrectly predict the new text as non-hate. Sentence-level attacks directly rewrite the sentence. In Table 1, rephrasing the text “I want to kill you” with “I would love to send you to heaven today” misleads the detector into predicting the text as non-hate. Attacks also occur at multiple levels (i.e., more than one of the above three levels). Prior studies have examined the impact of each type of attack, as shown in Table 2.

Table 2 shows that all four attack types considerably reduce model performance, commonly evaluated by Attack Success Rate (ASR) or after-attack classification metrics. ASR is defined as the proportion of adversarially crafted samples that are misclassified by the target model (Wang et al. 2022). For instance, in Ocampo et al. (2023), 90.7% of the crafted samples can successfully mislead the detector (HateBERT), and hence the ASR is 90.7%. After-attack classification metrics are computed on a combined dataset comprising both adversarially crafted samples (from initially correctly classified samples) and initial clean samples that were misclassified. Based on this dataset, classification metrics such as accuracy, precision, recall, and F1-score are calculated to evaluate the model’s performance under adversarial conditions (Huang et al. 2022). For instance, Aggarwal and Vishwakarma (2024) used a character-level attack to generate adversarial samples and combined them with initially misclassified ones to create a new dataset. On this combined dataset, the ALBERT-based hate speech classifier achieved an after-attack accuracy of only 13.1%.

**Table 1. Examples of Character-, Word-, and Sentence-Level Adversarial Attacks**

Types	Clean Sample	Adversarial Sample
Character-level	The South is full of white trash. The Midwest is full of white trash. The West Coast is full of white trash.	The South is full of white trash. The Midwest is full of white trash. The West Coast is full of white trash <b>h</b> .
	Predicted label: hate	Predicted label: non-hate
Word-level	Derrick said if I cover my face and leave just my eyes visible I'll have tons of <b>bitches</b> .	Derrick said if I cover my face and leave just my eyes visible I'll have tons of <b>knuckleheads</b> .
	Predicted label: hate	Predicted label: non-hate
Sentence-level	<b>I want to kill you</b>	<b>I would love to send you to heaven today</b>
	Predicted label: hate	Predicted label: non-hate

Note: character- and word-level examples are from (Aggarwal and Vishwakarma 2024); sentence-level example is from (Azumah et al. 2024).

**Table 2. Recent Research on Adversarial Attacks in Harmful Online Content Detection**

Types	Year	Authors	Harmful Content	Detection Models	Attack Methods	Impact of Attacks
Character-level	2024	Aggarwal and Vishwakarma	Hate Speech	DistilBERT, LSTM, etc.	Visually confusable glyphs, Zero-width characters	Accuracy: 91.8% → 13.1% on ALBERT

	2022	Li and Chai	Spam	CNN, GRU, LR, NB, etc.	DeepWordBug	F1-score: 82% → 44% on GRU
	2019	Oak and Berkeley	Hate Speech	RF, GB	Word splitting, Word merging, Drop-a-Letter	F1-score: 75% → 56% on RF
Word-level	2024	Zhou et al.	Machine-Generated	RoBERTa	Synonym replacement	AUC: 99.63% → 51.06% on RoBERTa
	2023	Herel et al.	Hate Speech	RoBERTa	TextFooler, TFAdjusted	ASR: 68.3% on RoBERTa
	2023	K. C. Chen et al.	Misinformation	LSTM, XLNet, RoBERTa, etc.	Synonym replacement, Swap noun and adjective	Accuracy: 77.8% → 22.7% on XLNet
	2024	Przybyła	Misinformation	LSTM, BERT, Gemma	Rephrasing generated by LLM with prompts	ASR: 15.7% on BERT
Sentence-level	2023	Ocampo et al.	Hate Speech	HateBERT	Few-shot prompting using LLMs	ASR: 90.7% on HateBERT
	2025	Kumbam et al.	Hate Speech	BERT, LSTM, CNN	Explainability-driven synonym replacement and character-level edit	Accuracy after attack/accuracy before attack: 0.7 on LSTM
Multi-level	2023	Chang et al.	Hate Speech, Spam	LSTM, CNN, RCNN	Synonym replacement, Dictionary paraphrasing	Accuracy: 99.1% → 32.7% on LSTM

Given the severe ramifications of adversarial attacks, enhancing robustness is essential. As noted earlier, such enhancement has two requirements: first, detectors should handle a wide range of known and new attacks to ensure strong worst-case performance (high generalizability); second, since real-world attacks vary widely, detectors must also maintain strong average performance (high accuracy). Next, we review the robustness enhancement methods to examine whether they satisfy these two requirements.

## 2.2 Adversarial Robustness Enhancement Methods

Various methods have been proposed to enhance adversarial robustness in fields such as natural language processing (NLP) and computer vision. Since some methods developed in other fields may also be used to enhance harmful content detectors, this section reviews methods from both NLP and other fields.

Existing enhancement methods fall into two categories: passive and active (Qiu et al. 2022). Passive methods detect and correct adversarial inputs without modifying ML models. Due to structural differences in data types, these methods are often field-specific. Thus, we focus on the text-based methods, commonly including spelling correction (Pruthi et al. 2019) and abnormal text detection (Mozes et al. 2021). Passive methods work well on character-level attacks. For example, in the aforementioned example that changes “fu\*\*ing immigrants” to “fuking immgrants,” spelling correction can effectively work. They can also defend against some word-level attacks, such as those replacing words with rare synonyms. However, they are less effective against more complex attacks, including word-level attacks that use common synonyms

or sentence-level attacks. Meanwhile, since they rely on certain patterns, attackers can bypass them by simply avoiding those patterns. Therefore, passive methods are limited in both generalizability and accuracy.

Active methods improve ML models and are generally more effective than the passive ones, making them the focus of most studies (Qiu et al. 2022). Improvement can be approached from three aspects. First, model structure design, which defines the hypothesis space (the set of functions the model can represent, (Anguita et al. 2011)), should favor robust over vulnerable model instances. Second, the parameter learning aspect focuses on how to select, within the hypothesis space, the model instance with the highest adversarial robustness. Third, the model coordination aspect focuses on how to combine the learned model instances, typically by ensemble learning, to enhance robustness. Based on these aspects, existing methods can be grouped into structure-based, learning-based, and ensemble model-based ones, as summarized in Table 3.

**Table 3. Recent Research on Active Methods for Enhancing Adversarial Robustness**

Types	Year	Authors	Methods	Enhanced Models	Data
Structure-based	2022	Nguyen and Tuan	Insert an InfoGAN structure to project adversarial samples onto the embedding space learned from clean samples.	BERT, RoBERTa, etc.	Text
	2022	Zhang et al.	Insert a layer between BERT's output and the classifier to preserve robust features while filtering non-robust ones.	BERT	Text
	2021	S. Zhang et al.	Design a residual-block network to learn precise mappings from adversarial images into clean images.	ResNet, Inception	Image
Regularization-based	2024	Liu et al.	Apply gradient norm regularization to reduce prediction variation from adversarial attacks.	HyperIQA, DBCNN, etc.	Image
	2022	Dong et al.	Use a KL divergence to align the model's outputs for clean and adversarial samples.	CNN, LSTM	Text
	2022	Yang et al.	Use triplet loss to bring words closer to their synonyms and push them away from non-synonyms in embedding space	CNN, LSTM	Text
	2024	X. Zhang et al.	Model word deletion/ insertion/ substitution/ reordering as probability distributions and sample from distributions.	LSTM, BERT	Text
Learning-based	2023	L. Li et al.	Randomly mask words in the input text and fill in the masked words using BERT as a denoising step.	RoBERTa, BERT	Text
	2022	Huang et al.	Randomly perturb input based on word frequency for perturbations disruption and distribution alignment.	LSTM, BERT	Text
	2020	Ye et al.	Create a synonym set for each word and replace the word by sampling from its synonym set.	CNN, BERT	Text
	2025	Yang et al.	Fast adversarial training in embedding space by single-step gradient ascent and historical perturbation initialization.	RoBERTa, BERT	Text
Adversarial training-based	2024	Hu et al.	Compute the median of historical model weights during adversarial training to obtain model weights.	WRN	Image
	2022	Chen and Ji	Guide the model to treat each word and its substitution in clean and adversarial sample pairs as equally important.	CNN, LSTM, BERT, etc.	Text
	2021	Zhao et al.	Combine clean-adversarial representations to create mixup samples, and align their predictive distributions.	CNN, LSTM, BERT	Text
	2024	Waghela et al.	Dynamic ensemble with a meta-model to weight base models for ensemble predictions.	BERT, ALBERT, etc.	Text
Ensemble model-based	2023	Qin et al.	Dynamic ensemble selection: choose the base mode	WRN	Image

		prediction with the lowest uncertainty.		
2022	Li and Chai	Train base models on varied samples, enhance robustness via adversarial training, and ensemble predictions.	LSTM, GRU, LR, etc.	Text
2020	Sen et al.	Combine a full-precision (32-bit) model with a low-precision (4- or 2-bit) one.	CNN, AlexNet, etc.	Image

### 2.2.1 Structure-Based Adversarial Robustness Enhancement Methods

Structure-based methods refine the hypothesis space by modifying the model's structure, such as adding an embedding projection module (Nguyen and Tuan 2022) or a robust feature extraction module (Zhang et al. 2022). For instance, Nguyen and Tuan (2022) add an InfoGAN-based module to project adversarial samples onto the embedding space of the initial clean samples. However, these methods often require careful structural changes, limiting their compatibility since existing ML models must be redesigned. Meanwhile, complex ML models have broad hypothesis spaces (Leshno et al. 1993). Even if the initial model instance is not robust, the space may still contain many robust alternatives. Conversely, even if the space is refined to include a higher proportion of robust instances, the selected one may still have low robustness. The critical factor, therefore, lies in the selection process, i.e., how the parameters are learned.

### 2.2.2 Learning-Based Adversarial Robustness Enhancement Methods

These methods improve the training process to increase the chance of selecting a robust model from the hypothesis space, including regularization-, random noise-, and adversarial training-based methods.

#### 1) Regularization-Based Methods

Regularization-based methods add regularization terms to the training objective to bias learning toward robust models. Since text is discrete, regularizations in other fields, such as gradient regularization (Liu et al. 2024) and Lipschitz regularization (Fazlyab et al. 2023) for images, are less effective for textual data. Common text-based regularizations include word embedding regularization, which encourages synonyms to have similar embeddings (Yang et al. 2022), and output-level regularization, which aligns the predictive distribution of adversarial samples with those of their initial clean samples (Dong et al. 2021). However, regularizations are typically attack-specific and lack generalizability. For example, the word embedding regularization targets word-level attacks like synonym substitutions but fails against character- or sentence-level attacks, while the output-level regularization relies on specific adversarial samples,

limiting its effectiveness on new attacks. Besides, choosing the right regularization strength is challenging: too much may harm accuracy on clean samples, while too little provides limited benefits (Waseda et al. 2025). Thus, regularization-based methods may struggle to achieve high generalizability and accuracy.

## 2) Random Noise-Based Methods

Random noise-based methods introduce random perturbations (noise) to input samples during training. For images, this can involve adding Gaussian or Laplacian noise (Lecuyer et al. 2019). For text, words can be randomly replaced with synonyms (Ye et al. 2020, Zhou et al. 2021) or masked and then reconstructed using a language model (Li et al. 2023), generating multiple input variants. By enforcing consistent predictions between the variants and the original input, these methods encourage the model to learn representations robust to noise, including adversarial perturbations. A key limitation is that such noise is easy to apply at the character or word level but difficult at the sentence level, reducing generalizability.

These methods also struggle to meet the accuracy requirement. During testing, random noise generates multiple input variants, thus producing multiple predictions. The final prediction is obtained using statistical or aggregation methods. Statistical methods assume predictions follow a specific distribution (e.g., binomial distribution for binary classification (Zeng et al. 2023)), and compute the lower confidence bound of the predictions. If the bound exceeds a threshold (e.g., 0.5 for binary classification (Zeng et al. 2023)), the predictions are considered certified. Certified radius, i.e., the maximum allowable perturbation to the input, can also be calculated based on the predictions. This approach can obtain the final prediction with certified robustness, guaranteeing that the model remains robust under perturbations within a certain radius. However, its accuracy is limited due to two reasons. First, it assumes that all constituent parts of an input (e.g., words) are perturbed with equal probability. However, adversarial attacks tend to target the most sensitive parts (e.g., words with greater influence on the prediction (Jin et al. 2020)), reducing both the practical utility of the computed radius and the defense accuracy. Second, this approach assumes all predictions are identically distributed, neglecting that some may be more accurate and thus should carry more weight. Unlike statistical methods, aggregation methods focus on weighting predictions to aggregate them. For example, in Zhou et al. (2021), predictions are aggregated using a CBW-D algorithm, which

gives higher weights to predictions with larger margins (the gap between the highest and other probabilities), addressing the second limitation of statistical methods. But the accuracy of this approach is still limited. First, like the statistical approach, it also fails to consider the more sensitive parts when generating variants. Second, it considers prediction differences only during testing, not training, reducing its effectiveness.

### 3) Adversarial Training-Based Methods

Adversarial training (AT) was first proposed in the image field by Goodfellow et al. (2015). It emulates attackers by using existing attack methods to generate adversarial samples, and an ML model is then trained on these samples with the objective of producing correct predictions for adversarial inputs. AT is also popular in NLP. For instance, Zhao et al. (2021a) proposed mixup regularized adversarial training (MRAT), which first uses attack methods (e.g., DeepWordBug (Gao et al. 2018)) to generate adversarial samples and then optimizes the model using a mixup-based strategy on paired clean and adversarial samples. AT addresses the limitation of random noise-based methods by focusing on the most sensitive parts through prioritizing the most threatening variants, namely adversarial samples. Learning directly from these samples significantly enhances adversarial robustness. However, AT has a key limitation: it requires prior knowledge of attacks to generate adversarial samples. As a result, its robustness is mostly confined to attacks seen during training and remains vulnerable to new ones, thereby limiting its generalizability. Meanwhile, AT alone is insufficient and is often combined with ensemble learning to enhance robustness. However, the current combinations are still limited and can reduce accuracy (illustrated next).

#### 2.2.3 Ensemble Model-Based Adversarial Robustness Enhancement Methods

Ensemble model-based methods combine multiple learned ML models (called *base models*) and aggregate their predictions. In this case, adversarial samples must deceive a majority of the base models, which is substantially more difficult than fooling a single model. This increased difficulty raises the barrier for attackers, thereby enhancing the overall adversarial robustness (Li and Chai 2022). These methods have been widely applied in fields such as images and text. For image, Sen et al. (2020) combined a full-precision (32-bit) model with a low-precision (4- or 2-bit) model, leveraging the former's strength on clean samples and the latter's on adversarial ones. For text, Li and Chai (2022) combined multiple base models such as

CNN, LSTM, and GRU, aggregating their predictions to detect adversarial spam emails and fake reviews.

However, current methods fall short of the generalizability requirement, as advanced transferable attacks can deceive multiple base models simultaneously. For instance, Jin et al. (2020) demonstrated that adversarial samples carefully crafted for a CNN-based text classifier not only achieved a 100% ASR on the CNN but also transferred to LSTM- and BERT-based classifiers with ASRs of 84.9% and 90.2%. This reduces the robustness of ensemble models against such attacks. Meanwhile, they fail to meet the accuracy requirement. The ensemble’s robustness depends on its base models, which are often vulnerable, limiting overall robustness. Some studies combine ensemble learning with AT, applying it to each base model to improve their robustness (Li and Chai 2022, Waghela et al. 2024). However, the enhancement remains limited because these studies primarily apply AT to strengthen the base models, while neglecting the weight assignment component (i.e., the weight assignor). Since the weight assignor directly determines each model’s influence on the ensemble’s final prediction, neglecting its robustness may result in assigning higher weights to less robust base models, thereby reducing the ensemble’s overall adversarial robustness.

### 3. An Overview of Our Proposed Method

Enhancing adversarial robustness requires both generalizability and accuracy. Drawing on transfer learning (Arjovsky et al. 2019), where generalizability is measured by the worst-case performance across domains, we extend this idea to our study. Let  $\mathcal{A}$  denote the set of all textual adversarial attacks. We define the generalizability of a detector  $D$  as its worst-case performance:  $\text{Gen}(D) := \min_{a \in \mathcal{A}} P(D, a)$ , where  $P(D, a)$  denotes the performance of detector  $D$  under attack  $a$ . We define the accuracy as the expected performance:  $\text{Acc}(D) := \mathbb{E}_{a \in \mathcal{A}} P(D, a)$ . We aim to maximize both  $\text{Gen}(D)$  and  $\text{Acc}(D)$  in this study.

The key difference between our study and prior studies is that prior studies mainly maximize the expected performance over a subset of attacks, i.e.,  $\mathbb{E}_{a \in \mathcal{A}'} P(D, a)$ , where  $\mathcal{A}' \subset \mathcal{A}$  (e.g., character-level attacks in spelling error correction (Pruthi et al. 2019) or known attacks in AT (Goodfellow et al. 2015)). Prior studies typically overlook  $\text{Gen}(D)$ . As a result,  $\text{Gen}(D)$  decreases, meaning the detector may perform well on some attacks but fail on others. This flaw poses a critical risk because it allows attackers to craft

targeted attacks that exploit the detector’s specific weaknesses, an issue that is especially pronounced given the inherently adversarial nature of such attacks. Meanwhile,  $\text{Acc}(D)$  also declines, not only because the detector is less effective to defend against attacks outside  $\mathcal{A}'$ , but also because its ability to handle attacks within  $\mathcal{A}'$  is constrained by the limitations we discussed in the literature review. This is also critical because  $\text{Acc}(D)$  reflects the detector’s overall performance. Over time, a detector may face a diverse array of attacks initiated by distinct adversaries, and a lower  $\text{Acc}(D)$  elevates the risk of frequent failures across them.

However, directly maximizing  $\text{Gen}(D)$  and  $\text{Acc}(D)$  is intractable. A detector  $D$  is a discrete ML model rather than a continuous variable as in classical optimization, resulting in a discrete search space (i.e., the set of all possible model configurations) that is hard to optimize. To address this, we follow the computational design science paradigm, developing a new IT artifact that addresses current limitations and performs the focal task more effectively. Instead of computing  $\text{Gen}(D)$  and  $\text{Acc}(D)$  and then optimizing over  $D$ , we design a new  $D$  to address the limitations and empirically evaluate its improvements on real data. Since the ideal detector corresponds to optimal performance, observed improvements indicate the proposed  $D$  is closer to the ideal and solves the optimization problem more effectively than prior studies.

Even following the computational design science paradigm, two challenges remain. First, a vast number of adversarial attacks have been devised, and new ones continue to emerge. Moreover, attacks are discrete in nature and difficult to characterize mathematically. Consequently, the set  $\mathcal{A}$  is vast, potentially infinite, and intractable. Designing a detector to achieve both objectives across such a complex set is therefore highly challenging. Second, jointly achieving the two objectives is itself difficult. Traditional ML focuses on maximizing expected accuracy by optimizing a loss defined on a set of training samples, aiming to obtain a model that performs well on general cases. Consequently, the model may overfit to common attacks: improving  $\text{Acc}(D)$  by boosting performance on frequent attacks while degrading performance on rarer attacks, thereby reducing  $\text{Gen}(D)$ . Although techniques such as transfer learning and multi-task learning can leverage knowledge across domains or coordinate learning across tasks, they are not suitable for our setting. They assume that the objectives are computable so that coordination can be performed. For

example, in multi-task learning, a common approach involves computing losses for samples across different tasks, summing these losses, calculating the gradients of the sum with respect to model parameters, and updating the parameters accordingly (Zhang and Yang 2018). In our case, however,  $\text{Acc}(D)$  and  $\text{Gen}(D)$  are defined over an intractable attack set  $\mathcal{A}$ , rendering both their values and their gradients hard to compute. To address these two challenges, we adopt a sequential approach. We first propose a framework ensuring that any detector instantiated within it can defend against a broad range of attacks, thereby securing high generalizability. We then propose a specific instantiation within this framework that focuses on improving accuracy. In this way, our instantiated detector achieves high generalizability and high accuracy.

## 4. An LLM-based Sample Generation and Aggregation Framework (LLM-SGA)

### 4.1 Core Idea of Our LLM-SGA Framework

Textual adversarial attacks occur at the character, word, and sentence levels, with new attacks continually emerging. This challenges defenses, which must counter a variety of known and new attacks. Our core idea is to identify the key invariances of all attacks and base our framework on these invariances. Before introducing our framework, we define the concept of the identical meaning set.

**Definition (Identical Meaning Set):** It is defined as the collection of all texts that convey the same underlying meaning. Formally,  $\mathcal{S}(h) = \{x \mid x \text{ is a text AND } s(x) = h\}$ , where  $s(x)$  denotes the underlying meaning of text  $x$  and  $\mathcal{S}(h)$  denotes the set of all texts whose meaning is  $h$ . For example, the two texts “I want to kill you” and “I would love to send you to heaven today” in Table 1 convey the same underlying meaning (i.e.,  $h$  represents “a threat to kill”), and thus they belong to the same identical meaning set.

Let an initial clean sample be  $x^C$  with ground truth  $y^C$ . An adversarial sample ( $x^A$ ) preserves the meaning of  $x^C$  but causes the detector to make an incorrect prediction, whereas it predicts  $x^C$  correctly. Hence, an adversarial sample  $x^A$  is defined by two properties. First,  $x^A$  and  $x^C$  belong to the same identical meaning set (*Invariance 1*). This is essential because if the meaning is altered, even if it evades the detection, the functional intent of the attack is lost. For instance, if the text “I want to kill you” is changed to “I want to play basketball,” the new text may evade detection, but it no longer conveys the attacker’s malicious intent, rendering the attack ineffective. Hence, an attacker will avoid such modifications. The second

invariance is that attacks typically arise when the targeted detector performs well, particularly when it correctly predicts the initial clean sample  $x^C$  (*Invariance 2*). Only in such cases do attackers need to craft adversarial samples to evade detection; otherwise,  $x^C$  already fulfills its intended function.

From Invariance 2, the detector is expected to correctly predict samples that share the same meaning as the clean input. However, this is not always the case, as adversarial samples can still fool the detector. Our LLM-SGA enhances robustness by making predictions over multiple samples rather than a single one, thereby diluting the impact of any individual sample, including a potential adversarial one. This mechanism is effective against all adversarial samples, ensuring strong worst-case performance for high generalizability.

In practice, the input sample may be adversarial or clean, but it is unclear to the detector. When the input is adversarial ( $x^A$ ), it implies that its corresponding clean sample  $x^C$  has been detected. But the detector does not know  $x^C$ . However, since  $x^A$  and  $x^C$  share the same meaning, we can generate multiple samples (denoted as  $\hat{x}_1, \hat{x}_2, \dots, \hat{x}_N$ ) that preserve the meaning of  $x^A$ , and therefore also that of  $x^C$  (as per Invariance 1). When the input is clean ( $x^C$ ), we can also generate multiple samples preserving the same meaning as  $x^C$ . For simplicity, we denote the input as  $x_0$ , which can be  $x^A$  or  $x^C$ . We generate samples that preserve the meaning of  $x_0$ , and make a detection by aggregating the predictions for them. Since  $x_0$  can be adversarial or clean, and adversarial samples can include character-, word-, or sentence-level perturbations, generating such samples is nontrivial. To address this, we use LLMs for generation. Since many advanced LLMs are restricted from responding to potentially harmful content, we adopt the open-source LLaMA.

## 4.2 Description of Our LLM-SGA Framework

Our LLM-SGA framework includes three steps.

**Step 1:** Given an input  $x_0$ , we prompt the LLaMA to generate samples ( $\hat{x}_1, \hat{x}_2, \dots, \hat{x}_N$ ):

*“The following text may contain adversarial perturbations generated by techniques such as word misspelling, synonym substitution, and sentence rephrasing. Please generate N new texts by rephrasing the input text while preserving its original meaning.*

*INPUT {text}*

*OUTPUT:”*

**Step 2:** We fed  $x_0$  and the generated  $\hat{x}_1, \hat{x}_2, \dots, \hat{x}_N$  into the detector to obtain predictive probabilities  $p_0, \dots, p_N \in [0,1]$ . Each value represents the likelihood that the label is 1 (harmful) according to the detector.

**Step 3:** We aggregate the predictive probabilities by computing their average ( $\bar{p}$ ):

$$\bar{p} = \frac{1}{N+1} \sum_{n=0}^N p_n \quad (1)$$

We then compare  $\bar{p}$  with a threshold  $\varepsilon$  to get the predicted label  $\hat{y}$  to decide whether the input  $x_0$  is harmful:

$$\hat{y} = \begin{cases} 0 & (\text{i. e., non-harmful}), \text{if } \bar{p} \leq \varepsilon \\ 1 & (\text{i. e., harmful}), \text{if } \bar{p} > \varepsilon \end{cases} \quad (2)$$

### 4.3 Theoretical Properties of Our LLM-SGA Framework

Let  $p$  denote the predictive probability of sample  $x_0$ , and  $y$  its ground truth label. The expectation and variance of  $p$  are denoted as:  $\mu_0 = \mathbb{E}[p]$  and  $\sigma_0^2 = \text{VAR}[p]$ . Since  $\hat{x}_1, \hat{x}_2, \dots, \hat{x}_N$  and  $x_0$  belong to the same identical meaning set, each corresponding  $p_n$  has the same expectation  $\mu_0$  and variance  $\sigma_0^2$ . Thus, the  $\bar{p}$  has expectation  $\mu_0$  and variance  $\sigma_0^2/(N+1)$ . Let  $P(\hat{y} = y)$  denote the probability that the  $\hat{y}$  is correct.

We consider a basic random guessing case where the detector's output is uniformly distributed over  $[0,1]$ . If the value exceeds  $\varepsilon$ , the predicted label is 1; otherwise, it is 0. Assuming the detector performs better than random guessing (a reasonable assumption given its overall excellent performance), we define  $\delta = |\mu_0 - \varepsilon|$ . We then have the following inequality (see Appendix B for details):

$$P(\hat{y} = y) \geq 1 - \sigma_0^2 / [(N+1)\delta^2] \quad (3)$$

Hence, the probability of correct detection is lower bounded. Moreover, increasing the number of samples  $N$  raises this lower bound, indicating that generating and aggregating more samples is advantageous.

## 5. Instantiation: Adversarially Robust Harmful Online Content Detector (ARHOCD)

### 5.1 Overview of Our Instantiated Detector

The LLM-SGA ensures that a detector instantiated within it is generalizable. But the accuracy still depends on a specific instantiation. As mentioned earlier, accurate detection faces three key challenges, which we address with three corresponding novel design components. Briefly, first, to tackle the single-detector challenge where relying on a single detector is highly vulnerable, we propose a two-dimensional ensemble that integrates multiple base detectors (Design Component 1). Second, to address the weighting

challenge where more accurate predictions should receive higher weights, we propose a Bayesian two-dimensional weight assignment method that combines prior knowledge with actual data to obtain a neural network-based weight assignor that determines weight for each prediction in the matrix (Design Component 2). Third, to overcome the learning challenge where the parameters of both the base detectors and the weight assignor should be jointly made adversarially robust, we introduce an iterative adversarial training strategy that iteratively optimizes the base detectors and the weight assignor (Design Component 3). Together, these three design components constitute our instantiated detector (ARHOCD) as illustrated in Figure 1.

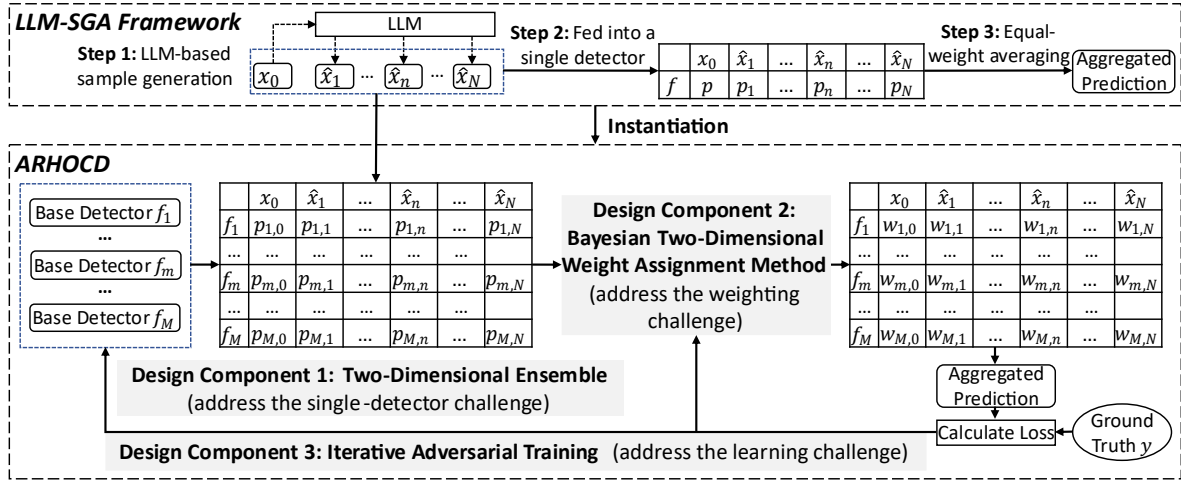


Figure 1. Overview of Our ARHOCD

## 5.2 Design Component 1: A Two-Dimensional Ensemble

We propose to ensemble  $M$  existing detectors. Each detector, such as a BERT-based model, is referred to as a base detector to distinguish it from the overall instantiated detector, ARHOCD, which is composed of multiple base detectors. We denote the  $m$ -th base detector as  $f_m$ , whose predictive probability for the input sample  $x_0$  is  $p_{m,0}$ , and for a generated sample  $\hat{x}_n$  is  $p_{m,n}$ . The predictive probabilities of  $f_m$  form a vector  $\mathbf{p}_m = [p_{m,0}, p_{m,1}, \dots, p_{m,n}, \dots, p_{m,N}]$ . The predictive probabilities of all base detectors form a two-dimensional matrix  $\mathbf{P} = [\mathbf{p}_1, \dots, \mathbf{p}_m, \dots, \mathbf{p}_M]^T$ . We then aggregate them by average:

$$\bar{p} = \frac{1}{M(N+1)} \sum_{m=1}^M \sum_{n=0}^N p_{m,n} \quad (4)$$

Then,  $\bar{p}$  is compared with a threshold  $\varepsilon$  to determine whether the input  $x_0$  is harmful, as in Equation (2).

Introducing multiple base detectors enhances accuracy. We assume that each base detector performs better than random guessing. For samples sharing the same meaning as  $x_0$ , each base detector's predictive

probability is a random variable with expectation  $\mu_m$  and variance  $\sigma_m^2$ . We can prove that (Appendix C):

$$P(\hat{y} = y) \geq 1 - \frac{1}{(N+1)M^2\delta^2} \sum_{m=1}^M \sigma_m^2 \quad (5)$$

where  $\delta = |(1/M) \sum_{m=1}^M \mu_m - \varepsilon|$ . As  $M$  increases, the numerator  $\sum_{m=1}^M \sigma_m^2$  grows linearly, while  $M^2$  in the denominator grows quadratically and  $\delta$  remains relatively stable. As a result, the lower bound of  $P(\hat{y} = y)$  increases, indicating that ensembling more base detectors is beneficial, provided that each one performs better than random guessing, which is typically easy to meet. Meanwhile, increasing  $N$  also raises the lower bound, suggesting that incorporating more samples is advantageous.

In summary, by ensembling multiple base detectors, we obtain a two-dimensional matrix of predictive probabilities for aggregation. Unlike prior ensemble studies that aggregate either samples or base models into a one-dimensional prediction vector, our study simultaneously incorporates both to form a matrix. We also theoretically demonstrate the advantage of our two-dimensional ensemble structure.

### 5.3 Design Component 2: A Bayesian Two-Dimensional Weight Assignment Method

#### 5.3.1 Overview of the Second Design Component

Consistent with prior studies (Glenn 1950), we use the Brier Score, defined as  $(p_{m,n} - y)^2$ , to measure the accuracy of each predictive probability  $p_{m,n}$ . A lower score indicates a prediction closer to the ground truth, reflecting better calibration and accuracy (Glenn 1950). Since different predictive probabilities correspond to different accuracy, a viable approach is weighted aggregation, assigning higher weights to more accurate ones. Hence, Equation (4) becomes:

$$\bar{p} = \sum_{m=1}^M \sum_{n=0}^N w_{m,n} p_{m,n} \quad (6)$$

$w_{m,n}$  is the weight assigned for  $p_{m,n}$ , satisfying two constraints:  $\sum_{m=1}^M \sum_{n=0}^N w_{m,n} = 1$  and  $w_{m,n} \geq 0, \forall m, n$ . We denote the likelihood of making the correct prediction  $y$  as  $p(y|\mathbf{P})$ . Since  $p(y|\mathbf{P})$  depends on the values of  $w_{m,n}, \forall m, n$ , assigning appropriate weights  $w_{m,n}$  for each  $p_{m,n}$  is crucial.

Weight assignment methods can be categorized as selection or weighting ones. For selection method, it selects a subset of predictions (each from a base model or for a sample) for the final output (Qin et al.

2023). It eliminates the influence of less accurate predictions by assigning them zero weights. However, enforcing exact zero weights may impair flexibility and compromise performance. Weighting method, by contrast, is more general and flexible, as it is not strictly forced to zero out any predictions. Hence, we focus on this approach, which can be further divided into fixed- and dynamic-weight methods. Fixed-weight methods assign constant weights to each base model during training, which remain fixed at runtime (Li and Chai 2022). However, this is unsuitable in our context because samples  $(\hat{x}_1, \hat{x}_2, \dots, \hat{x}_N)$  are generated at runtime and thus their weights cannot be predetermined. Dynamic-weight methods adapt weights based on the given sample (Zhou et al. 2021). While valuable, they still face two limitations. First, they assign weights to a vector of predictions, considering either multiple samples or multiple base models, but not both. In our case, prediction accuracy depends on both the sample and the base model, making weight assignment more complex. Second, these methods usually assume that higher predictive probabilities indicate higher accuracy. This assumption fails in the context of adversarial attacks, where adversarial samples can still yield high predictive probabilities (e.g., an adversarial image was misclassified as a gibbon with 99.3% predictive probability (Goodfellow et al. 2015)). Hence, determining the values of  $w_{m,n}$  for each sample and base detector under adversarial conditions remains a challenging task.

We propose a dynamic weight assignment method with three phases. Phase 1 follows prior studies by introducing intermediate weights and log-normal distributions to satisfy the two constraints. Since the values of  $w_{m,n}$  are unobserved, we employ Bayesian learning to infer them based on both prior knowledge and observed data. Such integration results in more effective weight assignment. Phase 2 designs the prior. Since the accuracy of each prediction depends jointly on the sample and the base detector, we decompose it into two factors: the sample’s predictability and the base detector’s capability. We theoretically show that a sample’s predictability is negatively correlated with the variance of predictions across base detectors, while a base detector’s capability is negatively correlated with the variance of its predictions across samples. These relationships guide us in designing a prior, which serves as the core technical novelty of our Bayesian weight assignment method. Phase 3 infers the posterior weights. As the true posterior  $p(w_{m,n}|\mathbf{P}, y)$  is

intractable, we approximate it using variational inference with a self-attention-based neural network.

### 5.3.2 Phase 1: Introduce Intermediate Weight and Log-Normal Distribution to Satisfy Constraints

We introduce intermediate weights  $\tilde{w}_{m,n}$  to meet the first constraint (i.e.,  $\sum_{m=1}^M \sum_{n=0}^N w_{m,n} = 1$ ):

$$w_{m,n} = \tilde{w}_{m,n} / \sum_{m=1}^M \sum_{n=0}^N \tilde{w}_{m,n} \quad (7)$$

We further require  $\tilde{w}_{m,n} \geq 0$  to meet the second constraint (i.e.,  $w_{m,n} \geq 0$ ). Thus, the task becomes how to determine  $\tilde{w}_{m,n}$ . Each  $\tilde{w}_{m,n}$  is modeled as a log-normal distribution to ensure its non-negativity. Formally,

$$p(\tilde{w}_{m,n}) = \text{LogNormal}(\psi_{m,n}, \sigma^2) \quad (8)$$

$\psi_{m,n}$  and  $\sigma^2$  are the mean and variance of the Gaussian distribution underlying the log-normal distribution.

### 5.3.3 Phase 2: Design the Prior Distribution

#### 1) Disentangle Factors of Sample and Base Detector

The accuracy of  $p_{m,n}$  depends on two factors: sample  $\hat{x}_n$ 's predictability (when  $n = 0$ ,  $\hat{x}_n$  refers to  $x_0$ ) and detector  $f_m$ 's capability. A *sample's predictability* reflects how likely it is to be correctly predicted and is measured by the Brier Score of its predictions across models:  $e_n = \frac{1}{M} \sum_{m=1}^M (p_{m,n} - y)^2$ . A *detector's capability* reflects its overall ability to make correct predictions and is measured by the Brier Score of its predictions across samples:  $e_m = \frac{1}{N+1} \sum_{n=0}^N (p_{m,n} - y)^2$ . Higher weights should be assigned to samples with greater predictability and to base detectors with stronger capability. To capture this, we factorize  $w_{m,n}$  as:  $w_{m,n} = w_m w_n$ , where  $w_m$  is the overall weight for detector  $f_m$  ( $w_m = \sum_n w_{m,n}$ ) and  $w_n$  is the overall weight for sample  $\hat{x}_n$  ( $w_n = \sum_m w_{m,n}$ ). We prove in Appendix D that the intermediate weight  $\tilde{w}_{m,n}$  can also be factorized as:  $\tilde{w}_{m,n} = \tilde{w}_m \tilde{w}_n$  with  $w_m \propto \tilde{w}_m$  and  $w_n \propto \tilde{w}_n$ , where  $\propto$  denotes proportionality. Thus, it suffices to determine  $\tilde{w}_m$  and  $\tilde{w}_n$ . Since both are non-negative, log-normal distributions are adopted:

$$p(\tilde{w}_m) = \text{LogNormal}(\psi_m, \sigma_{dt}^2); p(\tilde{w}_n) = \text{LogNormal}(\psi_n, \sigma_{sp}^2) \quad (9)$$

#### 2) Identify Domain Knowledge

In matrix  $\mathbf{P}$ , each column represents the predictive probabilities of a sample. For the  $n$ -th column, the mean and variance are  $\bar{p}_n = \frac{1}{M} \sum_{m=1}^M p_{m,n}$  and  $\sigma_n^2 = \frac{1}{M} \sum_{m=1}^M (p_{m,n} - \bar{p}_n)^2$ . We have (see Appendix E):

$$\mathbb{E}[e_n] = \mathbb{E}[\sigma_n^2] + \mathbb{E}[(\bar{p}_n - y)^2] \quad (10)$$

Since all the samples have the same meaning, their expected predictive probabilities are identical, i.e.,  $\mathbb{E}[\bar{p}_n]$  is the same for all samples. With the same  $y$ ,  $\mathbb{E}[(\bar{p}_n - y)^2]$  is also identical across samples. Hence, a larger  $\mathbb{E}[\sigma_n^2]$  implies a larger  $\mathbb{E}[e_n]$ . This makes the observed  $\sigma_n^2$  a useful indicator of sample  $\hat{x}_n$ 's lower predictability. Hence, a larger  $\sigma_n^2$  should correspond to a smaller  $w_n$  and thus a smaller  $\tilde{w}_n$ . Since a smaller  $\psi_n$  in the log-normal distribution leads to a smaller expected  $\tilde{w}_n$ ,  $\psi_n$  should also be smaller.

A similar conclusion holds for detector  $f_m$ , whose predictions correspond to the  $m$ -th row of matrix  $\mathbf{P}$ , with mean  $\bar{p}_m = \frac{1}{N+1} \sum_{n=0}^N p_{m,n}$  and variance  $\sigma_m^2 = \frac{1}{N+1} \sum_{n=0}^N (p_{m,n} - \bar{p}_m)^2$ . Then,  $\mathbb{E}[e_m] = \mathbb{E}[\sigma_m^2] + \mathbb{E}[(\bar{p}_m - y)^2]$  (see Appendix E). In our ensemble, base detectors perform comparably across a wide range of samples. While predictive probabilities for individual samples may vary across detectors, these variations tend to cancel out when averaged over many samples. Thus, we assume  $\mathbb{E}[\bar{p}_m]$  is identical across detectors, which is also empirically validated in Appendix F. Estimating  $\mathbb{E}[\sigma_m^2]$  with the observed  $\sigma_m^2$ , a larger  $\sigma_m^2$  implies a larger  $\mathbb{E}[e_m]$ , which corresponds to a smaller  $w_m$  (and thus  $\tilde{w}_m$ ), and consequently, a smaller  $\psi_m$ .

### 3) Design Prior Distribution based on Disentangled Factors and Domain Knowledge

Since  $\sigma_n^2$  and  $\sigma_m^2$  are inversely related to  $\psi_n$  and  $\psi_m$ , we define  $\psi_n$  and  $\psi_m$  as,

$$\psi_n = \exp[-\alpha \cdot \sigma_n^2]; \psi_m = \exp[-\beta \cdot \sigma_m^2] \quad (11)$$

$\alpha$  and  $\beta$  are positive hyperparameters. The exponential function helps strictly suppress the impact of highly inaccurate predictions (e.g., such as adversarial ones that can greatly increase variance). Since we factorize  $\tilde{w}_{m,n}$  into two factors,  $\tilde{w}_{m,n} = \tilde{w}_m \tilde{w}_n$ , we show in Appendix G that for the  $p(\tilde{w}_{m,n})$  in Equation (8), its  $\psi_{m,n}$  and  $\sigma^2$  can be expressed as  $\psi_{m,n} = \psi_m + \psi_n$ ,  $\sigma^2 = \sigma_{dt}^2 + \sigma_{sp}^2$ . Then, we have:

$$p(\tilde{w}_{m,n}) = \text{LogNormal}(\exp[-\alpha \cdot \sigma_n^2] + \exp[-\beta \cdot \sigma_m^2], \sigma_{dt}^2 + \sigma_{sp}^2) \quad (12)$$

In Equation (12), we actually design a mapping function from  $\mathbf{P}$  (from which  $\sigma_n^2$  and  $\sigma_m^2$  are computed) to  $\psi_{m,n}$  and then get  $p(\tilde{w}_{m,n})$ . Technically, it should be denoted as  $p(\tilde{w}_{m,n} | \mathbf{P})$ , but we still use  $p(\tilde{w}_{m,n})$  for simplicity.  $p(\tilde{w}_{m,n})$  serves as a prior for two reasons. First, it embeds useful domain knowledge (assigning smaller weights to higher-variance predictions), but the expectations are estimated from a single instance (e.g., using  $\sigma_m^2$  to estimate  $\mathbb{E}[\sigma_m^2]$ ), introducing randomness that may weaken the domain knowledge.

Second, while valuable, the multiplicative disentanglement and exponential functional form may not be optimal and oversimplify the underlying relationship. Thus,  $p(\tilde{w}_{m,n})$  is useful but still needs refinement. Hence, we use it as a prior to guide the learning of assigning more appropriate weights, i.e., the posterior.

#### 5.3.4 Phase 3: Obtain the Posterior

The posterior is advantageous as the mapping function from  $\mathbf{P}$  is refined with the observed ground truth  $y$ , resulting in more appropriate weight assignments. We denote the posterior of  $\tilde{w}_{m,n}$  as  $p(\tilde{w}_{m,n}|\mathbf{P}, y)$ , modeled as  $\text{LogNormal}(\varphi_{m,n}^{\text{post}}, (\sigma^{\text{post}})^2)$ . The task is to get the parameters  $\varphi_{m,n}^{\text{post}}$  and  $\sigma^{\text{post}}$ . However, their exact values are intractable. Hence, we adopt the neural network-based variational inference (Kingma and Welling 2014), using a neural network (*inference network*) to output the parameters of the variational distribution (i.e.,  $\varphi_{m,n}^{\text{post}}$  and  $\sigma^{\text{post}}$ ). To simplify inference and reduce complexity, we focus on inferring  $\varphi_{m,n}^{\text{post}}$  and set  $(\sigma^{\text{post}})^2$  directly as  $\sigma_{\text{dt}}^2 + \sigma_{\text{sp}}^2$  (same as the prior). Since the ground truth  $y$  is unobserved at runtime, the inference network cannot rely on it as input and should instead take only  $\mathbf{P}$  as input. We denote the inference network for obtaining  $\varphi_{m,n}^{\text{post}}$  as  $\varphi_{m,n}^{\text{post}} = f^{\text{infer}}(\mathbf{P})$ , which is trained to make the variational distribution approximate the true posterior  $p(\tilde{w}_{m,n}|\mathbf{P}, y)$ . Thus, the task reduces to learning  $f^{\text{infer}}(\mathbf{P})$ .

Our inference network is built on self-attention. Since each row of  $\mathbf{P}$  corresponds to a base detector, and each column corresponds to a sample, we first apply self-attention to the rows and columns to capture dependencies within each detector and sample, and then combine them to model their interactions. Let  $\mathbf{p}_m$  denote the predictions of detector  $f_m$  and  $\mathbf{p}_n$  those of sample  $\hat{x}_n$ . We use self-attention to get representation  $\mathbf{z}_m$  for  $\mathbf{p}_m$  and  $\mathbf{z}_n$  for  $\mathbf{p}_n$ , and then combine them to predict  $\varphi_{m,n}^{\text{post}}$  with a multilayer perceptron (MLP):

$$\mathbf{z}_m = \text{SelfAttention}(\mathbf{p}_m); \mathbf{z}_n = \text{SelfAttention}(\mathbf{p}_n); \varphi_{m,n}^{\text{post}} = \text{MLP}(\mathbf{z}_m; \mathbf{z}_n) \quad (13)$$

The structural details of the  $\text{SelfAttention}(\cdot)$  and  $\text{MLP}(\cdot)$  are in Appendix H. Compared with the prior that only uses variance, self-attention allows us to capture more intricate and useful dependencies. Moreover, the factors of the sample and the base detector are combined through an MLP instead of a specific multiplicative form, allowing to model richer interactions. In addition, a neural network is used as the inference network instead of a specific exponential function, enabling more effective extraction of

information from  $\mathbf{P}$  to determine weights. Let  $\widetilde{\mathbf{W}}$  collectively denote  $\widetilde{w}_{m,n}$  and  $\mathbf{W}$  denote  $w_{m,n}$ . Let  $\boldsymbol{\phi}$  denote the parameters of the inference network, which outputs  $\varphi_{m,n}^{\text{post}}$  to define the variational distribution  $q_{\boldsymbol{\phi}}(\widetilde{\mathbf{W}})$  over weights  $\widetilde{\mathbf{W}}$  (and thus over  $\mathbf{W}$ ). Hence, the inference network serves as the *weight assignor*.

Since we approximate the posterior  $p(\widetilde{\mathbf{W}}|\mathbf{P}, y)$  with a variational distribution  $q_{\boldsymbol{\phi}}(\widetilde{\mathbf{W}})$ , the log-likelihood  $\log p(y|\mathbf{P})$  computed with  $q_{\boldsymbol{\phi}}(\widetilde{\mathbf{W}})$  is a lower bound of the true  $\log p(y|\mathbf{P})$  (see Appendix I):

$$\mathcal{L} = \mathbb{E}_{q_{\boldsymbol{\phi}}(\widetilde{\mathbf{W}})}[\log p(y|\mathbf{P}, \widetilde{\mathbf{W}})] - \sum_{m=1}^M \sum_{n=0}^N \text{KL}\left(q_{\boldsymbol{\phi}}(\widetilde{w}_{m,n})\|p(\widetilde{w}_{m,n})\right) \quad (14)$$

where  $\mathcal{L}$  denotes the lower bound. The first term of the lower bound represents the model's likelihood of making a correct prediction based on  $\widetilde{\mathbf{W}}$  from the variational distribution. The second term measures the Kullback-Leibler divergence between the variational and the prior distribution. Their detailed computations are in Appendix J. We learn  $\boldsymbol{\phi}$  by maximizing  $\mathcal{L}$ . In this way, the weight assignor is learned from both the observed data ( $\mathbf{P}$  and  $y$ ) and the identified domain knowledge that has been embedded in our prior.

#### 5.4 Design Component 3: An Iterative Adversarial Training (IAT) Strategy

Adversarial training (AT) has been shown to learn models with robust parameters, and we adopt this idea in our study. However, unlike the prior AT studies that focus only on enhancing base models, we use AT to enhance both the base detectors and the weight assignor. This introduces a key challenge: the base detectors and the weight assignor jointly determine the final prediction, yet the dataset for training base detectors cannot be reused for training the weight assignor, which must evaluate the base detectors on a separate dataset to assign weights accordingly. Reusing the same data would cause overfitting and biased weight assignment. To address this issue, we propose an iterative adversarial training (IAT) strategy.

We denote the dataset to train base detectors and the weight assignor as  $\mathcal{D}^{\text{bd}}$  and  $\mathcal{D}^{\text{ag}}$ , respectively. As with prior work, we use existing attack methods to craft adversarial samples for each sample in  $\mathcal{D}^{\text{bd}}$  and  $\mathcal{D}^{\text{ag}}$ , yielding datasets  $\widetilde{\mathcal{D}}^{\text{bd}}$  and  $\widetilde{\mathcal{D}}^{\text{ag}}$ . They are then combined with the initial datasets to get two augmented datasets:  $\mathcal{D}^{\text{bd}} \cup \widetilde{\mathcal{D}}^{\text{bd}}$  and  $\mathcal{D}^{\text{ag}} \cup \widetilde{\mathcal{D}}^{\text{ag}}$ . Detailed process is in Appendix K. For each  $(x_i^{\text{bd}}, y_i^{\text{bd}}) \in \mathcal{D}^{\text{bd}} \cup \widetilde{\mathcal{D}}^{\text{bd}}$ , we generate  $N$  samples with the same meaning as  $x_i^{\text{bd}}$  using LLM, denoted as  $\hat{x}_{i,1}^{\text{bd}}, \dots, \hat{x}_{i,N}^{\text{bd}}$ . The initial

$x_i^{\text{bd}}$  and the generated  $\hat{x}_{i,1}^{\text{bd}}, \dots, \hat{x}_{i,N}^{\text{bd}}$  are collectively denoted as  $\mathbf{x}_i^{\text{bd}}$ . The predictive probabilities for  $\mathbf{x}_i^{\text{bd}}$  form a two-dimensional matrix  $\mathbf{P}_i^{\text{bd}}$ . Its weight matrix is denoted as  $\mathbf{W}_i^{\text{bd}}$ . The final prediction is computed as  $\text{tr}[(\mathbf{W}_i^{\text{bd}})^T \mathbf{P}_i^{\text{bd}}]$ . We define the loss over  $\mathcal{D}^{\text{bd}} \cup \tilde{\mathcal{D}}^{\text{bd}}$  as the cross-entropy (CE) loss. Then, we have:

$$\text{Loss}^{\text{bd}} = \sum_{i=1}^{|\mathcal{D}^{\text{bd}} \cup \tilde{\mathcal{D}}^{\text{bd}}|} \text{CE} \left( \text{tr}[(\mathbf{W}_i^{\text{bd}})^T \mathbf{P}_i^{\text{bd}}], y_i^{\text{bd}} \right) \quad (15)$$

The  $m$ -th row of  $\mathbf{P}_i^{\text{bd}}$  is produced by the detector parameterized by  $\boldsymbol{\theta}_m$ , while  $\mathbf{W}_i^{\text{bd}}$  comes from the weight assignor parameterized by  $\boldsymbol{\phi}$ . Since  $\mathcal{D}^{\text{bd}} \cup \tilde{\mathcal{D}}^{\text{bd}}$  is used to train the base detectors,  $\text{Loss}^{\text{bd}}$  updates only  $\boldsymbol{\theta}_m$  ( $\forall m$ ) with  $\boldsymbol{\phi}$  fixed. We update  $\boldsymbol{\theta}_m$  using the Adam optimizer with an initial learning rate  $\eta$ :

$$\boldsymbol{\theta}_m \leftarrow \boldsymbol{\theta}_m - \text{AdamUpdate}(\partial \text{Loss}^{\text{bd}} / \partial \boldsymbol{\theta}_m, \eta) \quad (16)$$

Using similar notations, we define the objective over  $\mathcal{D}^{\text{ag}} \cup \tilde{\mathcal{D}}^{\text{ag}}$  as maximizing the sum of the lower bounds of each sample it contains (as shown in Equation 14). The corresponding loss is then defined as:

$$\text{Loss}^{\text{ag}} = \sum_{i=1}^{|\mathcal{D}^{\text{ag}} \cup \tilde{\mathcal{D}}^{\text{ag}}|} \left[ -\mathbb{E}_{q_{\boldsymbol{\phi}}(\tilde{\mathbf{W}}_i^{\text{ag}})} [\log p(y_i^{\text{ag}} | \mathbf{P}_i^{\text{ag}}, \tilde{\mathbf{W}}_i^{\text{ag}})] + \text{KL} \left( q_{\boldsymbol{\phi}}(\tilde{\mathbf{W}}_i^{\text{ag}}) \| p(\tilde{\mathbf{W}}_i^{\text{ag}}) \right) \right] \quad (17)$$

Since  $\mathcal{D}^{\text{ag}} \cup \tilde{\mathcal{D}}^{\text{ag}}$  is used to train the weight assignor,  $\text{Loss}^{\text{ag}}$  is used to update only  $\boldsymbol{\phi}$  with  $\boldsymbol{\theta}_m$  ( $\forall m$ ) fixed:

$$\boldsymbol{\phi} \leftarrow \boldsymbol{\phi} - \text{AdamUpdate}(\partial \text{Loss}^{\text{ag}} / \partial \boldsymbol{\phi}, \eta) \quad (18)$$

We alternate between Equations (16) and (18) until convergence (pseudocode in Appendix L), jointly learning the parameters of base detectors and the weight assignor for enhanced robustness. A technical challenge is that  $\mathbf{W}_i^{\text{ag}}$  is a random sample from the distribution  $q_{\boldsymbol{\phi}}$ , making gradient computation and the update process difficult. We address this using the reparameterization trick, with details in Appendix M.

While some studies combine AT with ensemble learning, they apply AT only to the base detectors, neglecting the weight assignor and its interactions with base detectors. In contrast, our IAT robustifies both the base detectors and the weight assignor and captures their interactions. Notably, in practice, base detectors may already be deployed, so practitioners may keep them fixed to ensure higher compatibility or reduce training costs. This consideration is particularly relevant for base detectors with a large number of parameters, such as transformer-based models, where retraining can be costly. In such case, our IAT can be simplified: only using Equation (18) to train the weight assignor, without updating the base detectors.

## 5.5 Predicting New Samples

After training, we obtain our ARHOCD. For a new input  $x^{\text{new}}$ , its prediction involves three steps.

First, we prompt the LLM to generate  $N$  samples:  $\hat{x}_1^{\text{new}}, \dots, \hat{x}_n^{\text{new}}, \dots, \hat{x}_N^{\text{new}}$ . Second, we apply its base detectors to all samples to obtain a two-dimensional matrix of predictive probabilities  $\mathbf{P}^{\text{new}}$ , with each element denoted as  $p_{m,n}^{\text{new}}$ . Third, we apply its weight assignor to get the weight  $w_{m,n}^{\text{new}}$  for  $p_{m,n}^{\text{new}}$ . As  $w_{m,n}^{\text{new}}$  is a random variable, we compute the expectation. Then, the predictive probability  $\hat{p}^{\text{new}}$  is given by,

$$\hat{p}^{\text{new}} = \sum_{m=1}^M \sum_{n=0}^N (\mathbb{E}[w_{m,n}^{\text{new}}] \cdot p_{m,n}^{\text{new}}) \quad (19)$$

If  $\hat{p}^{\text{new}} \leq \varepsilon$ , the input  $x^{\text{new}}$  is classified as non-harmful; otherwise, it is classified as harmful. However,  $\mathbb{E}[w_{m,n}^{\text{new}}]$  is intractable. We propose two solutions: using Monte Carlo (MC) method to approximate  $\mathbb{E}[w_{m,n}^{\text{new}}]$ , or computing a lower bound of  $\mathbb{E}[w_{m,n}^{\text{new}}]$  to represent it. The corresponding ARHOCDs are denoted as Ours (MC) and Ours (LB), respectively. The details of these two solutions are in Appendix N.

## 6. Evaluation

### 6.1 Experiment Settings

#### 6.1.1 Datasets

We evaluated our method on three widely used datasets: ETHOS, PHEME and White Supremacist (De Gibert et al. 2018, Mollas et al. 2022). ETHOS is a dataset for hate speech detection. It contains tweets from Hatebusters and Reddit, each annotated by five Figure-Eight crowdworkers to indicate if the tweet contains hate speech. PHEME is a rumor detection dataset with tweets on news events, labeled by professional journalists. White Supremacist is an extremist content detection dataset, with posts from the Stormfront forum, each labeled by three experts. Table 4 shows their statistics (details in Appendix O). To handle class imbalance in the PHEME and White Supremacist datasets, we used the cost-sensitive learning strategy proposed in (Ting 2002) during training, where higher weights are assigned to the minority class.

**Table 4. Statistics of the Datasets**

Datasets	#Samples	Class Ratio (Positive/Negative)	Dataset Split (Train/Val/Test)	Avg. Len.	Max. Len.	Min. Len.
ETHOS	998	Hate (44.39%)/ Non-hate (55.61%)	798/100/100	23.24	606	2
PHEME	6425	Rumor (37.39%)/ Non-rumor (62.61%)	5140/642/643	21.46	38	3
White Supremacist	10,319	Hate (11.59%)/ Non-hate (88.41%)	8255/1032/1032	18.68	366	1

### 6.1.2 The Assumption of Attacker and Defender’s Knowledge in the Experiments

We assume attackers know the details of the detector being used, which is a common assumption in prior studies (Yoo and Qi 2021). This assumption is grounded in two reasons. First, many detectors’ structures or source codes are often publicly accessible, and even if not, attackers could infer or obtain them through various means, such as inference or network intrusion. Second, following Kerckhoffs’s principle, which states that a system should remain secure even if all its information is public, adversarial robustness should be evaluated and enhanced assuming the detector’s details are known to attackers.

Defenders, however, are often unaware of which attack will be launched. Since the attack set is vast, potentially infinite, it is infeasible to enumerate every possible attack. Based on the literature, we selected four representative attacks covering four levels to simulate adversaries. For character-level attack, we chose DeepWordBug (Gao et al. 2018, Li and Chai 2022), which generates adversarial samples by performing four character-level perturbations: substitution, insertion, deletion, and neighboring swap. For word-level attack, we chose TFAdjusted (Herel et al. 2023, John X. Morris et al. 2020), which deletes each word and measures the change in the model’s prediction to identify key words, and then replaces the key words with synonyms. For sentence-level attack, we chose TREPAT (Przybyła et al. 2025), which splits long texts into smaller segments, rephrases these segments with an LLM using diverse prompts, extracts edits (e.g., substitutions, insertions, and deletions), and then applies these edits via beam search to generate adversarial samples. For multi-level attack, we chose Explainability-Driven adversarial attack (ExplainDrive, (Kumbam et al. 2025)). It first identifies the most important features using interpretability techniques (e.g., LIME, (Ribeiro et al. 2016)), which assign importance scores based on each feature’s contribution to the prediction. It then adversarially perturbs the most important features at different levels to generate adversarial samples.

## 6.2 Experiment 1: Generalizability Comparison

### 6.2.1 Baselines and Metrics

We evaluated the generalizability of our LLM-SGA by showing that a detector instantiated within it outperforms detectors robustified by baselines. Since encoder-only transformers excel in classification tasks,

we used BERT (the most popular model in this family) as the detector. The baselines cover the major types of adversarial robustness enhancement methods reviewed earlier, whose core ideas are summarized in Table 5 and details in Appendix P. For passive defenses, we combined BERT with LLM-puri and Det&Res. For active defenses, structure-based methods were excluded because they modify detector structures, whereas ours preserves them for better compatibility. We included learning-based methods where BERT was fine-tuned. We also included ensemble model-based methods. Since these methods use multiple base detectors, we included BERT and its four variants (DistilBERT, RoBERTa, XLNet, ALBERT) as base detectors. For fair comparison, we instantiated two detectors within LLM-SGA: one using only BERT (LLM-SGA (single)) and one using the same five base detectors as the ensemble baselines (LLM-SGA (multiple)).

**Table 5. Brief Descriptions of Baselines**

Baselines		Brief Descriptions	
Passive	LLM-puri (Moraaffah et al. 2024)	Prompt an LLM to purify adversarial samples.	
	Detection and Restoration (Det&Res) (Wang et al. 2022)	Detect and restore adversarial samples.	
Active	Learning-based	Random noise-based SAFER (Ye et al. 2020)	Generate multiple samples by synonym replacement.
		MASKFil (Li et al. 2023)	Generate multiple samples by masked word filling.
		FTML (Yang et al. 2022)	Bring words closer to synonyms and push them away from non-synonyms in the embedding space.
	Regularization-based	OutReg (Dong et al. 2021)	Align outputs for clean and adversarial sample pairs.
		FIM (Gloeckler et al. 2023)	Penalize gradient directions with high sensitivity.
		AT (Goodfellow et al. 2015)	Incorporate adversarial samples into the training set.
	Adversarial training-based	MRAT (Zhao et al. 2021)	Optimize the model using a mixup-based strategy.
		FAT (Yang et al. 2025)	Fast adversarial training in the embedding space.
		ARText (Li and Chai 2022)	Use adversarial training and model ensemble.
Ensemble model-based	ARDEL (Waghela et al. 2024)	Use a meta-model to weight base models.	
	EnsSel (Qin et al. 2023)	Select predictions with the lowest uncertainties.	

We used the four aforementioned attacks to generate adversarial samples from test set for evaluation. For each detector, we computed ASR and after-attack classification metrics (described in Section 2.1, with computation details in Appendix Q). The worst-case performance across attacks reflects generalizability.

### 6.2.2 Results

We repeated the experiment 20 times, reporting the mean and standard deviation (std) and examining statistical significance via the t-test. To save space, we only report the ASRs of the four attacks on the PHEME dataset in Table 6, while other metrics and the results of the other two datasets are reported in Appendix R.1. For simplicity, a robustified detector is denoted by the enhancement method applied to it. For instance, the detector robustified by Det&Res is denoted as “Det&Res” in Table 6.

**Table 6. Comparison with Baselines on Generalizability (ASR%)**

Detectors	DeepWordBug	TFAdjusted	TREPAT	ExplainDrive	Worst-Case
Raw BERT	56.86*** (2.81)	58.28*** (2.53)	43.60*** (3.89)	74.95*** (3.04)	74.95
LLM-puri	19.42** (3.77)	20.98*** (1.91)	19.80** (3.32)	34.54* (2.09)	34.54
Det&Res	31.79*** (2.28)	30.24*** (3.03)	33.54*** (3.91)	41.18*** (4.75)	41.18
SAFER	47.32*** (3.32)	47.20*** (2.63)	45.43*** (4.40)	61.43*** (3.89)	61.43
MASKFil	52.40*** (4.20)	63.49*** (2.60)	43.65*** (2.72)	73.81*** (4.08)	73.81
FTML	43.85*** (4.26)	43.84*** (2.81)	47.25*** (3.76)	64.53*** (4.70)	64.53
OutReg	44.53*** (2.71)	41.96*** (3.45)	37.64*** (4.25)	56.54*** (5.01)	56.54
FIM	56.53*** (2.81)	59.05*** (3.62)	52.26*** (4.16)	72.85*** (5.03)	72.85
AT	50.64*** (3.33)	48.70*** (2.94)	39.67*** (3.37)	63.41*** (3.36)	63.41
MRAT	46.04*** (2.88)	53.18*** (3.00)	46.52*** (2.58)	72.95*** (2.88)	72.95
FAT	56.32*** (3.33)	57.07*** (4.17)	43.63*** (4.66)	72.12*** (3.92)	72.12
LLM-SGA (single)	<b>16.02 (2.70)</b>	<b>16.36 (2.38)</b>	<b>23.34 (3.55)</b>	<b>31.91 (4.59)</b>	<b>31.91</b>
ARText	24.23*** (3.57)	21.35*** (3.20)	23.59*** (4.03)	26.97*** (3.66)	26.97
ARDEL	21.04*** (3.33)	18.75*** (3.27)	20.18*** (3.48)	26.95*** (5.35)	26.95
EnsSel	17.07*** (2.92)	15.96 (2.51)	24.43*** (3.58)	21.86* (2.72)	24.43
LLM-SGA (multiple)	<b>12.08 (2.47)</b>	<b>15.22 (1.99)</b>	<b>14.95 (2.91)</b>	<b>19.68 (3.74)</b>	<b>19.68</b>

Note: A higher ASR indicates that more adversarial samples bypass the detector, resulting in lower performance; \* $p < 0.05$ ; \*\* $p < 0.01$ ; \*\*\* $p < 0.001$ ; Values in brackets show std. Bold font marks the best results. Same below.

By comparing our LLM-SGA (single) with the baselines, we find that the BERT detector robustified by LLM-SGA is more generalizable. Specifically, it obtains the best worst-case performance across all attacks, with an ASR of 31.91%. This means that, in the worst case, when attackers generate 100 adversarial samples, only about 32 of them can fool the detector. In contrast, among the baselines, the detector robustified by LLM-puri performs best, with its worst-case results under the ExplainDrive attack. In this setting, it attains an ASR of 34.54%, significantly higher than that of ours ( $p < 0.05$ ). Meanwhile, by comparing LLM-SGA (multiple) with ensemble model-based baselines, we find that ensembling multiple base detectors and robustifying them with LLM-SGA yields the best performance, with a worst-case ASR of 19.68%. The baselines ARText, ARDEL, EnsSel obtain worst-case ASRs of 26.97%, 26.95% and 24.43%, respectively—all significantly higher than that of ours ( $p < 0.001$ ). By the way, comparing LLM-SGA (multiple) with LLM-SGA (single) shows that ensembling multiple base detectors increases detection accuracy, reducing the ASR across the four attacks from 16.02%, 16.36%, 23.34%, and 31.91% to 12.08%, 15.22%, 14.95%, and 19.68%. This demonstrates the effectiveness of our first design component.

### 6.3 Experiment 2: Accuracy Comparison

We compared our ARHOCD with detectors robustified by baselines to show its advantage in accuracy. ARHOCD includes five base detectors (BERT, DistilBERT, RoBERTa, XLNet, and ALBERT).

Since ARHOCD includes the processes of generating samples, aggregating predictions from the generated samples and base detectors, and training parameters, while some baselines only include one or two processes, we enhanced all baselines to include comparable processes. This ensures that any performance gain arises from our novel design components rather than from simply assembling more processes.

The enhancement principle is as follows: if a baseline already contains a given process, we retain its own version; otherwise, we enhance it with a well-performing one. For example, the regularization-based methods (FTML, OutReg, FIM) do not generate samples, so we incorporated SAFER (a well-performing sample generation method according to our experiments). Similarly, because these baselines use a single detector, we extended them to five base detectors as ours and then aggregated their outputs using CBW-D (a well-performing aggregation method according to our experiments). However, since these baselines have their own training processes, the detector parameters were learned using their respective own ones. With the same principle, we enhanced all the other baselines (details in Appendix S), as summarized in Table 7. Since all detectors used the same five base detectors, we omit this detail from Table 7 for brevity.

Experiments were conducted in two scenarios: defending known attacks and new attacks. For known attacks, each dataset was split into training ( $D^{\text{train}}$ ) and test ( $D^{\text{test}}$ ) sets. Adversarial samples were generated for each set by randomly applying one of three attacks: DeepWordBug, TFAdjusted, or TREPAT, yielding adversarial datasets:  $D_{\text{DTT}}^{\text{train}}$  (from  $D^{\text{train}}$ ) and  $D_{\text{DTT}}^{\text{test}}$  (from  $D^{\text{test}}$ ). Detectors were robustified (e.g., adversarially trained) on  $D_{\text{DTT}}^{\text{train}}$  and evaluated on  $D_{\text{DTT}}^{\text{test}}$ . For new attacks, an adversarial test set  $D_{\text{E}}^{\text{test}}$  was crafted from  $D^{\text{test}}$  using the ExplainDrive attack, which was unseen in the robustification process and thus regarded new. All methods were evaluated on  $D_{\text{E}}^{\text{test}}$ . Since baselines FTML, SAFER, MASKFil, and FAT do not use adversarial samples during robustification, all attacks are new for them. Hence, these baselines were included only in new-attack scenario. For a fair comparison, they were also evaluated on  $D_{\text{E}}^{\text{test}}$ .

**Table 7. Enhancements of Baselines in Experiment 2**

Types		Enhanced Baselines	Samples	Aggregation	Learning
Passive defense baselines		LLM-puri	Own	Lack (CBW-D)	AT
		Det&Res	Own	Lack (CBW-D)	AT
Active defense	Random noise-based	SAFER	Own	Lack (CBW-D)	Own
		MASKFil	Own	Lack (CBW-D)	Own

baselines	Regularization-based	FTML	Lack (SAFER)	Lack (CBW-D)	Own
		OutReg	Lack (SAFER)	Lack (CBW-D)	Own
		FIM	Lack (SAFER)	Lack (CBW-D)	Own
	Adversarial training-based	AT	Lack (SAFER)	Lack (CBW-D)	Own
		MRAT	Lack (SAFER)	Lack (CBW-D)	Own
		FAT	Lack (SAFER)	Lack (CBW-D)	Own
	Ensemble model-based	ARText	Lack (SAFER)	Own	Own
		ARDEL	Own	Own	Own
		EnsSel	Lack (SAFER)	Own	Own

For both scenarios, we conducted an ablation study to examine the contribution of each key design component in our ARHOCD. First, to examine the two-dimensional ensemble (Design Component 1), we removed the model ensemble, retaining only a single detector (Ours w/o ME). Second, we tested the weight assignment method (Design Component 2). We removed our variance-based prior (Ours w/o prior) and the data-driven refinement process that aims to approximate the posterior (Ours w/o data). We replaced our weight assignment method with a fixed-weight baseline (Ours w/ FEL), a dynamic-weight baseline using CBW-D (Ours w/ CBW-D), and a selection method that, for each sample, chooses the detector with the highest predictive probability (Ours w/ ES). While not explored in prior work, we also devised a probability-based prior that used the gap between the predictive probabilities of the two classes: a larger gap indicates higher reliability and thus gets a larger weight. We replaced our variance-based prior with it, yielding Ours w/ Prob-prior. Third, we tested our IAT (Design Component 3) by removing it (Ours w/o IAT). In addition, since current AT enhances only the base detectors, we also evaluated a variant where IAT was replaced with AT applied only to the base detectors (Ours w/ AT). Appendix T shows further details of these variants.

For both scenarios, we also investigated the sensitivity of key parameters in our detector, including the number of generated samples, the number of base detectors, and the  $\sigma^2$  of the log-normal distribution.

In summary, Experiment 2 comprises three sub-experiments: (1) baseline comparison, (2) ablation analysis, and (3) sensitivity analysis, each performed under two scenarios on three datasets. For brevity, we present results on the PHEME dataset in the manuscript, with the other two datasets in Appendix R.2.

### 6.3.1 Results of Experiment 2.1 (Comparison with Baselines in Defending Known and New Attacks)

Table 8 reports the experimental results. Ours (MC) and Ours (LB), which use Monte Carlo and lower-bound approximations of Equation (19), respectively, perform comparably and outperform all

enhanced baselines, showing strong robustness in harmful content detection against known and new attacks. For instance, for known attacks, Ours (LB) improves after-attack accuracy, precision, recall, and F1-score over the best baseline (LLM-puri (Enhanced)) by 2.3%, 2.0%, 4.2%, and 3.0% ( $p < 0.001$ ). For new attacks, Ours (MC) reduces ASR from 15.38% of the best baseline (MRAT (Enhanced)) to 13.16% ( $p < 0.001$ ).

**Table 8. Results of Comparison with Baselines in Defending Known and New Attacks**

Attack Scenario	Method	Performance after attack <sup>†</sup> (%)				ASR $\downarrow$ (%)
		Accuracy	Precision	Recall	F1-score	
Known Attacks (DeepWordBug, TFAdjusted, TREPAT)	LLM-puri (Enhanced)	83.66*** (0.67)	82.73*** (0.71)	82.09*** (0.80)	82.38*** (0.75)	12.55*** (0.67)
	Det&Res (Enhanced)	81.38*** (0.77)	80.42*** (0.81)	79.27*** (0.95)	79.74*** (0.89)	14.99*** (1.12)
	OutReg (Enhanced)	81.15*** (0.62)	80.60*** (0.63)	78.36*** (0.80)	79.16*** (0.75)	15.26*** (1.22)
	AT (Enhanced)	81.59*** (0.85)	80.82*** (0.89)	79.23*** (1.04)	79.85*** (0.99)	15.03*** (1.14)
	MRAT (Enhanced)	83.54*** (1.06)	82.74*** (1.21)	81.71*** (1.09)	82.15*** (1.13)	13.96*** (0.96)
	ARTText (Enhanced)	80.95*** (0.75)	79.62*** (0.80)	79.82*** (0.78)	79.71*** (0.78)	12.79*** (0.81)
	ARDEL (Enhanced)	80.78*** (0.96)	80.10*** (1.08)	78.08*** (1.11)	78.81*** (1.10)	15.03*** (1.14)
	EnsSel (Enhanced)	81.81*** (0.84)	81.32*** (0.97)	79.13*** (0.92)	79.93*** (0.93)	15.35*** (0.74)
	Ours (MC)	<b>85.59 (0.76)</b>	<b>84.42 (0.78)</b>	<b>85.54 (0.86)</b>	<b>84.85 (0.80)</b>	10.59 (1.04)
	Ours (LB)	85.49 (0.82)	84.32 (0.85)	85.45 (0.93)	84.76 (0.87)	<b>10.59 (1.03)</b>
New Attacks (ExplainDrive)	LLM-puri (Enhanced)	82.41 (0.92)	81.41 (1.03)	80.65*** (0.98)	81.02*** (1.01)	14.24** (0.55)
	Det&Res (Enhanced)	80.05*** (0.94)	78.93*** (1.01)	77.89*** (1.08)	78.32*** (1.05)	16.27*** (1.40)
	SAFER (Enhanced)	77.27*** (1.11)	75.78*** (1.22)	75.20*** (1.17)	75.45*** (1.18)	17.54*** (1.13)
	MASKFil (Enhanced)	77.15*** (1.23)	75.77*** (1.38)	74.61*** (1.33)	75.06*** (1.34)	18.69*** (1.04)
	FTML (Enhanced)	78.13*** (0.76)	76.98*** (0.88)	75.40*** (0.82)	75.99*** (0.83)	19.20*** (1.36)
	OutReg (Enhanced)	79.88*** (0.77)	79.36*** (0.85)	76.71*** (0.91)	77.59*** (0.90)	17.52*** (1.38)
	FIM (Enhanced)	73.51*** (0.97)	73.05*** (1.17)	68.21*** (1.21)	68.98*** (1.32)	25.36*** (1.56)
	AT (Enhanced)	80.57*** (0.81)	79.63*** (0.87)	78.19*** (0.96)	78.76*** (0.92)	16.29*** (0.88)
	MRAT (Enhanced)	82.05** (0.99)	81.22 (1.17)	79.91*** (1.05)	80.44*** (1.07)	15.38*** (1.20)
	FAT (Enhanced)	73.59*** (0.94)	73.32*** (1.19)	68.17*** (1.15)	68.94*** (1.27)	26.42*** (1.06)
	ARTText (Enhanced)	79.16*** (1.23)	77.74*** (1.30)	77.82*** (1.35)	77.77*** (1.32)	15.11*** (1.27)
	ARDEL (Enhanced)	79.04*** (0.99)	78.29*** (1.13)	75.94*** (1.16)	76.73*** (1.15)	16.29*** (0.88)
	EnsSel (Enhanced)	79.90*** (0.94)	79.68*** (1.05)	76.42*** (1.11)	77.43*** (1.11)	18.44*** (1.28)
	Ours (MC)	<b>82.91 (0.66)</b>	<b>81.67 (0.67)</b>	<b>82.61 (0.63)</b>	<b>82.03 (0.66)</b>	<b>13.16 (1.12)</b>
	Ours (LB)	82.88 (0.66)	81.64 (0.68)	82.58 (0.58)	82.00 (0.65)	13.24 (1.13)

### 6.3.2 Results of Experiment 2.2 (Ablation Analysis in Defending Known and New Attacks)

Table 9 presents the results, revealing three observations. First, using a single detector without model ensemble greatly degrades performance. For instance, defending known attacks with only BERT lowers the F1-score from 84.85% to 75.99%, showing lower robustness. Second, removing the variance-based prior (Ours w/o prior) or replacing it (Ours w/ Prob-prior) degrades performance. Removing the data-driven refinement process (Ours w/o data) also worsens performance. Meanwhile, alternative weighting methods, including Ours w/ FEL, Ours w/ CBW-D and Ours w/ ES, perform worse. For instance, in defending new attacks, Ours w/ CBW-D rises ASR from 13.16% to 15.26%. Finally, removing or replacing IAT (Ours w/o

IAT, Ours w/ AT) notably reduces robustness. For instance, removing IAT reduces after-attack accuracy from 85.59% to 81.70% for known attacks and from 82.91% to 79.29% for new attacks. Overall, removing or replacing any key design component degrades performance, highlighting the contribution of each.

**Table 9. Results of Ablation Analysis in Defending Known and New Attacks**

Attack Scenario	Method	Performance after attack <sup>†</sup> (%)				ASR <sup>↓</sup> (%)	
		Accuracy	Precision	Recall	F1-score		
Known Attacks (DeepWordBug, TFAdjusted, TREPAT)	Ours w/o ME	BERT	77.26*** (0.45)	75.73*** (0.47)	76.35*** (0.50)	75.99*** (0.48)	14.88*** (0.53)
		DistilBERT	75.23*** (0.75)	73.74*** (0.78)	74.64*** (0.81)	74.04*** (0.79)	18.08*** (0.85)
		RoBERTa	78.94*** (0.65)	77.58*** (0.66)	78.67*** (0.69)	77.95*** (0.67)	14.78*** (0.70)
		XLNet	75.81*** (0.56)	74.64*** (0.59)	75.97*** (0.65)	74.93*** (0.60)	13.56*** (0.65)
		ALBERT	77.32*** (0.72)	75.85*** (0.81)	74.98*** (0.72)	75.35*** (0.75)	17.88*** (0.64)
	Ours w/o prior	Ours w/o prior	84.77** (0.87)	83.57* (0.91)	84.36*** (0.93)	83.91** (0.91)	11.24* (0.69)
		Ours w/o data	85.03* (0.59)	83.90 (0.64)	84.31*** (0.64)	84.09** (0.62)	11.29* (0.54)
		Ours w/ FEL	84.55*** (0.55)	83.40*** (0.60)	83.75*** (0.55)	83.56*** (0.56)	11.83*** (0.50)
		Ours w/ CBW-D	84.91* (0.69)	83.90 (0.75)	83.80*** (0.75)	83.84*** (0.74)	11.67*** (0.65)
		Ours w/ ES	84.98* (0.75)	84.06 (0.83)	83.65*** (0.78)	83.84** (0.79)	12.07*** (0.98)
		Ours w/ Prob-prior	84.75** (0.66)	83.58** (0.65)	84.41*** (0.85)	83.90** (0.71)	11.63** (0.85)
		Ours w/o IAT	81.70*** (0.80)	80.61*** (0.88)	79.96*** (0.84)	80.25*** (0.85)	13.64*** (1.10)
		Ours w/ AT	84.23*** (0.54)	83.07*** (0.56)	83.52*** (0.62)	83.27*** (0.58)	11.25* (0.68)
		Ours (MC)	<b>85.59 (0.76)</b>	<b>84.42 (0.78)</b>	<b>85.54 (0.86)</b>	<b>84.85 (0.80)</b>	10.59 (1.04)
		Ours (LB)	85.49 (0.82)	84.32 (0.85)	85.45 (0.93)	84.76 (0.87)	<b>10.59 (1.03)</b>
New Attacks (ExplainDrive)	Ours w/o ME	BERT	65.08*** (0.59)	63.21*** (0.58)	63.63*** (0.60)	63.33*** (0.59)	30.67*** (0.76)
		DistilBERT	63.85*** (0.78)	62.76*** (0.79)	63.50*** (0.84)	62.71*** (0.80)	31.80*** (0.89)
		RoBERTa	69.23*** (0.50)	67.86*** (0.54)	68.74*** (0.59)	68.03*** (0.54)	26.17*** (0.60)
		XLNet	68.77*** (0.79)	67.40*** (0.81)	68.26*** (0.86)	67.56*** (0.82)	23.05*** (0.74)
		ALBERT	66.42*** (0.90)	63.96*** (0.96)	63.72*** (0.93)	63.82*** (0.94)	30.51*** (0.81)
	Ours w/o prior	Ours w/o prior	81.95** (1.01)	80.67** (1.06)	81.05*** (1.15)	80.84*** (1.09)	14.21* (1.30)
		Ours w/o data	82.38* (0.77)	81.20 (0.80)	81.10*** (0.94)	81.14** (0.87)	14.04* (0.86)
		Ours w/ FEL	81.69*** (0.68)	80.49*** (0.72)	80.22*** (0.80)	80.35*** (0.75)	14.80*** (0.84)
		Ours w/ CBW-D	81.91*** (0.94)	80.86** (1.06)	80.15*** (0.98)	80.46*** (1.00)	15.26*** (1.68)
		Ours w/ ES	81.84*** (0.95)	80.84** (1.06)	79.92*** (1.02)	80.31*** (1.03)	16.48*** (1.01)
		Ours w/ Prob-prior	82.26** (0.65)	81.07** (0.60)	81.43** (1.34)	81.16** (0.92)	14.57** (1.30)
		Ours w/o IAT	79.29*** (1.00)	78.04*** (1.07)	77.19*** (1.16)	77.55*** (1.12)	16.80*** (1.32)
		Ours w/ AT	82.47 (0.64)	81.23 (0.68)	81.51*** (0.71)	81.36** (0.69)	13.89* (0.85)
		Ours (MC)	<b>82.91 (0.66)</b>	<b>81.67 (0.67)</b>	<b>82.61 (0.63)</b>	<b>82.03 (0.66)</b>	<b>13.16 (1.12)</b>
		Ours (LB)	82.88 (0.66)	81.64 (0.68)	82.58 (0.58)	82.00 (0.65)	13.24 (1.13)

### 6.3.3 Results of Experiment 2.3 (Sensitivity Analysis in Defending Known and New Attacks)

Figure 2 shows results for defending known (a-1 to a-3) and new (b-1 to b-3) attacks. First, increasing the number of generated samples  $N$  improves after-attack performance (accuracy, recall, precision, F1) and reduces ASR, aligning with our theoretical analysis that more samples enhance performance. Second, more base detectors  $M$  also boost performance, consistent with our theoretical analysis that ensembling more base detectors enhances detection accuracy. Third, the variance term  $\sigma^2$  of the log-normal distribution does not significantly affect performance, validating our focus on the mean term (i.e.,  $\psi$ ) rather than on  $\sigma^2$ .

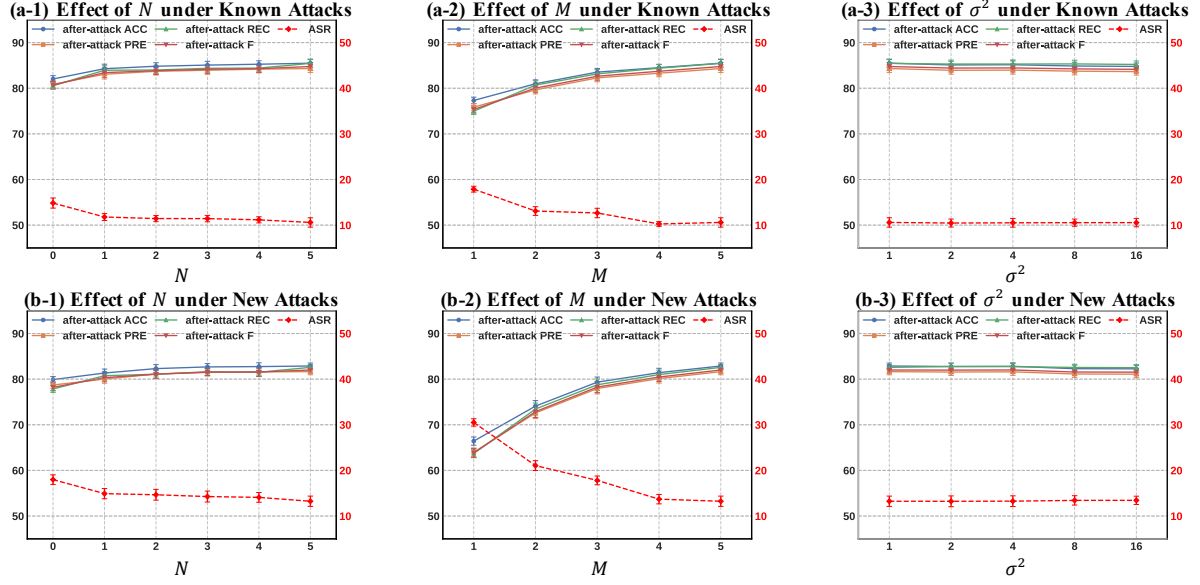


**Figure 2. Results of Sensitivity Analysis in Defending Known and New Attacks**

#### 6.4 Experiment 3: Accuracy Comparison without Updating Detectors

As noted earlier, defenders may choose to keep the base detector parameters fixed. In this case, only the weight assignor is updated. Under this setting, we compared our detector with the baselines (Experiment 3.1), conducted ablation analysis (Experiment 3.2) and sensitivity analysis (Experiment 3.3) across the three datasets. Results are in Appendix U. Conclusions align with those from Experiment 2. Meanwhile, we find that fixing the base detectors leads to inferior performance than updating them, which is expected because updating enhances base detectors and thereby enhances the robustness of our ARHOCD. Whether to update the base detectors depends on practitioners' judgment: if the attacks are severe enough, they should update base detectors' parameters; otherwise, they can reduce costs by updating only the weight assignor.

#### 6.5 Other Experiments

While this study focuses on a text-based task, some design components also apply to other data types, such as images (Appendix V). We tested an alternative defense strategy, i.e., adversarial sample detection, but found it less effective (Appendix W). In addition, we tested the computational efficiency of our detector and found it to be practical for real-world use (Appendix X). Finally, we conducted a case study to analyze how our detector performs on specific samples and across different attack types or topics (Appendix Y).

## 7. Discussion and Conclusion

### 7.1 Research Implication

Following the computational design science paradigm (Abbasi et al. 2024, Padmanabhan et al. 2022), we develop a harmful online content detector (ARHOCD) with a LLM-SGA framework and three design components, enhancing adversarial robustness in generalizability and accuracy. We contribute prescriptive knowledge to IS research in social media management, AI security, and computational design science.

### **7.1.1 Social Media Management in IS**

Effectively managing social media to harness its benefits while mitigating adverse effects is a central topic in IS. Among various adverse effects, harmful content has received growing attention. Most studies focus on developing IT artifacts to improve the detection accuracy under safe, non-adversarial conditions (Etudo and Yoon 2024, Wei et al. 2022). However, the accuracy often drops sharply under adversarial conditions, which are common given the adversarial nature of this task. This study proposes an adversarially robust detector, emphasizing robustness as a core design dimension in these studies. Moreover, robust detection is essential for studies analyzing the mechanisms or user behaviors related to harmful content. For instance, Wu et al. (2021) first use an ML-based detector to identify online harmful content (e.g., spam), then identify the users who posted it, and finally analyze the effects of different intervention strategies on mitigating such behavior. Hence, the validity of such studies largely depends on detection accuracy because a compromised detection may misidentify users and lead to a biased conclusion. By highlighting adversarial robustness and providing a principled approach to achieve it, this study also supports this line of research.

### **7.1.2 AI Security in IS**

With the rapid advancement of AI, AI security has become a critical topic in IS. Adversarial attacks pose major threats and have drawn growing attention. This study advances IS research on AI security by proposing a framework and design components that improve the generalizability and accuracy of defenses against such attacks. Our study also offers insights into other AI security issues, such as privacy. A classic privacy threat is the membership inference attack (MIA), which infers whether a specific sample was in the training set by exploiting a model's behavioral differences between training and unseen data (Shokri et al. 2017). Our study mitigates this threat in two ways. First, our weight assignment method can be adapted to assign higher weights to base models that better protect data privacy, making MIA more difficult. This

requires updating the prior from reflecting adversarial robustness to reflecting privacy-preserving ability. Second, our training set combines raw and generated samples, which protects privacy in two aspects: (1) the enlarged dataset reduces overfitting, making it harder for a model to memorize samples, and (2) even if an attacker infers that a sample was used in the training, they still cannot tell whether it is a raw or generated sample, preventing confirmation of any specific sample's presence in the original training set.

### 7.1.3 Design Science Research

This study contributes to the computational design science research paradigm, exemplifying it by tackling a practical problem (detecting harmful online content under adversarial conditions) and a situated implementation (ARHOCD) to illustrate how this paradigm solves real-world challenges. From this work, we derive two design principles. First, adversarial robustness is a critical consideration when designing new IT artifacts, especially for tasks that are inherently adversarial, such as harmful content detection (as in this study), phishing detection, and hacker asset identification. This does not mean every study must invent new robustness techniques; existing ones can often be adopted directly. In such cases, compatibility matters. Our ARHOCD, including the LLM-SGA framework and the three design components, is built on off-the-shelf models without requiring structure changes, making it a principled approach for future studies seeking to enhance adversarial robustness. We also release code at <https://github.com/YiLiuHFUT/ARHOCD> to further support future studies. Second, ensemble learning is critical in complex cases where a single model may fall short. Our ARHOCD assigns weights to predictions from different base detectors and across samples, leveraging their complementary strengths to achieve stronger performance. Meanwhile, as shown in our case study (Appendix Y), while the overall performance differences among base detectors are small, their performance can vary greatly on specific samples. This indicates that no single model is all-purpose to handle all cases (e.g., predicting diverse samples in our study), making ensemble learning necessary.

## 7.2 Practical Implication

This study offers important practical implications for users, social media platforms, and regulators. Users' exposure to harmful content can lead to psychological distress or misconceptions (Pennycook et al. 2020). Our study enhances the robustness of harmful content detection, helping users avoid such content

and thereby improving their online experience. For social media platforms, AI has been widely used to detect harmful content, but the security issues related to AI have emerged and attracted increasing attention. Our study enhances robustness against adversarial attacks and also mitigates other AI security issues such as MIA, as discussed above. Therefore, our work helps online platforms develop more trustworthy AI-based information systems for automatically detecting harmful content, creating a beneficial and wholesome public environment for society. For regulators, reliably harnessing AI to generate social good has become an urgent priority. This requires addressing AI security issues such as adversarial attacks, which have become central topics in AI governance (Zhang and Li 2020). This study provides a technical approach to counter adversarial attacks and also sheds light on other threats such as privacy inference attacks (e.g., MIA), offering valuable insights for developing more secure and trustworthy AI-based information systems.

### 7.3 Limitations and Future Directions

This study has several limitations that suggest directions for future research. First, in harmful content detection, we enhance adversarial robustness through technical solutions. While useful, technical measures alone may not be enough. Future work can explore complementary operational strategies to achieve more dependable management. Second, our focus is on adversarial attacks and does not consider other principles such as fairness and transparency. Integrating these principles is challenging due to potential trade-offs. For example, prior work has shown a tension between adversarial robustness and transparency (Chai et al. 2023). Future work can explore how to balance these principles to build more trustworthy AI-based information systems. Third, our case study shows that some adversarial attacks are harder to defend against than others. While our method demonstrates strong worst-case performance and generalizability across diverse attacks, certain attack types are more challenging than others. Future work can focus on these more complex attacks.

### Online Appendix

#### Appendix A: Representative Studies on Harmful Online Content Detection

**Table A1. Representative Studies on Harmful Online Content Detection**

Year	Authors	Detected Content	Methods	ML Models
------	---------	------------------	---------	-----------

2025	Huang et al.	Fake News	Utilize TF-IDF to extract features from news texts and input them into a BiGRU-enhanced Transformer model.	BiGRU, Transformer
2025	Hashmi et al.	Hate Speech	Enhance self-learning with Barlow Twins, and use lexical and semantic augmentation to enhance text representation.	Nor-BERT, NB-BERT, etc.
2024	Vishwamitra et al.	Hate Speech	Use automatic prompt generation and updating to capture new hate terms, and leverage the Chain-of-Thought prompting to detect new hate speech.	GPT-4
2024	Ayetiran and Özgöbek	Hate Speech Fake News	Unify all data modalities into text form, followed by a cross-attention mechanism to fuse the features.	CNN, LSTM
2024	Etudo et al.	Extremist Rhetoric	Use deep learning to extract entities and relations from text, and construct a structured ontology of extremist ideologies.	ELMo, LSTM, CNN, ALBERT
2024	Pereira et al.	Sexual Exploitation	Detection based solely on file metadata, i.e., the file path information (textual data about the file's path and name)	CNN, LSTM, BERT, LR, NB, etc.
2023	Yin et al.	Hate Speech	Integrate annotator characteristics and label text to enrich textual representations.	BERT
2023	Kim et al.	Hate Speech	Leverage machine-generated toxic text for contrastive learning-based pre-training.	BERT
2023	Lee and Ram	Misinformation	Calculate semantic consistency between claims (tweets) and evidence (news texts) based on Toulmin's model.	LSTM, BERT, RoBERTa, etc.
2022	Oswald et al.	Spam	Capture both semantic and textual features of the text messages based on pre-defined intention labels.	BERT, DistilBERT, RoBERTa, SpanBERT
2022	Wei et al.	Fake News	Combine crowd and machine judgment from news and crowd intelligence with a Bayesian aggregation model.	CNN, LSTM, BERT, SVM

## Appendix B: The Proof of Inequality 3

First, by Chebyshev's inequality, we have

$$P\left(|\bar{p} - \mu_0| \geq \frac{k\sigma_0}{\sqrt{N+1}}\right) \leq \frac{1}{k^2} \quad (\text{A. 1})$$

where  $k$  is any positive constant. We replace  $t$  with  $\frac{k\sigma_0}{\sqrt{N+1}}$ , and thus we have  $k = \frac{t\sqrt{N+1}}{\sigma_0}$ . Then, we have

$$P(|\bar{p} - \mu_0| \geq t) \leq \frac{1}{k^2} = \frac{\sigma_0^2}{(N+1)t^2} \quad (\text{A. 2})$$

This inequality holds as long as  $t$  is positive.

Next, we analyze the cases when the ground truth label is  $y = 1$  or  $y = 0$ .

**Case 1** (Ground truth label  $y = 1$ ):

In this case,  $P(\hat{y} = y)$  is equivalent to  $P(\bar{p} > \varepsilon)$ . Meanwhile, since  $p$  denotes the probability of being label 1, the expected probability of a correct prediction becomes  $\mu_0$ . Note that:

$$P(\bar{p} \leq \varepsilon) = P(\bar{p} \leq \mu_0 - (\mu_0 - \varepsilon)) \quad (\text{A. 3})$$

Let  $\delta = \mu_0 - \varepsilon$ . Then, we have

$$P(\bar{p} \leq \varepsilon) = P(\bar{p} \leq \mu_0 - \delta) \quad (\text{A.4})$$

Recall that the detector performs better than random guessing, where the output is uniformly distributed over  $[0,1]$  and labeled as 1 if it exceeds  $\varepsilon$  and 0 otherwise. Hence, the expected probability of a correct prediction satisfies  $\mu_0 > \varepsilon$  in Case 1. Consequently, we have  $\delta > 0$  and  $\delta$  can be written as  $\delta = |\mu_0 - \varepsilon|$ .

Note that if  $\bar{p} \leq \mu_0 - \delta$ , then we have  $\bar{p} - \mu_0 \leq -\delta$ . Since  $\delta > 0$ , we have  $|\bar{p} - \mu_0| \geq \delta$ . In other words, if  $\bar{p} \leq \mu_0 - \delta$ , we have  $|\bar{p} - \mu_0| \geq \delta$ . Hence, we have

$$P(\bar{p} \leq \mu_0 - \delta) \leq P(|\bar{p} - \mu_0| \geq \delta) \quad (\text{A.5})$$

Since  $\delta > 0$ , according to Chebyshev's inequality, we have

$$P(|\bar{p} - \mu_0| \geq \delta) \leq \frac{\sigma_0^2}{(N+1)\delta^2} \quad (\text{A.6})$$

Hence, we have

$$P(\bar{p} \leq \varepsilon) = P(\bar{p} \leq \mu_0 - \delta) \leq P(|\bar{p} - \mu_0| \geq \delta) \leq \frac{\sigma_0^2}{(N+1)\delta^2} \quad (\text{A.7})$$

Therefore,

$$P(\hat{y} = y) = P(\bar{p} > \varepsilon) \geq 1 - \frac{\sigma_0^2}{(N+1)\delta^2} \quad (\text{A.8})$$

**Case 2** (Ground truth label  $y = 0$ ):

In this case,  $P(\hat{y} = y)$  is equivalent to  $P(\bar{p} \leq \varepsilon)$ . Since the detector performs better than random guessing, the expected probability of a correct prediction satisfies  $\mu_0 < \varepsilon$ .

Note that:

$$P(\bar{p} > \varepsilon) \leq P(\bar{p} \geq \varepsilon) = P(1 - \bar{p} \leq 1 - \varepsilon) = P(1 - \bar{p} \leq 1 - \mu_0 - (\varepsilon - \mu_0)) \quad (\text{A.9})$$

Let  $\delta = \varepsilon - \mu_0$ . Since  $\mu_0 < \varepsilon$ , we have  $\delta > 0$ . Hence,  $\delta$  can be written as  $\delta = |\varepsilon - \mu_0|$ . Meanwhile, we have

$$P(\bar{p} > \varepsilon) \leq P(1 - \bar{p} \leq 1 - \mu_0 - \delta) \quad (\text{A.10})$$

Note that if  $1 - \bar{p} \leq 1 - \mu_0 - \delta$ , then we have  $(1 - \bar{p}) - (1 - \mu_0) \leq -\delta$ . Since  $\delta > 0$ , we have

$|(1 - \bar{p}) - (1 - \mu_0)| \geq \delta$ . In other words, if  $1 - \bar{p} \leq 1 - \mu_0 - \delta$ , we have  $|(1 - \bar{p}) - (1 - \mu_0)| \geq \delta$ .

Hence, we have

$$P(1 - \bar{p} \leq 1 - \mu_0 - \delta) \leq P(|(1 - \bar{p}) - (1 - \mu_0)| \geq \delta) = P(|\bar{p} - \mu_0| \geq \delta) \quad (\text{A.11})$$

Since  $\delta > 0$ , according to Chebyshev's inequality, we have

$$P(|\bar{p} - \mu_0| \geq \delta) \leq \frac{\sigma_0^2}{(N+1)\delta^2} \quad (\text{A.12})$$

Hence, we have

$$P(\bar{p} > \varepsilon) \leq P(1 - \bar{p} \leq 1 - \mu_0 - \delta) \leq P(|\bar{p} - \mu_0| \geq \delta) \leq \frac{\sigma_0^2}{(N+1)\delta^2} \quad (\text{A.13})$$

Therefore,

$$P(\hat{y} = y) = P(\bar{p} \leq \varepsilon) \geq 1 - \frac{\sigma_0^2}{(N+1)\delta^2} \quad (\text{A.14})$$

To sum up, in both cases, with  $\delta = |\mu_0 - \varepsilon|$ , we have proved  $P(\hat{y} = y) \geq 1 - \frac{\sigma_0^2}{(N+1)\delta^2}$ .

## Appendix C: The Proof of Inequality 5

Since the average predictive probability of the base detector  $f_m$  is  $\bar{p}_m = \frac{1}{N+1} \sum_{n=0}^N p_{m,n}$ , it is also a

random variable. The expectation of  $\bar{p}_m$  is  $\mu_m$ , and its variance is  $\frac{\sigma_m^2}{N+1}$ . Since  $\bar{p} = \frac{1}{M(N+1)} \sum_{m=1}^M \sum_{n=0}^N p_{m,n}$ , it can be further written as

$$\bar{p} = \frac{1}{M(N+1)} \sum_{m=1}^M \sum_{n=0}^N p_{m,n} = \frac{1}{M} \sum_{m=1}^M \frac{1}{N+1} \sum_{n=0}^N p_{m,n} = \frac{1}{M} \sum_{m=1}^M \bar{p}_m \quad (\text{A.15})$$

Hence, the expectation of  $\bar{p}$  is  $\mu_{\bar{p}} = \frac{1}{M} \sum_{m=1}^M \mu_m$ . The variance of  $\bar{p}$  is  $\sigma_{\bar{p}}^2 = \frac{1}{M^2} \sum_{m=1}^M \frac{\sigma_m^2}{N+1} = \frac{1}{(N+1)M^2} \sum_{m=1}^M \sigma_m^2$ . We analyze the cases when the ground truth label is  $y = 1$  or  $y = 0$ .

**Case 1** (Ground truth label  $y = 1$ ):

In this case,  $P(\hat{y} = y)$  is equivalent to  $P(\bar{p} > \varepsilon)$ . Note that:

$$P(\bar{p} \leq \varepsilon) = P\left(\bar{p} \leq \mu_{\bar{p}} - (\mu_{\bar{p}} - \varepsilon)\right) \quad (\text{A.16})$$

Let  $\delta = \mu_{\bar{p}} - \varepsilon$ . Since we assume that each base detector  $f_m$  performs better than random guessing, the average probability of a correct prediction satisfies  $\mu_m > \varepsilon$  in Case 1. Since  $\mu_{\bar{p}} = \frac{1}{M} \sum_{m=1}^M \mu_m$  we have  $\mu_{\bar{p}} > \varepsilon$ . Hence, we have  $\delta > 0$  and  $\delta$  can be written as  $\delta = |\mu_{\bar{p}} - \varepsilon|$ . Hence, we have

$$P(\bar{p} \leq \varepsilon) = P(\bar{p} \leq \mu_{\bar{p}} - \delta) \quad (\text{A.17})$$

Note that if  $\bar{p} \leq \mu_{\bar{p}} - \delta$ , then we have  $\bar{p} - \mu_{\bar{p}} \leq -\delta$ . Since  $\delta > 0$ , we have  $|\bar{p} - \mu_{\bar{p}}| \geq \delta$ . In other words, if  $\bar{p} \leq \mu_{\bar{p}} - \delta$ , we have  $|\bar{p} - \mu_{\bar{p}}| \geq \delta$ . Hence, we have

$$P(\bar{p} \leq \mu_{\bar{p}} - \delta) \leq P(|\bar{p} - \mu_{\bar{p}}| \geq \delta) \quad (\text{A.18})$$

Since  $\delta > 0$ , according to Chebyshev's inequality, we have

$$P(|\bar{p} - \mu_{\bar{p}}| \geq \delta) \leq \frac{\sigma_{\bar{p}}^2}{\delta^2} = \frac{1}{(N+1)M^2\delta^2} \sum_{m=1}^M \sigma_m^2 \quad (\text{A.19})$$

Hence, we have

$$\begin{aligned} P(\bar{p} \leq \varepsilon) &= P(\bar{p} \leq \mu_{\bar{p}} - \delta) \leq P(|\bar{p} - \mu_{\bar{p}}| \geq \delta) \\ &\leq \frac{1}{(N+1)M^2\delta^2} \sum_{m=1}^M \sigma_m^2 \end{aligned} \quad (\text{A.20})$$

Therefore,

$$P(\hat{y} = y) = P(\bar{p} > \varepsilon) \geq 1 - \frac{1}{(N+1)M^2\delta^2} \sum_{m=1}^M \sigma_m^2 \quad (\text{A.21})$$

**Case 2** (Ground truth label  $y = 0$ ):

In this case,  $P(\hat{y} = y)$  is equivalent to  $P(\bar{p} \leq \varepsilon)$ . Since each base detector  $f_m$  performs better than random guessing, the average probability of a correct prediction satisfies  $\mu_m < \varepsilon$  in Case 2. Hence, we have

$$\frac{1}{M} \sum_{m=1}^M \mu_m = \mu_{\bar{p}} < \varepsilon,$$

Note that:

$$P(\bar{p} > \varepsilon) \leq P(\bar{p} \geq \varepsilon) = P(1 - \bar{p} \leq 1 - \varepsilon) = P(1 - \bar{p} \leq 1 - \mu_{\bar{p}} - (\varepsilon - \mu_{\bar{p}})) \quad (\text{A.22})$$

Let  $\delta = \varepsilon - \mu_{\bar{p}}$ . Since  $\mu_{\bar{p}} < \varepsilon$ , we have  $\delta > 0$ . Hence,  $\delta$  can be written as  $\delta = |\varepsilon - \mu_{\bar{p}}|$ . Meanwhile,

we have

$$P(\bar{p} > \varepsilon) \leq P(1 - \bar{p} \leq 1 - \mu_{\bar{p}} - \delta) \quad (\text{A.23})$$

Note that if  $1 - \bar{p} \leq 1 - \mu_{\bar{p}} - \delta$ , then we have  $(1 - \bar{p}) - (1 - \mu_{\bar{p}}) \leq -\delta$ . Since  $\delta > 0$ , we have

$|(1 - \bar{p}) - (1 - \mu_{\bar{p}})| \geq \delta$ . In other words, if  $1 - \bar{p} \leq 1 - \mu_{\bar{p}} - \delta$ , we have  $|(1 - \bar{p}) - (1 - \mu_{\bar{p}})| \geq \delta$ .

Hence, we have

$$P(1 - \bar{p} \leq 1 - \mu_{\bar{p}} - \delta) \leq P(|(1 - \bar{p}) - (1 - \mu_{\bar{p}})| \geq \delta) = P(|\bar{p} - \mu_{\bar{p}}| \geq \delta) \quad (\text{A.24})$$

Since  $\delta > 0$ , according to Chebyshev's inequality, we have

$$P(|\bar{p} - \mu_{\bar{p}}| \geq \delta) \leq \frac{\sigma_{\bar{p}}^2}{\delta^2} = \frac{1}{(N+1)M^2\delta^2} \sum_{m=1}^M \sigma_m^2 \quad (\text{A.25})$$

Hence, we have

$$P(\bar{p} > \varepsilon) \leq P(1 - \bar{p} \leq 1 - \mu_{\bar{p}} - \delta) \leq P(|\bar{p} - \mu_{\bar{p}}| \geq \delta) \leq \frac{1}{(N+1)M^2\delta^2} \sum_{m=1}^M \sigma_m^2 \quad (\text{A.26})$$

Therefore,

$$P(\hat{y} = y) = P(\bar{p} \leq \varepsilon) \geq 1 - \frac{1}{(N+1)M^2\delta^2} \sum_{m=1}^M \sigma_m^2 \quad (\text{A.27})$$

To sum up, in both cases, with  $\delta = |\mu_{\bar{p}} - \varepsilon| = \left| \frac{1}{M} \sum_{m=1}^M \mu_m - \varepsilon \right|$ , we have proved  $P(\hat{y} = y) \geq 1 - \frac{1}{(N+1)M^2\delta^2} \sum_{m=1}^M \sigma_m^2$ .

## Appendix D: Factorization of $\tilde{w}_{m,n}$

We show that the intermediate weight  $\tilde{w}_{m,n}$  can be factorized as:

$$\tilde{w}_{m,n} = \tilde{w}_m \tilde{w}_n \quad (\text{A.28})$$

where  $\tilde{w}_m = S \cdot w_m$  and  $\tilde{w}_n = T \cdot w_n$ , with  $S = \sum_{m=1}^M \tilde{w}_m$  and  $T = \sum_{n=0}^N \tilde{w}_n$  being constants for  $\tilde{w}_m$  and  $\tilde{w}_n$ , respectively. We show such factorization of  $\tilde{w}_{m,n}$  can satisfy the factorization of  $w_{m,n}$ .

With the factorization in Equation (A.28), the overall weight for detector ( $w_m$ ) and the overall weight for sample ( $w_n$ ), can be expressed as,

$$w_m = \frac{\tilde{w}_m}{S} \quad (\text{A.29})$$

$$w_n = \frac{\tilde{w}_n}{T} \quad (\text{A.30})$$

Hence, the normalized weight  $w_{m,n}$  can be expressed as,

$$w_{m,n} = \frac{\tilde{w}_{m,n}}{\sum_{m=1}^M \sum_{n=0}^N \tilde{w}_{m,n}} = \frac{\tilde{w}_m \tilde{w}_n}{\sum_{m=1}^M \sum_{n=0}^N \tilde{w}_m \tilde{w}_n} = \frac{\tilde{w}_m \tilde{w}_n}{\sum_{m=1}^M \tilde{w}_m \sum_{n=0}^N \tilde{w}_n} = \frac{\tilde{w}_m \tilde{w}_n}{S \cdot T} = w_m w_n \quad (\text{A.31})$$

Hence, the factorization of  $w_{m,n}$  can be satisfied, i.e.,  $w_{m,n} = w_m w_n$ .

Hence, the factorization of  $\tilde{w}_{m,n}$  into  $\tilde{w}_m = S \cdot w_m$ ,  $\tilde{w}_n = T \cdot w_n$  satisfies  $w_{m,n} = w_m w_n$ , verifying the rationality of such factorization. Hence, if we obtain the intermediate weights  $\tilde{w}_m$  and  $\tilde{w}_n$ , we can determine  $\tilde{w}_{m,n}$ , and then determine  $w_{m,n}$ .

## Appendix E: Proof of Theorem 1

*Proof.*

First, for  $(p_{m,n} - y)^2$ , we have:

$$(p_{m,n} - y)^2 = (p_{m,n} - \bar{p}_n + \bar{p}_n - y)^2 = (p_{m,n} - \bar{p}_n)^2 + 2(p_{m,n} - \bar{p}_n)(\bar{p}_n - y) + (\bar{p}_n - y)^2 \quad (\text{A.32})$$

The overall Brier Score  $e_n$  can be derived as:

$$\begin{aligned} e_n &= \frac{1}{M} \sum_{m=1}^M (p_{m,n} - y)^2 = \frac{1}{M} \sum_{m=1}^M \left[ (p_{m,n} - \bar{p}_n)^2 + 2(p_{m,n} - \bar{p}_n)(\bar{p}_n - y) + (\bar{p}_n - y)^2 \right] \\ &= \frac{1}{M} \sum_{m=1}^M (p_{m,n} - \bar{p}_n)^2 + \frac{1}{M} \sum_{m=1}^M 2(p_{m,n} - \bar{p}_n)(\bar{p}_n - y) + \frac{1}{M} \sum_{m=1}^M (\bar{p}_n - y)^2 \\ &= \frac{1}{M} \sum_{m=1}^M (p_{m,n} - \bar{p}_n)^2 + \frac{2(\bar{p}_n - y)}{M} \sum_{m=1}^M (p_{m,n} - \bar{p}_n) + (\bar{p}_n - y)^2 \end{aligned} \quad (\text{A.33})$$

Since  $\bar{p}_n = \frac{1}{M} \sum_{m=1}^M p_{m,n}$ , we have  $\sum_{m=1}^M (p_{m,n} - \bar{p}_n) = 0$ . Recall that  $\sigma_n^2 = \frac{1}{M} \sum_{m=1}^M (p_{m,n} - \bar{p}_n)^2$ .

Hence, we can decompose the overall Brier Score  $e_n$  as:

$$e_n = \sigma_n^2 + (\bar{p}_n - y)^2 \quad (\text{A.34})$$

Since the  $e_n$ ,  $\sigma_n^2$  and  $\bar{p}_n$  in Equation (A.34) are computed based on a number of  $M$  base detectors, different base detectors may bring about different values. Hence, they are random variables. We further

take the expectation on both sides, we obtain:

$$\mathbb{E}[e_n] = \mathbb{E}[\sigma_n^2] + \mathbb{E}[(\bar{p}_n - y)^2] \quad (\text{A.35})$$

Similarly, by expanding  $(p_{m,n} - y)^2 = (p_{m,n} - \bar{p}_m + \bar{p}_m - y)^2$ , we have  $e_m = \sigma_m^2 + (\bar{p}_m - y)^2$ ,

and therefore:

$$\mathbb{E}[e_m] = \mathbb{E}[\sigma_m^2] + \mathbb{E}[(\bar{p}_m - y)^2] \quad (\text{A.36})$$

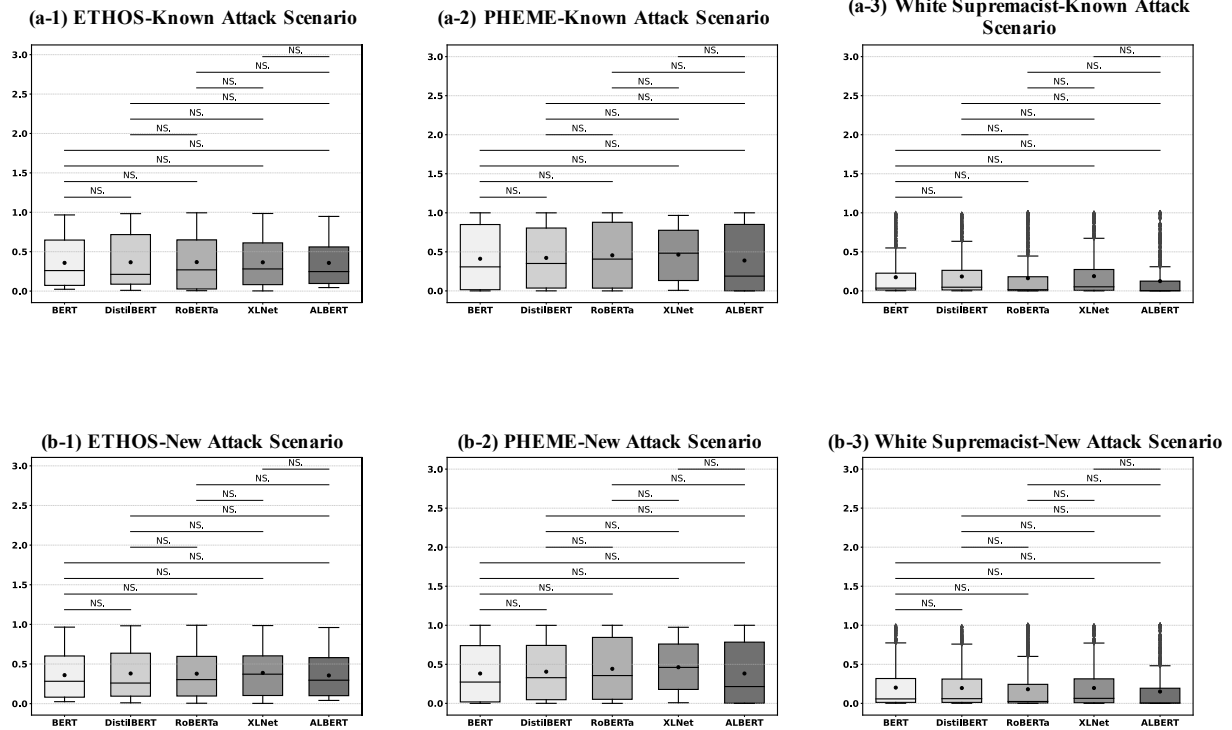
## Appendix F: Empirically Comparing $\mathbb{E}[\bar{p}_m]$ among Base Detectors

As the same experiment setting in Section 5.3 of the manuscript, we employed 5 base detectors: BERT, DistilBERT, RoBERTa, XLNet, and ALBERT. We aimed to examine the identity of the expected prediction probabilities ( $\mathbb{E}[\bar{p}_m]$ ) across all base detectors on datasets  $D_{\text{DTT}}^{\text{test}}$  and  $D_{\text{E}}^{\text{test}}$  —corresponding to the known and new attack scenarios, respectively.

For each sample in  $D_{\text{DTT}}^{\text{test}}$  or in  $D_{\text{E}}^{\text{test}}$ , we generated 5 samples  $(\hat{x}_1, \hat{x}_2, \dots, \hat{x}_5)$  with the same meaning and calculated  $\bar{p}_m = \frac{1}{6} \sum_{n=0}^5 p_{m,n}$ ,  $(m = 1, \dots, 5)$  for each base detector  $f_m$   $(m = 1, \dots, 5)$ . This computation yielded a vector of averaged predictive probabilities for each base detector, denoted as  $\mathbf{v}_1, \mathbf{v}_2, \dots, \mathbf{v}_5$ . The length of each vector  $\mathbf{v}_m$   $(m = 1, \dots, 5)$  is equal to the number of test samples. Finally, we applied a one-way repeated-measures ANOVA, treating base detectors as the within-subject factor and test samples as subjects. This choice is motivated by the fact that each test sample is evaluated by all base detectors, resulting in repeated measurements on the same subjects. The ANOVA examined whether different base detectors produce statistically different predictive probabilities. When the ANOVA indicated a significant overall effect, we conducted post-hoc pairwise comparisons using paired t-tests on the per-sample prediction differences. To control for multiple comparisons, Bonferroni correction was applied. Statistical significance was determined based on the corrected p-values.

Figure F1 shows the results of corrected p-values under the known attack (a-1 to a-3) and new attack (b-1 to b-3) scenarios. In the figure, the box represents the distribution of the predictions (i.e.,  $\mathbf{v}_m$   $(m = 1, \dots, 5)$ ), where the top and bottom edges of the box represent the upper and lower quartiles, the central horizontal line indicates the median, and the black dots represent the mean. The vertical error bars reflect

the variability within each detector. The horizontal bars above the boxes denote the pairwise statistical comparisons across detectors. Labels “NS.” above these bars denote non-significant differences, while labels with significance markers (e.g., \*) indicate statistically significant differences. For instance, in figure (a-1) for the ETHOS dataset under the known attack scenario, the upper and lower quartiles, median and mean values of BERT and DistilBERT are very close, and the significance test yields  $p>0.05$ , indicating a non-significant difference (NS.) between them. Overall, across the three datasets, there are no statistically significant differences in the expected prediction probabilities among the base detectors, verifying the validity of our assumption.



Note: NS. means non-significant differences ( $p > 0.05$ ).

**Figure F1. Results of the Paired T-tests on  $E[\bar{p}_m]$  across All Detectors**

#### Appendix G: The Derivation of the Mean and Variance of $\tilde{w}_{m,n}$

As the unnormalized weight can be factorized as  $\tilde{w}_{m,n} = \tilde{w}_m \tilde{w}_n$ , taking the logarithm yields,

$$\ln \tilde{w}_{m,n} = \ln \tilde{w}_m + \ln \tilde{w}_n \quad (\text{A.37})$$

Note that  $\tilde{w}_m$  and  $\tilde{w}_n$  follow two log-normal distributions as defined in Equation (9) in the manuscript, i.e.,  $p(\tilde{w}_m) = \text{LogNormal}(\psi_m, \sigma_{\text{dt}}^2)$ ;  $p(\tilde{w}_n) = \text{LogNormal}(\psi_n, \sigma_{\text{sp}}^2)$ .

Hence, we have,

$$\ln \tilde{w}_m \sim \mathcal{N}(\psi_m, \sigma_{\text{dt}}^2); \ln \tilde{w}_n \sim \mathcal{N}(\psi_n, \sigma_{\text{sp}}^2) \quad (\text{A.38})$$

As  $\ln \tilde{w}_m$  and  $\ln \tilde{w}_n$  are Gaussian random variables, the sum of  $\ln \tilde{w}_m$  and  $\ln \tilde{w}_n$  is also normally distributed, i.e.,

$$\ln \tilde{w}_{m,n} = \ln \tilde{w}_m + \ln \tilde{w}_n \sim \mathcal{N}(\psi_m + \psi_n, \sigma_{\text{dt}}^2 + \sigma_{\text{sp}}^2) \quad (\text{A.39})$$

Therefore,  $\tilde{w}_{m,n}$  also follows a log-normal distribution:

$$p(\tilde{w}_{m,n}) = \text{LogNormal}(\psi_m + \psi_n, \sigma_{\text{dt}}^2 + \sigma_{\text{sp}}^2) \quad (\text{A.40})$$

To sum up, for  $p(\tilde{w}_{m,n})$  in Equation (8) of the manuscript, its  $\psi_{m,n}$  and  $\sigma^2$  can be expressed as  $\psi_{m,n} = \psi_m + \psi_n$ ,  $\sigma^2 = \sigma_{\text{dt}}^2 + \sigma_{\text{sp}}^2$ .

## Appendix H: The Technical Details of the Attention( $\cdot$ ) and MLP( $\cdot$ ) in Our Inference Network

We first nonlinearly transform  $\mathbf{p}_m$  and  $\mathbf{p}_n$  to obtain their latent representations:

$$\mathbf{h}_m = \mathbf{p}_m \mathbf{W}^1 + \mathbf{b}^1, \quad \mathbf{h}_n = \mathbf{p}_n \mathbf{W}^2 + \mathbf{b}^2 \quad (\text{A.41})$$

where  $\mathbf{W}^1 \in \mathbb{R}^{(N+1)*d}$ ,  $\mathbf{W}^2 \in \mathbb{R}^{M*d}$ ,  $\mathbf{b}^1 \in \mathbb{R}^d$ ,  $\mathbf{b}^2 \in \mathbb{R}^d$  are learnable parameters,  $d$  is the dimension of the hidden representations.  $\mathbf{h}_m \in \mathbb{R}^d$  and  $\mathbf{h}_n \in \mathbb{R}^d$  represent the nonlinearly transformed representations. Then, we apply self-attention for  $\mathbf{h}_m$  and  $\mathbf{h}_n$  respectively to model the interactions among their elements. Formally,

$$\mathbf{Q}^{\text{dt}} = \mathbf{h}_m \mathbf{W}_Q^{\text{dt}}, \mathbf{K}^{\text{dt}} = \mathbf{h}_m \mathbf{W}_K^{\text{dt}}, \mathbf{V}^{\text{dt}} = \mathbf{h}_m \mathbf{W}_V^{\text{dt}} \quad (\text{A.42})$$

$$\mathbf{Q}^{\text{sp}} = \mathbf{h}_n \mathbf{W}_Q^{\text{sp}}, \mathbf{K}^{\text{sp}} = \mathbf{h}_n \mathbf{W}_K^{\text{sp}}, \mathbf{V}^{\text{sp}} = \mathbf{h}_n \mathbf{W}_V^{\text{sp}} \quad (\text{A.43})$$

$$\mathbf{z}_m = \text{softmax} \left( \frac{\mathbf{Q}^{\text{dt}} (\mathbf{K}^{\text{dt}})^T}{\sqrt{d}} \right) \mathbf{V}^{\text{dt}}, \mathbf{z}_n = \text{softmax} \left( \frac{\mathbf{Q}^{\text{sp}} (\mathbf{K}^{\text{sp}})^T}{\sqrt{d}} \right) \mathbf{V}^{\text{sp}} \quad (\text{A.44})$$

where  $\mathbf{W}_Q^{\text{dt}}, \mathbf{W}_K^{\text{dt}}, \mathbf{W}_V^{\text{dt}}, \mathbf{W}_Q^{\text{sp}}, \mathbf{W}_K^{\text{sp}}, \mathbf{W}_V^{\text{sp}} \in \mathbb{R}^{d*d}$  are learnable parameters. In this way, we obtain the representation  $\mathbf{z}_m$  and  $\mathbf{z}_n$ , which capture the relationships of the predictions of base detector  $f_m$  and the

relationships of the predictions of sample  $\hat{x}_n$ , respectively.

Then, we concatenate  $\mathbf{z}_m$  and  $\mathbf{z}_n$  and feed them into a MLP, i.e.,

$$\varphi_{m,n}^{\text{post}} = \text{MLP}(\mathbf{z}_m; \mathbf{z}_n) = [\mathbf{z}_m; \mathbf{z}_n] \mathbf{W}^3 + b^3 \quad (\text{A.45})$$

where  $\mathbf{W}^3 \in \mathbb{R}^{2d*1}$  and  $b^3 \in \mathbb{R}$  are learnable parameters.

### Appendix I: The Proof that the Objective Computed is a Lower Bound of $\mathcal{L}$

The proof procedure is standard in variational inference (Bishop and Nasrabadi 2006, Blei et al. 2017). Here, we demonstrate the proof in our case for interested readers.

*Proof.*

First, we compute the KL divergence between variational distribution  $q_{\phi}(\widetilde{\mathbf{W}})$  and the true posterior distribution  $p(\widetilde{\mathbf{W}}|\mathbf{P}, y)$  as

$$\begin{aligned} \text{KL}\left(q_{\phi}(\widetilde{\mathbf{W}}) \parallel p(\widetilde{\mathbf{W}}|\mathbf{P}, y)\right) &= \int q_{\phi}(\widetilde{\mathbf{W}}) \log \frac{q_{\phi}(\widetilde{\mathbf{W}})}{p(\widetilde{\mathbf{W}}|\mathbf{P}, y)} d\widetilde{\mathbf{W}} \\ &= \int q_{\phi}(\widetilde{\mathbf{W}}) [\log q_{\phi}(\widetilde{\mathbf{W}}) - \log p(\widetilde{\mathbf{W}}|\mathbf{P}, y)] d\widetilde{\mathbf{W}} \\ &= \int q_{\phi}(\widetilde{\mathbf{W}}) \log q_{\phi}(\widetilde{\mathbf{W}}) d\widetilde{\mathbf{W}} - \int q_{\phi}(\widetilde{\mathbf{W}}) \log p(\widetilde{\mathbf{W}}|\mathbf{P}, y) d\widetilde{\mathbf{W}} \\ &= \mathbb{E}_{q_{\phi}(\widetilde{\mathbf{W}})} \log q_{\phi}(\widetilde{\mathbf{W}}) - \mathbb{E}_{q_{\phi}(\widetilde{\mathbf{W}})} \log p(\widetilde{\mathbf{W}}|\mathbf{P}, y) \\ &= \mathbb{E}_{q_{\phi}(\widetilde{\mathbf{W}})} \log q_{\phi}(\widetilde{\mathbf{W}}) - \mathbb{E}_{q_{\phi}(\widetilde{\mathbf{W}})} \log \left( \frac{p(\widetilde{\mathbf{W}}, y|\mathbf{P})}{p(y|\mathbf{P})} \right) \\ &= \mathbb{E}_{q_{\phi}(\widetilde{\mathbf{W}})} \log q_{\phi}(\widetilde{\mathbf{W}}) - \mathbb{E}_{q_{\phi}(\widetilde{\mathbf{W}})} \log p(\widetilde{\mathbf{W}}, y|\mathbf{P}) + \mathbb{E}_{q_{\phi}(\widetilde{\mathbf{W}})} \log p(y|\mathbf{P}) \\ &= \mathbb{E}_{q_{\phi}(\widetilde{\mathbf{W}})} \log q_{\phi}(\widetilde{\mathbf{W}}) - \mathbb{E}_{q_{\phi}(\widetilde{\mathbf{W}})} \log p(\widetilde{\mathbf{W}}, y|\mathbf{P}) + \log p(y|\mathbf{P}) \end{aligned}$$

Since  $\text{KL}\left(q_{\phi}(\widetilde{\mathbf{W}}) \parallel p(\widetilde{\mathbf{W}}|\mathbf{P}, y)\right)$  is non-negative, we have

$$\mathbb{E}_{q_{\phi}(\widetilde{\mathbf{W}})} \log q_{\phi}(\widetilde{\mathbf{W}}) - \mathbb{E}_{q_{\phi}(\widetilde{\mathbf{W}})} \log p(\widetilde{\mathbf{W}}, y|\mathbf{P}) + \log p(y|\mathbf{P}) \geq 0 \quad (\text{A.46})$$

Hence, we have,

$$\begin{aligned}\log p(y|\mathbf{P}) &\geq \mathbb{E}_{q_\phi(\tilde{\mathbf{W}})} \log p(\tilde{\mathbf{W}}, y|\mathbf{P}) - \mathbb{E}_{q_\phi(\tilde{\mathbf{W}})} \log q_\phi(\tilde{\mathbf{W}}) \\ &= \mathbb{E}_{q_\phi(\tilde{\mathbf{W}})} \log [p(y|\tilde{\mathbf{W}}, \mathbf{P}) p(\tilde{\mathbf{W}}|\mathbf{P})] - \mathbb{E}_{q_\phi(\tilde{\mathbf{W}})} \log q_\phi(\tilde{\mathbf{W}})\end{aligned}\quad (\text{A.47})$$

where  $p(\tilde{\mathbf{W}}|\mathbf{P})$  is the prior distribution for  $\tilde{\mathbf{W}}$ , simplified as  $p(\tilde{\mathbf{W}})$ . Hence, we have,

$$\begin{aligned}\log p(y|\mathbf{P}) &\geq \mathbb{E}_{q_\phi(\tilde{\mathbf{W}})} \log [p(y|\tilde{\mathbf{W}}, \mathbf{P}) p(\tilde{\mathbf{W}})] - \mathbb{E}_{q_\phi(\tilde{\mathbf{W}})} \log q_\phi(\tilde{\mathbf{W}}) \\ &= \mathbb{E}_{q_\phi(\tilde{\mathbf{W}})} \log p(y|\tilde{\mathbf{W}}, \mathbf{P}) + \mathbb{E}_{q_\phi(\tilde{\mathbf{W}})} \log p(\tilde{\mathbf{W}}) - \mathbb{E}_{q_\phi(\tilde{\mathbf{W}})} \log q_\phi(\tilde{\mathbf{W}}) \\ &= \mathbb{E}_{q_\phi(\tilde{\mathbf{W}})} \log p(y|\tilde{\mathbf{W}}, \mathbf{P}) + \mathbb{E}_{q_\phi(\tilde{\mathbf{W}})} [\log p(\tilde{\mathbf{W}}) - \log q_\phi(\tilde{\mathbf{W}})] \\ &= \mathbb{E}_{q_\phi(\tilde{\mathbf{W}})} \log p(y|\tilde{\mathbf{W}}, \mathbf{P}) + \int q_\phi(\tilde{\mathbf{W}}) \log \frac{p(\tilde{\mathbf{W}})}{q_\phi(\tilde{\mathbf{W}})} d\tilde{\mathbf{W}} \\ &= \mathbb{E}_{q_\phi(\tilde{\mathbf{W}})} \log p(y|\tilde{\mathbf{W}}, \mathbf{P}) - \text{KL} (q_\phi(\tilde{\mathbf{W}}) || p(\tilde{\mathbf{W}}))\end{aligned}$$

Under the classic mean-field assumption (Bishop et al. 1997, Cohn et al. 2010), each  $\tilde{w}_{m,n}$  in  $\tilde{\mathbf{W}}$  is assumed to be independent. Hence,  $\text{KL} (q_\phi(\tilde{\mathbf{W}}) || p(\tilde{\mathbf{W}}))$  can be written as

$$\sum_{m=1}^M \sum_{n=0}^N \text{KL} (q_\phi(\tilde{w}_{m,n}) || p(\tilde{w}_{m,n})).$$

$$\log p(y|\mathbf{P}) \geq \mathbb{E}_{q_\phi(\tilde{\mathbf{W}})} \log p(y|\tilde{\mathbf{W}}, \mathbf{P}) - \sum_{m=1}^M \sum_{n=0}^N \text{KL} (q_\phi(\tilde{w}_{m,n}) || p(\tilde{w}_{m,n})) \quad (\text{A.48})$$

Above all, Equation (14) in the manuscript is proved.

## Appendix J: Detailed Computations of Equation (14) in the Manuscript

The first item in Eq. (14) is hard to compute because it involves integral in the expectation operation.

We use Monto Carlo method to draw a number of  $C$  samples for  $\tilde{\mathbf{W}}$  and the  $c$ -th sample is denoted as  $\tilde{\mathbf{W}}(c)$ .

Then, we can get  $\mathbf{W}(c), c = 1, \dots, C$  to estimate the first term by,

$$\mathbb{E}_{q_\phi(\tilde{\mathbf{W}})} \log p(y|\tilde{\mathbf{W}}, \mathbf{P}) \approx \frac{1}{C} \sum_{c=1}^C \log p(y|\mathbf{W}(c), \mathbf{P}) \quad (\text{A.49})$$

We use  $p(y|\mathbf{W}, \mathbf{P})$  to denote the ensemble predictive probability obtained from multiple base detectors, which suggests the probability that the label is positive (i.e.,  $y = 1$ ). As  $y$  equals 0 or 1,  $\log p(y|\mathbf{W}, \mathbf{P})$  can be expressed as  $y \cdot \log p(y|\mathbf{W}, \mathbf{P}) + (1 - y) \cdot \log(1 - p(y|\mathbf{W}, \mathbf{P}))$ , which is exactly the negative of cross-entropy. As cross-entropy is one of the mostly commonly used loss function for binary

classification, we replace  $\log p(y|\mathbf{W}(c), \mathbf{P})$  with its cross-entropy based form, i.e.,  $-\text{CE}(\log p(y|\mathbf{W}(c), \mathbf{P}), y)$ . Then,

$$\mathbb{E}_{q_\phi(\tilde{\mathbf{W}})} \log p(y|\tilde{\mathbf{W}}, \mathbf{P}) \approx \frac{1}{C} \sum_{c=1}^C -\text{CE}(\log p(y|\mathbf{W}(c), \mathbf{P}), y) \quad (\text{A.50})$$

where  $\text{CE}$  denotes the cross-entropy loss.

For the second term of the right-hand side in Equation (14) of the manuscript, as  $q_\phi(\tilde{w}_{m,n}) = \text{LogNormal}(\varphi_{m,n}^{\text{post}}, (\sigma^{\text{post}})^2)$ ,  $p(\tilde{w}_{m,n}) = \text{LogNormal}(\psi_{m,n}, \sigma^2)$  and  $(\sigma^{\text{post}})^2 = \sigma^2 = \sigma_{\text{dt}}^2 + \sigma_{\text{sp}}^2$ , their KL divergence is expressed by,

$$\text{KL}\left(q_\phi(\tilde{w}_{m,n})\|p(\tilde{w}_{m,n})\right) = \log \frac{\sigma}{\sigma^{\text{post}}} + \frac{(\sigma^{\text{post}})^2 + (\varphi_{m,n}^{\text{post}} - \psi_{m,n})^2}{2\sigma^2} - \frac{1}{2} = \frac{(\varphi_{m,n}^{\text{post}} - \psi_{m,n})^2}{2\sigma^2} \quad (\text{A.51})$$

Hence,  $\mathcal{L}$  can be computed as,

$$\mathcal{L} \approx \frac{1}{C} \sum_{c=1}^C -\text{CE}(\log p(y|\mathbf{W}(c), \mathbf{P}), y) - \sum_{m=1}^M \sum_{n=0}^N \frac{(\varphi_{m,n}^{\text{post}} - \psi_{m,n})^2}{2\sigma^2} \quad (\text{A.52})$$

## Appendix K: Detailed Construction of the Augmented Datasets

For each sample  $(x_i^{\text{bd}}, y_i^{\text{bd}}) \in \mathcal{D}^{\text{bd}}$ , we randomly select one attack method from DeepWordBug (Gao et al. 2018, Li and Chai 2022), TFAdjusted (Herel et al. 2023, John X. Morris et al. 2020), or TREPAT (Przybyła et al. 2025), denoted as  $a_{\text{ran}}$ . The selected attack is then applied to produce an adversarial example for the clean sample,  $x_i^{\text{bd}}$  i.e.,  $\tilde{x}_i^{\text{bd}} = \text{GenerateAdversarialSample}(a_{\text{ran}}, x_i^{\text{bd}}, y_i^{\text{bd}})$ . The ground truth label of  $\tilde{x}_i^{\text{bd}}$  remains the same as that of  $x_i^{\text{bd}}$ , i.e.,  $y_i^{\text{bd}}$ . In this way, we obtain an adversarial sample  $(\tilde{x}_i^{\text{bd}}, y_i^{\text{bd}})$  corresponding to the clean sample  $(x_i^{\text{bd}}, y_i^{\text{bd}})$ . All generated adversarial samples together constitute  $\tilde{\mathcal{D}}^{\text{bd}}$ . By this way, we obtain  $\mathcal{D}^{\text{bd}} \cup \tilde{\mathcal{D}}^{\text{bd}}$ . The construction of  $\mathcal{D}^{\text{ag}} \cup \tilde{\mathcal{D}}^{\text{ag}}$  follows the same procedure as described above.

## Appendix L: Pseudocode for Iterative Adversarial Training

---

### Algorithm 1 Pseudocode for Iterative Adversarial Training

---

**Input:** Training data  $\mathcal{D}^{\text{bd}}, \mathcal{D}^{\text{ag}}$ ; A set of  $R$  adversarial attack methods  $\{a_r\}_{r=1}^{r=R}$  ( $a_r \in \mathcal{A}$ ); Batch size  $b^{\text{bd}}, b^{\text{ag}}$ ; Max iterations  $T$ ; Early-stopping patience  $\rho$ .

**Output:** Trained base detectors and weight assignor

1: Initialize base detectors  $f_m$  with parameter  $\theta_m^{(0)}$  ( $m = 1, \dots, M$ ), and initialize the weight assignor

---

---

1:  $f^{\text{infer}}$  with parameter  $\phi^{(0)}$   
 2:  $t = 0$   
 3: Repeat until convergence (loss does not decrease for  $\rho$  consecutive iterations) or reach the max number of iterations (i.e.,  $t > T$ )  
 4: Initialize  $\tilde{\mathcal{D}}^{\text{bd}}$  with empty set  
 5: **for** each sample  $(x_i^{\text{bd}}, y_i^{\text{bd}})$  from  $\mathcal{D}^{\text{bd}}$  **do**  
 6:     Randomly choose an adversarial attack method  $a_{\text{ran}}$  from  $\{a_r\}_{r=1}^R$   
 7:     Generate adversarial sample:  $\tilde{x}_i^{\text{bd}} = \text{GenerateAdversarialSample}(a_{\text{ran}}, x_i^{\text{bd}}, y_i^{\text{bd}})$   
 8:     Add  $(\tilde{x}_i^{\text{bd}}, y_i^{\text{bd}})$  into  $\tilde{\mathcal{D}}^{\text{bd}}$   
 9: **end for**  
 10: Obtain  $\tilde{\mathcal{D}}^{\text{ag}}$  following the same step of (4-8)  
 11: **for** batch number  $b = 1, \dots, B^{\text{ag}}$  **do**  
 12:      $\{x^{\text{ag}}, y^{\text{ag}}\} \leftarrow \text{SampleMiniBatch}(\mathcal{D}^{\text{ag}} \cup \tilde{\mathcal{D}}^{\text{ag}}, b^{\text{ag}})$ .  
 13:     Calculate the total loss of weight assignor  $\text{Loss}^{\text{ag}}$  with Eq. (17) in the manuscript  
 14:     Update parameter  $\phi$  with Eq. (18)  
 15: **end for**  
 16: **for** batch number  $b = 1, \dots, B^{\text{bd}}$  **do**  
 17:      $\{x^{\text{bd}}, y^{\text{bd}}\} \leftarrow \text{SampleMiniBatch}(\mathcal{D}^{\text{bd}} \cup \tilde{\mathcal{D}}^{\text{bd}}, b^{\text{bd}})$   
 18:     Calculate the total loss of base detector  $\text{Loss}^{\text{bd}}$  with Eq. (15) in the manuscript  
 19:     Update parameter  $\theta_m$  with Eq. (16)  
 20: **end for**  
 21:  $t = t + 1$   
 22: **return** trained base detectors and weight assignor (i.e., our trained ARHOCD)

---

## Appendix M: Reparameterization Trick for Learning Parameters $\phi$

A variety of ready-to-use optimizers are available in common DL platforms (e.g., PyTorch, TensorFlow) to minimize  $\text{Loss}^{\text{ag}}$  to learn parameters  $\phi$ . However, it is hard to directly use  $\text{Loss}^{\text{ag}}$  in Equation (17) to learn parameters  $\phi$ . The reason is that learning parameters  $\phi$  requires us to compute the gradient of  $\text{Loss}^{\text{ag}}$  with respect to parameters  $\phi$  such that we can update  $\phi$  based on the gradient. However, the computation of  $\text{Loss}^{\text{ag}}$  involves the sampling process, that is using Monto Carlo method to draw a number of  $C$  samples for  $\tilde{\mathbf{W}}_i^{\text{ag}}$  (the  $c$ -th sample is denoted as  $\tilde{\mathbf{W}}_i^{\text{ag}}(c)$  and the obtaining  $\mathbf{W}_i^{\text{ag}}(c)$  via normalization. As this process involves drawing from  $q_{\phi}(\tilde{\mathbf{W}}_i^{\text{ag}})$  to obtain weight  $\tilde{\mathbf{W}}_i^{\text{ag}}$  (thus  $\mathbf{W}_i^{\text{ag}}(c)$ ), the randomness in the sampling process hinders the computation of the gradient of  $\text{Loss}^{\text{ag}}$  with respect to  $\phi$ . Consequently, this impedes the learning process for parameter  $\phi$ .

This study introduces a reparameterization trick similar to previous methods such as variational autoencoder to tackle this challenge (Kingma and Welling 2014). We first draw random samples from an

external distribution, and then transform them to get new samples of  $\mathbf{W}_i^{\text{ag}}(c)$  in a deterministic manner. In this way, the randomness of  $\mathbf{W}_i^{\text{ag}}(c)$  comes from the sampling process of an external distribution, which is not our interest. Our focus is the information flow from  $\boldsymbol{\phi}$  to  $\mathbf{W}_i^{\text{ag}}(c)$  and then to  $\text{Loss}^{\text{ag}}$ , which has now become deterministic. Thus, we can compute the gradient of  $\text{Loss}^{\text{ag}}$  with respect to  $\boldsymbol{\phi}$  with chain rule.

Specifically, based on the properties of Gaussian distribution, if  $\epsilon \sim \mathcal{N}(0,1)$ , then  $\varphi + \epsilon\sigma$  follows a Gaussian distribution  $\mathcal{N}(\varphi, \sigma^2)$ . Consequently,  $\exp(\varphi + \epsilon\sigma)$  follows the log-normal distribution  $\text{LogNormal}(\varphi, \sigma^2)$ . Hence, we first generated  $\epsilon$  from the  $\mathcal{N}(0,1)$  and then transform it with  $\exp(\varphi + \epsilon\sigma)$ .

In our case, as  $\tilde{w}_{i,(m,n)}^{\text{ag}}$  follows  $\text{LogNormal}(\varphi_{i,(m,n)}^{\text{ag}}, (\sigma^{\text{post}})^2)$ , we generate it by

$$\tilde{w}_{i,(m,n)}^{\text{ag}} = \exp(\varphi_{i,(m,n)}^{\text{ag}} + \epsilon_{i,(m,n)}\sigma^{\text{post}}), \epsilon_{i,(m,n)} \sim \mathcal{N}(0,1) \quad (\text{A. 53})$$

We then obtain  $w_{i,(m,n)}^{\text{ag}}$  by normalization, i.e.,

$$w_{i,(m,n)}^{\text{ag}} = \tilde{w}_{i,(m,n)}^{\text{ag}} / \sum_{m=1}^M \sum_{n=0}^N \tilde{w}_{i,(m,n)}^{\text{ag}} \quad (\text{A. 54})$$

Although  $w_{i,(m,n)}^{\text{ag}}$  is still a random variable, the computation path from  $\varphi_{i,(m,n)}^{\text{ag}}$  to  $w_{i,(m,n)}^{\text{ag}}$  ( $m = 1, \dots, M; n = 0, \dots, N$ ) (i.e.  $\mathbf{W}_i^{\text{ag}}(c)$ ) becomes deterministic. As  $\varphi_{i,(m,n)}^{\text{ag}}$  is deterministically computed based on  $\boldsymbol{\phi}$ , this allows us to compute the gradient of  $\boldsymbol{\phi}$  for updating. In this way, we addressed the problem caused by randomness.

Denote the transformation process from  $\epsilon_{m,n}$  to  $w_{i,(m,n)}^{\text{ag}}$  as  $\mathbf{W}_i^{\text{ag}} = g(\boldsymbol{\epsilon}_i)$  where  $\boldsymbol{\epsilon}_i$  is a matrix whose element is  $\epsilon_{i,(m,n)}$ . Then, Equation (17) in the manuscript can be computed as,

$$\begin{aligned} \text{Loss}^{\text{ag}} &\approx \sum_{i=1}^{|\mathcal{D}^{\text{ag}} \cup \tilde{\mathcal{D}}^{\text{ag}}|} \text{CE} \left( \text{tr} \left[ (\mathbf{W}_i^{\text{ag}})^T \mathbf{P}_i^{\text{ag}} \right], y_i^{\text{ag}} \right) + \text{KL} \left( q_{\boldsymbol{\phi}}(\tilde{\mathbf{W}}_i^{\text{ag}}) \parallel p(\tilde{\mathbf{W}}_i^{\text{ag}}) \right) \\ &= \frac{1}{C} \sum_{c=1}^C \sum_{i=1}^{|\mathcal{D}^{\text{ag}} \cup \tilde{\mathcal{D}}^{\text{ag}}|} \left[ \text{CE} \left( \text{tr} \left[ (g(\boldsymbol{\epsilon}_i(c)))^T \mathbf{P}_i^{\text{ag}} \right], y_i^{\text{ag}} \right) + \sum_{m=1}^M \sum_{n=0}^N \frac{(\varphi_{i,(m,n)}^{\text{ag}} - \psi_{i,(m,n)}^{\text{ag}})^2}{2\sigma^2} \right] \quad (\text{A. 55}) \end{aligned}$$

where  $\boldsymbol{\epsilon}_i(c)$  refers to the  $c$ -th sample of  $\boldsymbol{\epsilon}_i$  from Monte Carlo method, and  $p(\tilde{\mathbf{W}}_i^{\text{ag}}) = \text{LogNormal}(\psi_{i,(m,n)}^{\text{ag}}, \sigma^2)$ ,  $\psi_{i,(m,n)}^{\text{ag}}$  and  $\sigma^2$  are the mean and variance of the Gaussian distribution

underlying the log-normal distribution.

## Appendix N: Two Solutions for Calculating the Expectation $\mathbb{E}[w_{m,n}^{\text{new}}]$

### (1) Monte Carlo method:

The first solution is employing the Monte Carlo method for approximation. Then, the predictive probability  $\hat{p}^{\text{new}}$  is:

$$\hat{p}^{\text{new}} \approx \sum_{m=1}^M \sum_{n=0}^N \left( \frac{1}{C_{\text{MC}}^w} \sum_{c=1}^{C_{\text{MC}}^w} w_{m,n}^{\text{new}}(c) \cdot p_{m,n}^{\text{new}} \right) \quad (\text{A.56})$$

where  $C_{\text{MC}}^w$  is the sample number of  $w_{m,n}^{\text{new}}$ .

Then, the predict label  $\hat{y}^{\text{new}}$  is given by,

$$\hat{y}^{\text{new}} = \begin{cases} 0 & (\text{i. e. , non-harmful}), \text{ if } \hat{p}^{\text{new}} \leq \varepsilon \\ 1 & (\text{i. e. , harmful}), \text{ if } \hat{p}^{\text{new}} > \varepsilon \end{cases} \quad (\text{A.57})$$

### (2) Compute lower bound:

The second solution is to derive a closed-form estimate for  $\mathbb{E}[w_{m,n}^{\text{new}}]$ . The lower bound of  $\mathbb{E}[w_{m,n}^{\text{new}}]$  is given by (see proof later in this Appendix),

$$\mathbb{E}[w_{m,n}^{\text{new}}] \geq \xi \frac{\exp(\varphi_{m,n}^{\text{new}})}{\sum_{m=1}^M \sum_{n=0}^N \exp(\varphi_{m,n}^{\text{new}})} \quad (\text{A.58})$$

where  $\xi$  is a constant that is the same for different predictions.

We utilize the lower bound to represent  $\mathbb{E}[w_{m,n}^{\text{new}}]$ . Since the constant  $\xi$  is identical across all predictions, it does not influence the relative weights following normalization and thus can be safely omitted. Then, the predictive probability  $\hat{p}^{\text{new}}$  is given by

$$\hat{p}^{\text{new}} \approx \sum_{m=1}^M \sum_{n=0}^N \left( \frac{\exp(\varphi_{m,n}^{\text{new}})}{\sum_{m=1}^M \sum_{n=0}^N \exp(\varphi_{m,n}^{\text{new}})} \cdot p_{m,n}^{\text{new}} \right) \quad (\text{A.59})$$

Then, the predict label  $\hat{y}^{\text{new}}$  is obtained with Equation (A.57). Though the second method for computing  $\hat{y}^{\text{new}}$  in Equation (A.59) may not as accurate as the first method, our experiments demonstrate that actually its performance is close to that obtained from Equation (A.57). Moreover, the second method does not need a sampling process and thus is more efficient.

*Proof of Equation (A.58).*

Assume  $\tilde{w}_{m,n}^{\text{new}}$  follows a log-normal distribution parameterized by  $(\varphi_{m,n}^{\text{new}}, (\sigma^{\text{post}})^2)$ , the expectation of the normalized weight can be approximated as:

$$\mathbb{E}[w_{m,n}^{\text{new}}] = \mathbb{E}\left[\frac{\tilde{w}_{m,n}^{\text{new}}}{\sum_{m=1}^M \sum_{n=0}^N \tilde{w}_{m,n}^{\text{new}}}\right] \approx \frac{\exp(\varphi_{m,n}^{\text{new}} + \frac{1}{2}(\sigma^{\text{post}})^2)}{\sum_{m=1}^M \sum_{n=0}^N \exp(\varphi_{m,n}^{\text{new}} + \frac{1}{2}(\sigma^{\text{post}})^2)}$$

According to (Daunizeau 2017),  $\mathbb{E}[\log w_{m,n}^{\text{new}}]$  can be approximated by,

$$\mathbb{E}[\log w_{m,n}^{\text{new}}] \approx \log \frac{\exp(\varphi_{m,n}^{\text{new}})}{\sum_{m=1}^M \sum_{n=0}^N \exp(\varphi_{m,n}^{\text{new}})} + \frac{1}{2} \text{tr} \left[ (\mathbf{V}\mathbf{V}^T - \text{diag}(\mathbf{V})) \text{diag}((\sigma^{\text{post}})^2) \right]$$

$$\text{where } \mathbf{V} = [v_{1,0}, \dots, v_{m,n}, \dots, v_{M,N}]^T, v_{m,n} = \frac{\exp(\varphi_{m,n}^{\text{new}})}{\sum_{m=1}^M \sum_{n=0}^N \exp(\varphi_{m,n}^{\text{new}})}.$$

The second term on the right-hand side can be written as,

$$\frac{1}{2} \text{tr} \left[ (\mathbf{V}\mathbf{V}^T - \text{diag}(\mathbf{V})) \text{diag}((\sigma^{\text{post}})^2) \right] = \frac{(\sigma^{\text{post}})^2}{2} \sum_{m=1}^M \sum_{n=0}^N [v_{m,n}^2 - v_{m,n}]$$

Hence, the  $\mathbb{E}[\log w_{m,n}^{\text{new}}]$  can be written as,

$$\mathbb{E}[\log w_{m,n}^{\text{new}}] \approx \log \frac{\exp(\varphi_{m,n}^{\text{new}})}{\sum_{m=1}^M \sum_{n=0}^N \exp(\varphi_{m,n}^{\text{new}})} + \frac{(\sigma^{\text{post}})^2}{2} \sum_{m=1}^M \sum_{n=0}^N [v_{m,n}^2 - v_{m,n}]$$

Since  $\frac{(\sigma^{\text{post}})^2}{2} \sum_{m=1}^M \sum_{n=0}^N [v_{m,n}^2 - v_{m,n}]$  is the same for all different  $(m, n)$ , it can be treated as a constant  $\xi'$ . Hence, we have,

$$\mathbb{E}[\log w_{m,n}^{\text{new}}] \approx \log \frac{\exp(\varphi_{m,n}^{\text{new}})}{\sum_{m=1}^M \sum_{n=0}^N \exp(\varphi_{m,n}^{\text{new}})} + \xi'$$

Since the log function is concave, according to Jensen's Inequality (Jensen 1906), we have,

$$\log \mathbb{E}[w_{m,n}^{\text{new}}] \geq \mathbb{E}[\log w_{m,n}^{\text{new}}]$$

Hence, we are expected to have,

$$\begin{aligned} \mathbb{E}[w_{m,n}^{\text{new}}] &\geq \exp \left( \log \frac{\exp(\varphi_{m,n}^{\text{new}})}{\sum_{m=1}^M \sum_{n=0}^N \exp(\varphi_{m,n}^{\text{new}})} + \xi' \right) = \frac{\exp(\varphi_{m,n}^{\text{new}})}{\sum_{m=1}^M \sum_{n=0}^N \exp(\varphi_{m,n}^{\text{new}})} \cdot \exp(\xi') \\ &= \frac{\exp(\varphi_{m,n}^{\text{new}})}{\sum_{m=1}^M \sum_{n=0}^N \exp(\varphi_{m,n}^{\text{new}})} \cdot \xi \end{aligned}$$

where  $\xi = \exp(\xi')$  is a constant.

Above all, Equation (A.58) is proved.

## Appendix O: Details of Datasets

The ETHOS (Ethics in Text - Hate and Offensive Speech) binary dataset (Mollas et al. 2022) is designed for hate speech detection. According to Mollas et al. (2022), the dataset construction followed a three-stage annotation process. First, an active learning strategy was employed: classifiers (including SVM, random forest, logistic regression, and neural networks) were trained on existing labeled data and used to predict newly collected, unlabeled comments. Samples with high uncertainty were selected for manual annotation, while semantically similar comments were avoided to maintain diversity. This process was iteratively repeated until approximately 1,000 comments were collected. Second, the dataset underwent crowdsourced validation on the Figure-Eight platform, where high-quality annotators answered questions related to hate speech. Annotation consistency was evaluated using Fleiss' Kappa, with most labels achieving values above 0.85, indicating good to excellent agreement. Finally, the crowdsourced annotations were aggregated and manually checked, and the labels were binarized by treating samples with an aggregated score of at least 0.5 as positive.

The PHEME dataset<sup>2</sup> comprises a collection of Twitter rumors and non-rumors associated with breaking news events. It was curated in collaboration with journalists, who manually labeled each tweet as a rumor or non-rumor based on its veracity at the time of posting. In total, the dataset comprises 6,425 annotated tweets, including 2,402 rumors (37.39%) and 4,023 non-rumors (62.61%). It covers nine events: Sydney Siege (522 rumors and 699 non-rumors), Germanwings Crash (238 rumors and 231 non-rumors), Prince-Toronto (229 rumors and 4 non-rumors), Ferguson (284 rumors and 859 non-rumors), Charlie Hebdo (458 rumors and 1,621 non-rumors), Ottawa Shooting (470 rumors and 420 non-rumors), Ebola-Essien (14 rumors and 0 non-rumors), Gurlitt (61 rumors and 77 non-rumors), and Putinmissing (126

---

<sup>2</sup>

[https://figshare.com/articles/dataset/PHEME\\_dataset\\_for\\_Rumour\\_Detection\\_and\\_Veracity\\_Classification/6392078](https://figshare.com/articles/dataset/PHEME_dataset_for_Rumour_Detection_and_Veracity_Classification/6392078)

rumors and 112 non-rumors). Only tweets with at least 100 retweets were included in the dataset. This filtering ensures that the dataset contains high-quality and representative content, making it a reliable benchmark for rumor detection.

The White Supremacist dataset (De Gibert et al. 2018) is a highly imbalanced dataset for extremist detection. According to De Gibert et al. (2018), it was constructed from forum posts published on Stormfront, a white supremacist online forum, between 2002 and 2017. The data were collected using web crawling techniques. To ensure thematic and user diversity, posts were randomly sampled from 22 subforums. The collected posts were preprocessed by filtering out non-English content and segmenting them into sentences. Then, annotation was conducted at the sentence level using a web-based annotation tool that allowed annotators to inspect the full post and the surrounding conversational context. Each sentence was labeled by three annotators following collaboratively developed annotation guidelines..

## Appendix P: Technical Details of Baselines

### Passive Methods

- (1) LLM-guided Purification (LLM-puri) (Moraffah et al. 2024): it employs a role-playing strategy, using a prompt to ask an LLM to purify adversarial samples. The purification process is guided by a structured prompt, as shown in Table P1. Note this prompt relies on the ground truth, which is impractical during testing. For a fair comparison, we excluded the ground truth information from the prompt. In this baseline, we used the same LLM as in our method, i.e., Llama-3.1-8B-Instruct<sup>3</sup>.

**Table P1. Prompt Used in LLM-puri**

'Human: You are a teacher tasked with grading a quiz. The quiz consists of a sentence (the question) and a classification label (the student's answer). Unfortunately, the sentence has been manipulated by an adversarial attack, leading to a misclassification.

Given the altered sentence and its incorrect label, your job is to generate a new sentence that is semantically similar to the altered one but will be classified correctly according to the correct label.

The categories for classification are: [list of classification categories]

ALTERED SENTENCE (QUESTION): [altered sentence]

MISCLASSIFIED LABEL (STUDENT ANSWER): [misclassified label]

CORRECT LABEL (TRUE ANSWER): [correct label]

Please create a new sentence that conveys the same meaning as the altered sentence but will be classified under the CORRECT LABEL when graded. Even if there is not a misclassification, provide/construct the sentence to the best of your capability.

The output format must be json: "Original Sentence": "[New sentence here]" Begin!"

- (2) Detection and Restoration (Det&Res) (Wang et al. 2022): it first uses a binary classifier to detect adversarial samples. For samples detected as anomalous, it randomly applies one of the four

---

<sup>3</sup> <https://huggingface.co/meta-llama/Llama-3.1-8B-Instruct>

restoration strategies (random synonym substitution, adverb insertion, MLM-based suggestion, and back translation) to generate a purified sample for prediction. For samples detected as normal, it retains their original form for prediction. Following the original paper, we trained a BERT-based anomaly detector to identify adversarial samples.

### Active Methods: Learning-based

#### Random noise-based

- (1) SAFER (Ye et al. 2020): it first uses synonym replacement to generate multiple variants of the input text and then makes predictions on them to provide certified robustness. We used TextAttack Python package (John X Morris et al. 2020) to replace words in the input text with their WordNet synonyms (Miller 1995). Since our focus is not on certified robustness, following common practice (Wang et al. 2023), we report the empirical results. Specifically, we aggregated the predictions of these variants through a weighted averaging scheme (i.e., CBW-D, (Zhou et al. 2021)) to obtain the final prediction.
- (2) MASKFil (Li et al. 2023): it generates several input variants by randomly masking words in the input text and filling in the masked words with a masked language model. Predictions are then made on all variants and aggregated through equal-weight averaging. Following the original paper, we used BERT as the masked language model to generate multiple variants for each input and compute the final prediction by averaging their outputs with equal weights.

#### Regularization-based

- (1) FTML (Yang et al. 2022): it uses triplet loss to bring words closer to their synonyms and push them away from non-synonyms in embedding space. We followed its source code released in github<sup>4</sup> to train the base models used in our study.
- (2) OutReg (Dong et al. 2022): it encourages the output distributions of clean samples and their corresponding adversarial samples to be close. We used clean samples and their corresponding adversarial samples (generated by DeepWordBug, TFAdjusted, and TREPAT) as training data, and used a KL divergence term, as in the original paper, to align the output distributions.
- (3) FIM (Gloeckler et al. 2023): it proposes a regularization method for improving the robustness of amortized Bayesian inference. In amortized inference, a neural network is trained to approximate the posterior distribution conditioned on observed data. Consequently, the goal of an adversarial attack is to maximize the discrepancy (e.g., KL divergence) between the posterior inferred from a clean input and that from a perturbed input. To defend against such attacks, it introduces a Fisher Information Matrix (FIM)-based regularization method. The FIM captures the sensitivity of the estimated posterior distribution to input perturbations by computing gradients with respect to the input. By penalizing directions associated with high sensitivity, the method encourages the model to be more robust against perturbations along these vulnerable directions. However, this defense strategy is not directly applicable to text classification models because textual inputs are discrete, preventing the computation of input-level gradients required by the original FIM formulation. To adapt this method to text classification model, we followed the common practice of operating in the embedding space (Yoo and Qi 2021). Specifically, instead of computing gradients with respect to the discrete tokens, we computed the gradients of the loss with respect to the input embeddings. This operation allows us to estimate the FIM. We then applied the same regularization strategy as in the original method, but used the embedding-level FIM to guide the regularization.

#### Adversarial training-based

---

<sup>4</sup> <https://github.com/JHL-HUST/FTML/tree/main>

- (1) AT (Goodfellow et al. 2015): it mixes clean and adversarial samples as training data. Following this, we trained the model using both clean samples and adversarial samples generated by DeepWordBug, TFAdjusted, and TREPAT.
- (2) MRAT (Zhao et al. 2021): it adds linear interpolation of the hidden representation of clean and adversarial samples, and uses Jensen-Shannon divergence to encourage the predictive distributions of the initial clean and mixup sample to be close. We followed its source code released in [github<sup>5</sup>](https://github.com/Opdoop/MRAT) to train the base detectors used in our study.
- (3) FAT (Yang et al. 2025): it proposes a fast adversarial training in the embedding space by single-step gradient ascent and historical perturbation initialization. Notably, it generates perturbations directly in the embedding space by computing the gradient of the loss with respect to the input embeddings, rather than relying on existing adversarial attack algorithms. We followed its source code released in [github<sup>6</sup>](https://github.com/JHL-HUST/FAT) to train the base detectors used in our study.

#### Active Methods: Ensemble model-based

- (1) ARTText (Li and Chai 2022): it trains multiple base models on varied samples, enhances robustness via adversarial training, and aggregates base models’ predictions via majority voting. Following this setting, we trained the five base detectors (BERT, DistilBERT, RoBERTa, XLNet, and ALBERT) used in our study on different bootstrap samples generated by bagging and finally aggregate their predictions via majority voting.
- (2) ARDEL (Waghela et al. 2024): it trains multiple base models on varied samples, incorporating adversarial training and randomized smoothing. During testing, it randomly masks words in the input text only once, resulting in a single variant for prediction. When aggregating predictions from multiple base models, it uses a random forest to dynamically assign weights to the models. We followed it to train base detectors on varied samples and adopt a random forest to aggregate predictions across multiple base models.
- (3) EnsSel (Qin et al. 2023): it models the prediction distribution of each base model using a Dirichlet prior, enabling the model to quantify predictive uncertainty. Moreover, it incorporates adversarial samples during training and designs a loss function that penalizes small uncertainty gaps between clean and adversarial inputs. During testing, it dynamically chooses the base model prediction with lowest uncertainty. Note that, the original design constructs multiple base models through low-rank projection of a shared backbone, it is not directly applicable to our setting that involves heterogeneous models. Therefore, we instead followed its idea of enhancing ensemble diversity by training base detectors on different subsets of the training data in our study.

#### Appendix Q: Computation Details of Attack Success Rate (ASR) and After-Attack Classification

##### Metrics

###### Q.1 Computation Details of ASR

ASR is the proportion of adversarial examples generated by the attacker that are misclassified by the model. Specifically, we applied the four attack methods—DeepWordBug, TFAdjusted, TREPAT, and ExplainDrive—to generate adversarial samples from the test set  $D^{\text{test}}$ , resulting in  $D_{\text{DW}}^{\text{test}}$ ,  $D_{\text{TF}}^{\text{test}}$ ,  $D_{\text{TR}}^{\text{test}}$ ,  $D_{\text{E}}^{\text{test}}$ ,

---

<sup>5</sup> <https://github.com/Opdoop/MRAT>

<sup>6</sup> <https://github.com/JHL-HUST/FAT>

respectively. The true labels of the adversarial samples are the same as those of their corresponding clean samples. Taking DeepWordBug as an example, for each class (e.g., POS and NEG), we first counted the total number of adversarial samples in  $D_{\text{DW}}^{\text{test}}$ , denoted as  $N_{\text{DW}}^{\text{POS}}, N_{\text{DW}}^{\text{NEG}}$ . Then, we counted the number of misclassified adversarial samples, i.e., adversarial examples that successfully mislead the model, denoted as  $N_{\text{DW}}^{\text{POS\_suc}}, N_{\text{DW}}^{\text{NEG\_suc}}$ . This enables us to calculate the attack success rate for each class, i.e.,

$$ASR_{\text{DW}}^{\text{POS}} = \frac{N_{\text{DW}}^{\text{POS\_suc}}}{N_{\text{DW}}^{\text{POS}}} \quad (\text{A. 60})$$

$$ASR_{\text{DW}}^{\text{NEG}} = \frac{N_{\text{DW}}^{\text{NEG\_suc}}}{N_{\text{DW}}^{\text{NEG}}} \quad (\text{A. 61})$$

The overall ASR of DeepWordBug is then obtained by averaging across the two classes:

$$ASR_{\text{DW}} = \frac{ASR_{\text{DW}}^{\text{POS}} + ASR_{\text{DW}}^{\text{NEG}}}{2} \quad (\text{A. 62})$$

The ASR for the other attack methods ( $ASR_{\text{TF}}, ASR_{\text{TR}}, ASR_{\text{E}}$ ) is computed in the same manner.

## Q.2 Computation Details of After-Attack Classification Metrics

Using a combined dataset consisting of adversarially crafted samples (derived from initially correctly classified samples) and initially misclassified clean samples, we apply the model to predict each sample in this dataset, yielding  $\hat{y}_i$ . Based on the ground-truth labels  $y_i$ , the after-attack classification metrics including accuracy, precision, recall, and F1-score are computed as follows,

$$TP = \sum_i \mathbb{I}[[\hat{y}_i = 1 \text{ AND } y_i = 1]], FP = \sum_i \mathbb{I}[[\hat{y}_i = 1 \text{ AND } y_i = 0]], \quad (\text{A. 63})$$

$$TN = \sum_i \mathbb{I}[[\hat{y}_i = 0 \text{ AND } y_i = 0]], FN = \sum_i \mathbb{I}[[\hat{y}_i = 0 \text{ AND } y_i = 1]] \quad (\text{A. 64})$$

$$Accuracy = \frac{TP + TN}{TP + TN + FP + FN} \quad (\text{A. 65})$$

$$Precision = \frac{TP}{TP + FP} \quad (\text{A. 66})$$

$$Recall = \frac{TP}{TP + FN} \quad (\text{A. 67})$$

$$F1\text{-score} = \frac{2 * Precision * Recall}{Precision + Recall} \quad (A.68)$$

## Appendix R: Results of Experiment 1 and 2 on the ETHOS and White Supremacist Datasets

### R.1 Experiment 1: Generalizability Comparison

Table R1 shows the generalizability comparison results on the PHEME, ETHOS and White Supremacist datasets. For each attack method, we report the after-attack classification metrics (accuracy (ACC), precision (PRE), recall (REC), and F1-score (F1)), and the attack success rate (ASR). To measure generalizability, we report the worst-case metric value (“Worst” in Table R1).

The results show that detectors instantiated with our LLM-SGA achieve the best generalizability. By comparing our LLM-SGA (single) with baselines that use a single BERT, we find our method demonstrates superior generalizability. For instance, on the PHEME dataset, across all attack methods, our method achieves the best worst-case performance, with accuracy, precision, recall and F1-score of 67.50%, 65.75%, 66.09% and 65.68%, respectively. By comparing our LLM-SGA (multiple) with ensemble-based baselines, our method again achieves the best performance. It attains the highest worst-case F1-score—73.91% on the PHEME dataset, 70.47% on the ETHOS dataset, and 58.00% on the White Supremacist dataset. Moreover, the worst-case ASR is lower than that of the baselines, with 19.68% on PHEME, 26.20% on ETHOS, and 30.98% on the White Supremacist dataset.

**Table R1. Comparison with Baselines on Generalizability**

Detectors	Attack	PHEME Dataset					ETHOS Dataset					White Supremacist Dataset				
		ACC%	PRE%	REC%	F1%	ASR%	ACC%	PRE%	REC%	F1%	ASR%	ACC%	PRE%	REC%	F1%	ASR%
Raw BERT	DW	44.55*** (3.20)	37.91*** (2.47)	39.47*** (2.40)	38.19*** (2.30)	56.86*** (2.81)	31.36*** (3.13)	31.13*** (3.28)	30.64*** (3.34)	30.67*** (3.25)	65.28*** (2.59)	43.65*** (2.01)	41.70*** (1.44)	30.26*** (2.61)	32.48*** (1.47)	65.06*** (2.70)
	TF	39.85*** (2.94)	34.46*** (2.95)	35.89*** (2.25)	34.89*** (2.61)	58.28*** (2.53)	39.43*** (3.29)	39.19*** (3.03)	38.97*** (3.07)	38.85*** (3.08)	53.58*** (2.24)	62.00*** (2.33)	48.61*** (1.13)	46.69*** (2.62)	44.11*** (1.40)	45.14*** (3.63)
	TR	53.85*** (5.08)	46.89*** (5.40)	47.01*** (5.36)	46.75*** (5.37)	43.60*** (3.89)	46.64*** (3.74)	41.25*** (4.01)	43.03*** (3.36)	40.85*** (3.42)	51.43*** (2.22)	71.00*** (2.46)	48.77*** (1.54)	48.18*** (2.20)	48.05*** (1.90)	45.69*** (3.47)
	ED	25.20*** (3.76)	22.24*** (3.11)	21.30*** (3.16)	21.63*** (2.94)	74.95*** (3.04)	28.29*** (3.46)	28.36*** (3.38)	27.84*** (3.51)	27.85*** (3.46)	68.23*** (2.35)	45.17*** (4.39)	40.35*** (1.71)	26.46*** (2.74)	31.48*** (2.18)	70.65*** (2.89)
	<b>Worst</b>	25.20	22.24	21.30	21.63	74.95	28.29	28.36	27.84	27.85	68.23	43.65	40.35	26.46	31.48	70.65
LLM-puri	DW	76.95 (2.96)	76.21 (3.49)	74.48 (3.21)	74.95 (3.27)	19.42** (3.77)	68.43*** (3.47)	69.75*** (4.01)	64.17*** (3.62)	63.56*** (4.35)	30.38*** (1.64)	80.15*** (2.01)	57.06*** (2.20)	58.58*** (2.36)	57.54*** (2.28)	34.35*** (3.80)
	TF	72.30* (2.92)	71.40* (3.13)	70.15** (2.78)	70.43* (2.88)	20.98*** (1.91)	66.50* (3.84)	70.27 (4.36)	62.18*** (2.80)	60.32*** (3.83)	35.18*** (2.30)	88.12*** (1.39)	65.61*** (3.58)	63.18 (3.12)	64.11** (3.02)	27.60*** (3.54)
	TR	76.45*** (2.48)	73.74*** (3.18)	72.35*** (2.49)	72.79** (2.68)	19.80** (3.32)	65.36 (3.82)	71.42* (5.63)	60.30 (2.23)	57.27* (3.28)	37.08*** (1.87)	83.75* (2.08)	58.32** (3.98)	54.92* (2.50)	55.55* (3.18)	42.23*** (2.65)
	ED	63.55*** (2.87)	61.66*** (3.39)	61.65*** (3.25)	61.54*** (3.32)	34.54* (2.09)	62.29** (3.42)	65.19 (4.07)	58.77** (2.99)	55.63*** (4.09)	39.99*** (2.29)	79.13* (2.26)	50.02** (1.60)	50.06** (1.70)	49.96** (1.63)	44.83*** (4.14)

	<b>Worst</b>	63.55	61.66	61.65	61.54	34.54	62.29	65.19	58.77	55.63	39.99	<b>79.13</b>	50.02	50.06	49.96	44.83
Det&Res	DW	68.50 *** (2.12)	66.17 *** (2.46)	64.88 *** (2.08)	65.06 *** (2.17)	31.79 *** (2.28)	60.79 *** (2.76)	59.25 *** (3.32)	57.40 *** (2.71)	56.48 *** (2.96)	36.17 *** (2.67)	73.95 *** (2.19)	52.94 *** (1.64)	54.73 *** (2.70)	52.75 *** (2.02)	39.18 *** (4.34)
	TF	64.20 *** (2.57)	62.39 *** (2.62)	61.83 *** (2.79)	61.78 ** (2.77)	30.24 ** (3.03)	68.14 (2.94)	68.02 ** (3.24)	65.75 (2.92)	65.69 (3.11)	26.32 ** (2.17)	84.65 (1.66)	61.07 (3.31)	63.53 (3.38)	61.93 (3.20)	30.27 *** (2.34)
	TR	64.80 *** (3.47)	59.08 *** (4.60)	57.83 *** (3.91)	57.86 ** (4.18)	33.54 ** (3.91)	61.93 ** (3.08)	61.59 ** (3.78)	57.77 ** (2.65)	55.83 *** (3.30)	39.35 ** (2.44)	79.55 ** (2.14)	56.04 (2.55)	56.35 ** (2.66)	56.14 *** (2.57)	44.25 *** (2.12)
	ED	56.05 *** (4.17)	51.23 *** (4.52)	51.13 *** (4.13)	50.83 *** (4.28)	41.18 *** (4.75)	58.64 *** (4.11)	56.82 *** (3.75)	55.95 *** (3.25)	55.43 *** (3.65)	37.98 *** (3.08)	79.20 * (2.09)	55.36 ** (3.97)	57.46 ** (5.91)	55.79 ** (4.53)	38.03 ** (3.53)
	<b>Worst</b>	56.05	51.23	51.13	50.83	41.18	58.64	56.82	55.95	55.43	39.35	73.95	52.94	54.73	52.75	44.25
SAFER	DW	50.80 *** (3.35)	46.57 *** (3.00)	46.84 *** (2.83)	46.50 *** (2.97)	47.32 *** (3.32)	31.36 ** (3.23)	31.46 *** (3.25)	31.16 *** (3.23)	31.09 *** (3.18)	62.52 *** (2.65)	37.33 *** (1.64)	41.46 *** (1.71)	30.20 *** (2.85)	29.98 *** (1.33)	62.45 *** (3.75)
	TF	49.90 *** (3.61)	46.07 *** (3.70)	46.43 *** (3.36)	45.85 *** (3.53)	47.20 *** (2.63)	34.21 ** (3.36)	33.49 *** (3.49)	33.35 *** (3.42)	33.34 *** (3.42)	60.96 *** (2.45)	55.00 *** (2.52)	49.35 *** (1.39)	48.32 *** (3.88)	42.24 *** (2.09)	39.19 *** (3.75)
	TR	53.30 *** (4.24)	47.18 ** (3.57)	47.14 ** (3.67)	46.97 ** (3.64)	45.43 ** (4.40)	47.71 ** (3.86)	44.07 ** (3.93)	45.09 ** (3.31)	43.36 ** (3.58)	46.87 ** (2.16)	61.35 ** (2.03)	49.56 ** (1.62)	48.95 ** (3.44)	45.90 *** (2.37)	43.59 *** (3.13)
	ED	36.80 *** (3.46)	32.98 ** (4.04)	33.14 *** (4.05)	32.83 *** (3.91)	61.43 ** (3.89)	29.14 ** (2.68)	28.04 ** (2.94)	27.69 ** (3.16)	27.74 ** (3.02)	67.94 ** (1.86)	36.95 ** (3.23)	39.78 ** (1.48)	24.10 ** (3.00)	27.98 *** (1.96)	69.94 *** (3.03)
	<b>Worst</b>	36.80	32.98	33.14	32.83	61.43	29.14	28.04	27.69	27.74	67.94	36.95	39.78	24.10	27.98	69.94
MASKfil	DW	42.05 *** (2.95)	41.17 ** (2.82)	40.76 *** (2.90)	40.61 *** (2.66)	52.40 ** (4.20)	34.71 ** (4.38)	30.81 *** (4.50)	32.39 ** (4.34)	31.24 *** (4.27)	63.97 *** (2.71)	56.73 *** (1.97)	42.31 *** (1.18)	34.03 *** (2.22)	37.24 *** (1.43)	61.98 *** (2.80)
	TF	32.55 *** (2.74)	31.93 ** (3.08)	31.29 ** (3.03)	31.32 *** (2.79)	63.49 ** (2.60)	40.29 ** (2.73)	38.32 ** (2.81)	38.81 ** (2.52)	38.34 ** (2.73)	56.27 *** (2.32)	69.10 *** (2.30)	48.15 *** (1.25)	46.33 *** (2.58)	45.90 *** (1.76)	45.01 *** (3.95)
	TR	50.55 *** (4.06)	47.91 *** (3.65)	47.79 *** (3.97)	47.31 *** (3.73)	43.65 *** (2.72)	48.71 *** (3.93)	43.65 *** (3.84)	44.99 *** (3.07)	42.93 *** (3.36)	49.11 *** (2.12)	72.97 *** (2.05)	46.32 *** (1.53)	45.27 *** (2.29)	45.71 *** (1.88)	47.96 *** (2.56)
	ED	22.55 *** (4.51)	23.41 *** (4.26)	21.92 ** (4.57)	21.98 ** (4.43)	21.98 ** (4.08)	73.81 *** (3.42)	33.64 *** (3.28)	31.39 *** (3.38)	31.49 *** (3.29)	31.36 *** (2.20)	62.67 *** (3.74)	54.25 *** (1.35)	41.70 *** (2.34)	31.81 *** (1.75)	35.72 *** (2.75)
	<b>Worst</b>	22.55	23.41	21.92	21.98	73.81	33.64	30.81	31.49	31.24	63.97	54.25	41.70	31.81	35.72	66.39
FTML	DW	51.80 *** (3.38)	50.10 ** (3.33)	50.11 *** (3.46)	49.89 *** (3.35)	43.85 ** (4.26)	53.71 ** (2.80)	53.52 *** (2.76)	53.55 *** (2.77)	53.32 *** (2.80)	42.88 *** (1.85)	59.92 *** (2.25)	42.71 *** (1.11)	35.94 *** (1.87)	38.64 *** (1.24)	59.40 *** (1.78)
	TF	49.75 *** (2.83)	46.76 *** (2.90)	46.86 *** (2.83)	46.65 *** (2.88)	43.84 ** (2.81)	61.86 ** (3.21)	60.90 *** (3.30)	60.69 *** (3.26)	60.63 *** (3.25)	31.26 ** (1.87)	67.60 *** (2.00)	49.08 *** (1.49)	48.11 *** (3.28)	46.54 *** (1.96)	44.55 *** (3.79)
	TR	47.95 *** (4.50)	43.63 *** (3.81)	43.36 *** (4.02)	43.30 *** (3.88)	47.25 ** (3.76)	45.71 ** (3.34)	42.14 ** (3.42)	42.95 ** (3.01)	41.98 ** (3.21)	49.98 ** (2.50)	78.72 ** (1.67)	54.63	55.18 ** (1.93)	54.77 ** (2.25)	37.67 *** (2.00)
	ED	35.05 *** (3.68)	30.99 ** (4.09)	30.65 *** (3.56)	30.59 *** (3.59)	64.53 ** (4.70)	31.71 ** (3.95)	30.75 ** (3.93)	30.60 ** (3.89)	30.59 ** (3.86)	65.18 ** (2.54)	53.08 *** (3.53)	41.21 *** (1.23)	30.12 *** (1.91)	34.73 *** (1.49)	66.43 *** (1.78)
	<b>Worst</b>	35.05	30.99	30.65	30.59	64.53	31.71	30.75	30.60	30.59	65.18	53.08	41.21	30.12	34.73	66.43
OutReg	DW	51.10 *** (3.02)	48.34 ** (2.95)	48.38 ** (2.97)	48.25 ** (2.94)	44.53 ** (2.71)	42.57 ** (3.26)	38.86 ** (3.00)	40.18 ** (2.70)	38.85 ** (2.81)	53.18 ** (1.94)	58.03 *** (2.47)	44.36 *** (1.35)	38.11 *** (2.73)	39.64 *** (1.77)	53.69 *** (3.19)
	TF	53.45 *** (3.43)	50.61 *** (3.59)	50.58 *** (3.43)	50.44 *** (3.52)	41.96 ** (3.45)	41.00 ** (3.85)	36.70 ** (3.87)	38.30 ** (3.66)	36.82 ** (3.45)	54.64 *** (2.12)	65.85 *** (2.35)	45.58 *** (1.35)	41.07 *** (2.80)	42.37 *** (1.70)	51.73 *** (3.06)
	TR	53.10 *** (3.99)	48.88 *** (4.31)	48.81 *** (4.62)	48.57 *** (4.38)	37.64 ** (4.25)	54.43 ** (3.73)	49.19 *** (3.81)	49.51 *** (2.43)	46.18 *** (3.18)	42.61 *** (2.50)	67.03 *** (1.78)	46.00 *** (1.96)	45.78 *** (1.31)	45.59 *** (2.13)	45.39 *** (1.58)
	ED	39.40 *** (5.04)	35.74 *** (4.68)	35.39 *** (4.86)	35.42 *** (4.81)	56.54 ** (5.01)	35.14 ** (2.87)	31.29 *** (3.36)	32.62 ** (2.82)	31.71 ** (3.13)	61.33 *** (2.21)	54.30 *** (3.21)	42.06 *** (1.44)	32.20 *** (1.64)	35.91 *** (1.27)	64.62 *** (2.29)
	<b>Worst</b>	39.40	35.74	35.39	35.42	56.54	35.14	31.29	32.62	31.71	61.33	54.30	42.06	32.20	35.91	64.62
FIM	DW	42.05 *** (3.24)	37.96 *** (2.70)	38.15 *** (2.91)	37.88 *** (2.66)	56.53 ** (2.81)	26.57 ** (2.98)	27.12 *** (3.09)	27.43 *** (3.19)	26.50 *** (2.95)	68.68 *** (2.33)	44.22 *** (2.45)	42.67 *** (1.35)	32.67 *** (2.41)	33.53 *** (1.52)	61.02 *** (2.56)
	TF	35.10 *** (3.92)	32.64 *** (3.85)	32.28 *** (4.11)	32.31 *** (3.97)	59.05 ** (3.62)	32.57 ** (4.19)	33.10 *** (4.30)	33.32 *** (4.40)	32.43 *** (4.21)	61.84 *** (2.63)	59.65 *** (2.31)	48.89 *** (0.75)	47.10 *** (2.01)	43.65 *** (1.34)	43.38 *** (3.71)
	TR	47.80 *** (3.46)	41.91 *** (3.27)	41.79 ** (3.21)	41.70 ** (3.17)	52.26 ** (4.16)	40.64 ** (3.23)	39.28 ** (3.08)	39.18 ** (3.03)	39.18 ** (3.04)	54.18 ** (2.55)	66.65 ** (1.29)	48.59 ** (1.44)	47.29 ** (2.82)	46.54 ** (2.03)	42.11 *** (3.05)
	ED	25.90 *** (2.94)	23.80 *** (2.55)	23.00 *** (2.95)	23.21 *** (2.58)	72.85 ** (5.03)	20.43 ** (2.50)	20.66 ** (2.50)	19.78 ** (2.58)	19.97 ** (2.51)	77.14 *** (2.30)	47.48 ** (2.85)	42.69 ** (2.30)	32.02 *** (2.85)	34.26 *** (4.31)	64.36 *** (2.13)
	<b>Worst</b>	25.90	23.80	23.01	23.21	72.85	20.43	20.66	19.78	19.97	77.14	44.23	42.67	32.02	33.53	64.36
AT	DW	48.30 *** (2.62)	44.57 *** (3.13)	44.73 *** (2.94)	44.54 *** (3.01)	50.64 ** (3.33)	44.00 ** (2.65)	42.16 ** (3.08)	42.30 ** (2.88)	42.11 ** (2.96)	52.48 *** (2.53)	55.93 *** (2.15)	44.68 *** (1.49)	38.37 *** (2.86)	39.30 *** (1.71)	54.46 *** (3.27)
	TF	48.10 *** (2.86)	44.02 *** (3.53)	44.47 *** (3.22)	43.94 *** (3.32)	48.70 ** (2.94)	41.79 ** (3.27)	40.99 *** (3.11)	40.88 ** (3.18)	40.80 ** (3.13)	52.12 *** (2.38)	62.38 *** (1.75)	47.44 *** (1.06)	44.08 *** (2.39)	43.29 *** (1.52)	48.76 *** (3.60)
	TR	52.05 *** (2.88)	47.49 *** (3.22)	47.36 *** (3.21)	47.16 *** (3.20)	39.67 *** (3.03)	43.93 *** (2.50)	41.34 *** (2.50)	41.78 *** (2.58)	41.32 *** (2.51)	53.94 *** (2.30)	65.62 *** (2.85)	49.45 *** (2.18)	49.03 *** (4.31)	47.33 *** (4.04)	40.54

		(3.73)	(3.58)	(3.84)	(3.72)	(3.37)	(3.40)	(3.09)	(2.88)	(3.00)	(2.38)	(2.15)	(1.59)	(2.90)	(2.01)	(3.67)
	ED	34.80 <sup>***</sup> (2.73)	29.81 <sup>***</sup> (2.94)	29.89 <sup>***</sup> (2.47)	29.72 <sup>***</sup> (2.58)	63.41 <sup>***</sup> (3.36)	32.07 <sup>***</sup> (3.60)	31.28 <sup>***</sup> (3.59)	30.99 <sup>***</sup> (3.53)	31.03 <sup>***</sup> (3.52)	63.64 <sup>***</sup> (1.90)	50.22 <sup>***</sup> (3.29)	41.41 <sup>***</sup> (1.38)	30.20 <sup>***</sup> (2.63)	34.27 <sup>***</sup> (1.78)	65.11 <sup>***</sup> (2.77)
	<b>Worst</b>	34.80	29.81	29.89	29.72	63.41	32.07	31.28	30.99	31.03	63.64	50.23	41.41	30.20	34.27	65.11
	DW	51.65 <sup>***</sup> (2.60)	47.82 <sup>***</sup> (3.11)	47.92 <sup>***</sup> (2.99)	47.64 <sup>***</sup> (2.88)	46.04 <sup>***</sup> (3.27)	53.00 <sup>***</sup> (3.47)	51.54 <sup>***</sup> (3.31)	51.41 <sup>***</sup> (3.27)	51.11 <sup>***</sup> (1.79)	41.01 <sup>***</sup> (2.29)	69.53 <sup>***</sup> (1.63)	43.63 <sup>***</sup> (1.16)	40.70 <sup>***</sup> (1.15)	42.01 <sup>***</sup> (1.00)	55.21 <sup>***</sup> (1.74)
MRAT	TF	46.35 <sup>***</sup> (4.11)	41.73 <sup>***</sup> (4.66)	42.21 <sup>***</sup> (4.46)	41.68 <sup>***</sup> (4.50)	53.18 <sup>***</sup> (3.00)	63.21 <sup>***</sup> (3.17)	62.42 <sup>***</sup> (3.88)	60.86 <sup>***</sup> (3.56)	60.49 <sup>***</sup> (3.75)	31.60 <sup>**</sup> (2.32)	73.78 <sup>***</sup> (1.76)	50.79 <sup>***</sup> (1.22)	51.32 <sup>***</sup> (2.15)	49.87 <sup>***</sup> (1.72)	40.71 <sup>***</sup> (2.67)
	TR	52.20 <sup>***</sup> (5.01)	45.32 <sup>***</sup> (3.55)	45.52 <sup>***</sup> (3.63)	45.19 <sup>***</sup> (3.46)	46.52 <sup>**</sup> (2.58)	50.64 <sup>***</sup> (2.80)	45.92 <sup>***</sup> (2.22)	47.11 <sup>***</sup> (1.61)	44.05 <sup>***</sup> (1.75)	44.39 <sup>***</sup> (1.79)	73.50 <sup>***</sup> (2.22)	50.08 <sup>***</sup> (2.05)	50.16 <sup>***</sup> (3.05)	49.71 <sup>***</sup> (2.38)	44.40 <sup>***</sup> (3.04)
	ED	31.40 <sup>***</sup> (2.96)	26.33 <sup>***</sup> (2.87)	26.22 <sup>***</sup> (3.02)	26.06 <sup>***</sup> (2.45)	72.95 <sup>***</sup> (2.88)	53.71 <sup>**</sup> (3.69)	51.37 <sup>***</sup> (3.65)	51.29 <sup>***</sup> (3.23)	50.64 <sup>***</sup> (3.66)	41.51 <sup>***</sup> (1.90)	60.48 <sup>***</sup> (3.40)	42.14 <sup>***</sup> (1.32)	34.08 <sup>***</sup> (1.84)	37.66 <sup>***</sup> (1.33)	63.01 <sup>***</sup> (1.48)
	<b>Worst</b>	31.40	26.34	26.22	26.06	72.95	50.64	45.92	47.11	44.05	44.39	60.48	42.14	34.08	37.66	63.01
	DW	43.20 <sup>***</sup> (3.52)	39.29 <sup>**</sup> (3.21)	39.58 <sup>***</sup> (3.12)	39.31 <sup>***</sup> (3.14)	56.32 <sup>**</sup> (3.33)	40.93 <sup>**</sup> (4.43)	37.11 <sup>**</sup> (4.20)	38.19 <sup>**</sup> (3.83)	37.34 <sup>**</sup> (4.03)	58.34 <sup>**</sup> (2.31)	57.40 <sup>**</sup> (1.99)	43.95 <sup>**</sup> (1.33)	37.63 <sup>**</sup> (2.33)	39.28 <sup>**</sup> (1.50)	56.51 <sup>**</sup> (3.92)
FAT	TF	42.20 <sup>***</sup> (3.66)	35.82 <sup>**</sup> (3.35)	37.41 <sup>***</sup> (2.91)	36.26 <sup>***</sup> (3.11)	57.07 <sup>**</sup> (4.17)	40.14 <sup>**</sup> (3.71)	38.69 <sup>**</sup> (3.83)	38.72 <sup>**</sup> (3.74)	38.60 <sup>**</sup> (3.74)	56.85 <sup>**</sup> (1.64)	69.08 <sup>**</sup> (2.34)	51.01 <sup>**</sup> (1.53)	52.14 <sup>**</sup> (3.51)	48.70 <sup>**</sup> (2.19)	40.84 <sup>**</sup> (4.00)
	TR	52.60 <sup>***</sup> (4.19)	46.20 <sup>***</sup> (4.35)	46.35 <sup>***</sup> (4.12)	46.14 <sup>***</sup> (4.24)	43.63 <sup>***</sup> (4.66)	47.50 <sup>***</sup> (4.22)	40.89 <sup>***</sup> (4.83)	42.80 <sup>***</sup> (3.88)	40.76 <sup>***</sup> (4.17)	52.02 <sup>***</sup> (2.58)	68.15 <sup>***</sup> (1.80)	46.55 <sup>***</sup> (1.40)	44.26 <sup>***</sup> (2.46)	44.82 <sup>***</sup> (1.89)	50.36 <sup>***</sup> (2.54)
	ED	31.30 <sup>***</sup> (3.29)	27.36 <sup>**</sup> (2.97)	27.11 <sup>***</sup> (2.92)	27.01 <sup>***</sup> (2.60)	72.12 <sup>**</sup> (3.92)	31.43 <sup>**</sup> (4.12)	30.34 <sup>**</sup> (4.22)	30.18 <sup>**</sup> (4.28)	30.19 <sup>**</sup> (4.22)	66.32 <sup>**</sup> (2.29)	53.30 <sup>***</sup> (2.65)	42.93 <sup>**</sup> (1.77)	34.08 <sup>**</sup> (3.43)	36.70 <sup>**</sup> (2.09)	61.14 <sup>***</sup> (4.01)
	<b>Worst</b>	31.30	27.36	27.11	27.01	72.12	31.43	30.34	30.18	30.19	66.32	53.30	42.93	34.08	36.70	61.14
	DW	78.65 <sup>***</sup> (3.01)	78.20 <sup>**</sup> (3.22)	76.29 <sup>**</sup> (3.11)	76.82 <sup>**</sup> (3.13)	16.02 <sup>**</sup> (2.70)	73.93 <sup>**</sup> (2.78)	76.77 <sup>**</sup> (2.46)	70.83 <sup>**</sup> (2.45)	70.94 <sup>**</sup> (2.84)	23.48 <sup>**</sup> (2.06)	84.65 <sup>**</sup> (1.53)	64.09 <sup>**</sup> (3.05)	65.02 <sup>**</sup> (2.92)	64.47 <sup>**</sup> (2.85)	23.17 <sup>**</sup> (3.46)
LLM-SGA (single)	TF	74.55 <sup>***</sup> (3.52)	73.66 <sup>**</sup> (3.71)	73.11 <sup>**</sup> (3.41)	73.17 <sup>**</sup> (3.50)	16.36 <sup>**</sup> (2.38)	68.86 <sup>**</sup> (2.99)	70.71 <sup>**</sup> (2.86)	65.56 <sup>**</sup> (2.41)	65.00 <sup>**</sup> (3.05)	29.33 <sup>**</sup> (1.82)	85.25 <sup>**</sup> (1.49)	60.68 <sup>**</sup> (2.31)	61.96 <sup>**</sup> (2.73)	61.15 <sup>**</sup> (2.29)	28.28 <sup>**</sup> (3.07)
	TR	70.60 <sup>***</sup> (4.27)	67.20 <sup>**</sup> (4.86)	67.25 <sup>**</sup> (4.78)	67.07 <sup>**</sup> (4.81)	23.34 <sup>**</sup> (3.55)	65.57 <sup>**</sup> (3.11)	67.58 <sup>**</sup> (3.39)	61.36 <sup>**</sup> (2.13)	59.83 <sup>**</sup> (2.70)	32.67 <sup>**</sup> (1.61)	82.03 <sup>**</sup> (2.07)	54.67 <sup>**</sup> (2.93)	53.06 <sup>**</sup> (1.85)	53.33 <sup>**</sup> (2.21)	41.96 <sup>**</sup> (3.29)
	ED	67.50 <sup>***</sup> (2.26)	65.75 <sup>**</sup> (2.56)	66.09 <sup>**</sup> (2.53)	65.68 <sup>**</sup> (2.58)	31.91 <sup>**</sup> (4.59)	65.43 <sup>**</sup> (2.52)	64.77 <sup>**</sup> (3.44)	61.34 <sup>**</sup> (2.84)	60.77 <sup>**</sup> (3.25)	34.06 <sup>**</sup> (1.67)	77.05 <sup>**</sup> (3.34)	52.10 <sup>**</sup> (2.50)	52.81 <sup>**</sup> (3.37)	52.01 <sup>**</sup> (2.90)	41.33 <sup>**</sup> (3.67)
	<b>Worst</b>	<b>67.50</b>	<b>65.75</b>	<b>66.09</b>	<b>65.68</b>	<b>31.91</b>	<b>65.43</b>	<b>64.77</b>	<b>61.34</b>	<b>60.77</b>	<b>34.06</b>	<b>77.05</b>	<b>52.10</b>	<b>52.81</b>	<b>52.01</b>	<b>41.96</b>
	DW	73.85 <sup>***</sup> (3.34)	72.48 <sup>***</sup> (3.44)	71.34 <sup>***</sup> (3.54)	71.67 <sup>***</sup> (3.54)	24.23 <sup>**</sup> (3.57)	64.07 <sup>**</sup> (3.86)	63.49 <sup>***</sup> (4.07)	63.45 <sup>***</sup> (4.04)	63.38 <sup>***</sup> (4.01)	31.71 <sup>***</sup> (2.59)	75.03 <sup>***</sup> (1.44)	56.08 <sup>**</sup> (1.57)	60.62 <sup>**</sup> (2.64)	56.32 <sup>***</sup> (1.93)	32.74 <sup>***</sup> (3.59)
ARText	TF	73.55 <sup>**</sup> (3.62)	72.81 <sup>**</sup> (4.19)	71.29 <sup>**</sup> (4.06)	71.61 <sup>**</sup> (4.08)	21.35 <sup>***</sup> (3.20)	70.29 <sup>***</sup> (2.73)	69.59 <sup>***</sup> (2.83)	69.38 <sup>**</sup> (2.96)	69.39 <sup>***</sup> (2.88)	31.63 <sup>***</sup> (1.86)	85.08 <sup>***</sup> (1.45)	66.48 <sup>***</sup> (2.42)	73.61 <sup>***</sup> (2.55)	68.81 <sup>*</sup> (2.51)	14.84 <sup>***</sup> (3.21)
	TR	74.55 <sup>***</sup> (2.86)	71.78 <sup>***</sup> (3.34)	69.73 <sup>**</sup> (3.90)	70.29 <sup>***</sup> (3.82)	23.59 <sup>***</sup> (4.03)	70.00 <sup>**</sup> (2.97)	69.64 <sup>***</sup> (3.06)	68.39 <sup>***</sup> (2.97)	68.55 <sup>***</sup> (3.05)	28.30 <sup>***</sup> (2.59)	82.28 <sup>***</sup> (1.46)	59.90 <sup>**</sup> (2.17)	61.09 <sup>***</sup> (2.13)	60.32 <sup>**</sup> (2.04)	24.92 <sup>***</sup> (3.28)
	ED	70.20 <sup>***</sup> (3.85)	68.31 <sup>***</sup> (4.20)	67.04 <sup>**</sup> (4.20)	67.28 <sup>***</sup> (4.27)	26.97 <sup>**</sup> (3.66)	62.57 <sup>**</sup> (3.70)	61.72 <sup>***</sup> (3.75)	61.17 <sup>***</sup> (3.51)	61.17 <sup>***</sup> (3.54)	33.16 <sup>**</sup> (3.58)	81.35 <sup>***</sup> (2.39)	60.84 <sup>***</sup> (3.19)	65.01 <sup>**</sup> (4.57)	62.03 <sup>***</sup> (3.60)	31.25 <sup>***</sup> (5.02)
	<b>Worst</b>	70.20	68.31	67.04	67.28	26.97	62.57	61.72	61.17	61.17	33.16	75.03	56.08	<b>60.62</b>	56.32	32.74
	DW	77.50 <sup>***</sup> (3.24)	76.55 <sup>***</sup> (3.56)	75.36 <sup>***</sup> (3.18)	75.74 <sup>***</sup> (3.25)	21.04 <sup>**</sup> (3.33)	61.07 <sup>**</sup> (3.82)	60.46 <sup>***</sup> (4.39)	58.37 <sup>***</sup> (3.67)	57.31 <sup>***</sup> (4.15)	34.12 <sup>***</sup> (2.54)	85.08 <sup>***</sup> (1.03)	60.50 <sup>**</sup> (4.04)	54.94 <sup>***</sup> (1.64)	55.75 <sup>***</sup> (2.13)	39.66 <sup>**</sup> (2.61)
ARDEL	TF	77.00 <sup>***</sup> (3.04)	76.38 <sup>**</sup> (3.49)	75.21 <sup>**</sup> (3.59)	75.52 <sup>**</sup> (3.54)	18.75 <sup>***</sup> (3.27)	68.93 <sup>**</sup> (3.07)	68.46 <sup>***</sup> (3.31)	66.95 <sup>***</sup> (3.32)	67.04 <sup>***</sup> (3.42)	30.43 <sup>***</sup> (2.98)	89.90 <sup>**</sup> (1.19)	75.72 <sup>**</sup> (4.46)	60.85 <sup>***</sup> (2.96)	64.03 <sup>***</sup> (3.65)	30.25 <sup>**</sup> (4.16)
	TR	72.10 <sup>***</sup> (2.83)	69.10 <sup>***</sup> (3.75)	68.74 <sup>***</sup> (3.41)	68.74 <sup>***</sup> (3.35)	20.18 <sup>***</sup> (3.48)	69.79 <sup>***</sup> (3.01)	69.71 <sup>***</sup> (3.48)	67.95 <sup>***</sup> (3.22)	68.03 <sup>**</sup> (3.29)	23.48 <sup>*</sup> (2.67)	88.58 <sup>***</sup> (1.31)	73.10 <sup>***</sup> (7.83)	57.03 <sup>**</sup> (2.45)	59.11 <sup>**</sup> (3.53)	40.27 <sup>**</sup> (2.95)
	ED	72.35 <sup>**</sup> (4.69)	70.60 <sup>**</sup> (5.30)	69.64 <sup>*</sup> (5.46)	69.82 <sup>*</sup> (5.35)	26.95 <sup>***</sup> (3.73)	63.21 <sup>***</sup> (3.89)	62.46 <sup>***</sup> (3.46)	61.46 <sup>***</sup> (3.61)	61.35 <sup>***</sup> (3.46)	33.75 <sup>***</sup> (2.69)	86.90 <sup>**</sup> (2.52)	59.48 <sup>***</sup> (2.08)	52.77 <sup>***</sup> (2.32)	52.60 <sup>***</sup> (3.66)	44.24 <sup>**</sup> (3.28)
	<b>Worst</b>	72.10	69.10	68.74	68.74	26.95	61.07	60.46	58.37	57.31	34.12	85.08	59.48	52.77	52.60	44.24
	DW	79.10 <sup>***</sup> (2.75)	78.84 <sup>***</sup> (2.92)	76.77 <sup>***</sup> (2.88)	77.36 <sup>***</sup> (2.88)	17.07 <sup>***</sup> (2.92)	71.43 <sup>***</sup> (3.37)	71.05 <sup>***</sup> (3.46)	71.11 <sup>**</sup> (3.51)	70.99 <sup>**</sup> (3.43)	24.48 <sup>***</sup> (1.89)	79.03 <sup>***</sup> (1.32)	56.53 <sup>***</sup> (2.16)	58.69 <sup>***</sup> (2.60)	57.10 <sup>***</sup> (2.36)	33.50 <sup>***</sup> (3.55)
EnsSel	TF	79.20 <sup>*</sup> (2.59)	78.69 <sup>*</sup> (2.54)	77.75 <sup>*</sup> (2.69)	78.02 <sup>*</sup> (2.65)	15.96	77.71 <sup>*</sup> (2.80)	77.62	77.19 <sup>***</sup> (2.83)	77.23 <sup>***</sup> (2.75)	22.44 <sup>***</sup> (2.78)	87.00 <sup>***</sup> (1.96)	66.55 <sup>***</sup> (1.48)	68.30 <sup>**</sup> (3.89)	67.24 <sup>**</sup> (3.75)	21.72 <sup>***</sup> (3.95)
	TR	77.55 <sup>***</sup> (3.05)	75.32 <sup>**</sup> (3.33)	73.64 <sup>**</sup> (3.41)	74.21 <sup>**</sup> (3.36)	24.43 <sup>***</sup> (3.58)	71.21 <sup>**</sup> (2.59)	71.19 <sup>***</sup> (3.42)	68.90 <sup>**</sup> (3.27)	69.05 <sup>**</sup> (3.27)	27.87 <sup>***</sup> (1.85)	84.12 <sup>**</sup> (1.61)	62.64 <sup>**</sup> (2.85)	63.38 <sup>**</sup> (2.76)	62.83 <sup>**</sup> (2.47)	30.74 <sup>**</sup> (3.98)
	ED	74.85 <sup>***</sup> (3.08)	73.57 <sup>**</sup> (3.52)	71.19 <sup>**</sup> (3.17)	71.66 <sup>**</sup> (3.10)	21.86 <sup>*</sup> (2.72)	67.14 <sup>**</sup> (3.62)	66.37 <sup>**</sup> (3.89)	65.56 <sup>**</sup> (3.90)	65.62 <sup>**</sup> (3.93)	26.81 <sup>*</sup> (2.69)	80.17 <sup>***</sup> (1.72)	57.06 <sup>***</sup> (2.10)	59.29 <sup>**</sup> (3.60)	57.73 <sup>***</sup> (4.66)	35.49 <sup>**</sup> (4.82)
	<b>Worst</b>	74.85	73.57	71.19	71.66	24.43	67.14	66.37	65.56	65.62	27.87	79.03	56.53	58.69	57.10	35.49
LLM-SGA (multiple)	DW	87.45 <sup>***</sup> (2.04)	87.00 <sup>***</sup> (2.20)	86.32 <sup>***</sup> (2.43)	86.58 <sup>***</sup> (2.29)	12.08 <sup>***</sup> (2.47)	77.21 <sup></sup>									

TF	77.15 (3.10)	76.67 (3.26)	75.35 (3.08)	75.69 (3.17)	15.22 (1.99)	75.50 (3.12)	79.54 (3.28)	72.25 (3.20)	72.42 (3.65)	26.20 (2.08)	90.22 (1.37)	75.50 (3.97)	68.52 (3.86)	71.00 (3.59)	25.92 (3.45)
TR	78.25 (2.95)	76.33 (3.43)	73.93 (3.88)	74.68 (3.66)	14.95 (2.91)	74.50 (2.14)	79.77 (2.17)	71.20 (1.77)	71.09 (2.14)	25.27 (2.60)	85.50 (1.17)	60.60 (4.30)	56.93 (2.66)	58.00 (3.19)	30.98 (3.27)
ED	76.40 (4.16)	75.68 (4.42)	73.37 (4.48)	73.91 (4.44)	19.68 (3.74)	73.57 (1.99)	77.59 (2.69)	70.66 (2.25)	70.47 (2.32)	24.80 (3.25)	88.17 (2.33)	71.30 (5.19)	66.76 (4.11)	68.23 (4.22)	29.86 (5.89)
<b>Worst</b>	<b>76.40</b>	<b>75.68</b>	<b>73.37</b>	<b>73.91</b>	<b>19.68</b>	<b>73.57</b>	<b>77.59</b>	<b>70.66</b>	<b>70.47</b>	<b>26.20</b>	<b>85.50</b>	<b>60.60</b>	<b>56.93</b>	<b>58.00</b>	<b>30.98</b>

Note: DW: DeepWordBug, TF: TFAjusted, TR: TREPAT, ED: ExplainDrive. Same below.

## R.2 Experiment 2: Accuracy Comparison

In this section, we report the results of Experiment 2 on the other two datasets: ETHOS and the White Supremacist datasets.

### R.2.1 Results of Experiment 2.1 on the ETHOS and White Supremacist Datasets (Comparison with Baselines in Defending Known and New Attacks)

Table R2 shows the comparison results with baselines in defending known attacks and new attacks on the ETHOS and White Supremacist datasets. Across both scenarios, our method outperforms all enhanced baselines and achieves the best performance. Specifically, for known attacks, compared to the baseline (LLM-puri (Enhanced)), Ours (LB) improves the after-attack accuracy, and F1-score by 5.5% and 9.1% on the ETHOS dataset, and by 1.8% and 13.0% on the White Supremacist dataset, respectively. For new attacks, Ours (MC) improves the after-attack F1-score from 73.77% (SAFER (Enhanced)) to 75.16% on the ETHOS dataset and from 65.01% (EnsSel (Enhanced)) to 74.10% on the White Supremacist dataset. It also reduces the ASR from 24.70% (ARText (Enhanced)) to 23.08% on the ETHOS dataset and from 24.98% (FIM (Enhanced)) to 21.89% on the White Supremacist dataset.

**Table R2. Results of Comparison with Baselines in Defending Known and New Attacks**

Attack Scenario	Method	ETHOS Dataset				White Supremacist Dataset				ASR $\downarrow$ (%)	
		Performance after attack $\uparrow$ (%)			ASR $\downarrow$ (%)	Performance after attack $\uparrow$ (%)					
		Accuracy	Precision	Recall		Accuracy	Precision	Recall	F1-score		
Known Attacks (DW, TF, TR)	LLM-puri (Enhanced)	75.25*** (2.24)	<b>80.51</b> <b>(2.45)</b>	71.88*** (2.54)	71.92*** (2.94)	26.31*** (3.56)	89.55*** (0.52)	74.75*** (1.92)	66.26*** (1.59)	69.22*** (1.71)	27.98*** (1.30)
	Det&Res (Enhanced)	74.35*** (3.12)	74.39*** (3.49)	72.83*** (3.13)	73.15*** (3.22)	22.36*** (3.59)	85.79*** (0.47)	65.74*** (1.08)	66.70*** (1.39)	66.18*** (1.19)	26.87*** (1.38)
	OutReg (Enhanced)	72.95*** (2.42)	74.65*** (2.70)	70.27*** (2.61)	70.44*** (2.82)	26.00*** (2.87)	84.94*** (0.44)	64.74*** (0.93)	67.02*** (1.30)	65.73*** (1.05)	25.72*** (1.34)
	FIM (Enhanced)	65.40*** (2.52)	65.39*** (2.34)	65.64*** (2.38)	65.18*** (2.47)	28.78*** (4.32)	83.09*** (0.76)	63.50*** (1.18)	68.52*** (1.54)	65.23*** (1.33)	22.46*** (1.70)
	AT (Enhanced)	73.40*** (3.94)	73.00*** (4.10)	72.37*** (3.97)	72.55*** (4.01)	24.47*** (3.74)	86.27*** (0.43)	67.03*** (0.81)	68.45*** (1.04)	67.68*** (0.83)	25.73*** (1.12)
	MRAT (Enhanced)	74.10*** (1.97)	74.38*** (2.10)	72.33*** (2.14)	72.65*** (2.18)	22.42*** (3.00)	87.28*** (0.44)	66.74*** (1.52)	61.89*** (1.24)	63.65*** (1.36)	30.94*** (2.01)

	ARText (Enhanced)	70.85*** (2.81)	70.34*** (2.97)	69.73*** (2.94)	69.87*** (2.96)	22.73*** (1.96)	87.56*** (0.50)	69.25*** (1.25)	68.37*** (1.26)	68.79*** (1.20)	23.97*** (1.64)
	ARDEL (Enhanced)	70.20*** (3.78)	69.68*** (3.90)	69.18*** (3.82)	69.28*** (3.87)	24.47*** (3.74)	88.18*** (0.35)	69.02*** (1.60)	60.08*** (1.18)	62.49*** (1.39)	25.73*** (1.12)
	EnsSel (Enhanced)	71.65*** (3.94)	71.42*** (4.19)	70.21*** (4.03)	70.40*** (4.11)	26.28*** (2.67)	86.49*** (0.73)	67.10*** (1.68)	67.55*** (1.79)	67.31*** (1.70)	24.52*** (1.21)
	Ours (MC)	79.30 (2.36)	79.68 (2.32)	77.92 (2.62)	78.33 (2.59)	17.86 (3.08)	91.11 (0.51)	78.22 (1.30)	78.11 (1.67)	78.14 (1.34)	16.62 (1.94)
	Ours (LB)	<b>79.40</b> <b>(2.21)</b>	79.78 (2.13)	<b>78.03</b> <b>(2.48)</b>	<b>78.45</b> <b>(2.44)</b>	<b>17.45</b> <b>(2.70)</b>	<b>91.13</b> <b>(0.54)</b>	<b>78.28</b> <b>(1.37)</b>	<b>78.18</b> <b>(1.70)</b>	<b>78.21</b> <b>(1.40)</b>	<b>16.47</b> <b>(1.98)</b>
New Attacks (ED)	LLM-puri (Enhanced)	72.50*** (2.93)	75.46 (3.79)	69.37*** (3.17)	69.27*** (3.73)	29.40*** (3.97)	88.40*** (0.41)	70.29*** (1.72)	62.03*** (1.09)	64.58*** (1.26)	35.58*** (1.43)
	Det&Res (Enhanced)	69.15*** (2.98)	68.68*** (3.31)	67.64*** (2.93)	67.82*** (3.01)	28.46*** (3.73)	84.83*** (0.56)	63.65*** (1.29)	64.67*** (1.69)	64.11*** (1.44)	28.83*** (1.59)
	SAFER (Enhanced)	74.25* (2.97)	73.84* (3.05)	73.83 (2.87)	73.77 (2.94)	25.42* (2.19)	79.04*** (0.78)	60.99*** (0.95)	68.55*** (1.63)	62.52*** (1.17)	25.12*** (2.14)
	MASKFil (Enhanced)	71.45*** (2.63)	71.59*** (2.93)	69.46*** (2.77)	69.69*** (2.89)	26.99*** (2.22)	83.63*** (0.74)	61.97*** (1.50)	63.83*** (1.90)	62.76*** (1.65)	31.27*** (1.60)
	FTML (Enhanced)	71.60*** (4.11)	71.21*** (4.38)	70.42*** (4.15)	70.59*** (4.23)	28.34*** (2.65)	84.21*** (0.63)	62.39*** (1.30)	63.45*** (1.51)	62.87*** (1.36)	29.04*** (1.84)
	OutReg (Enhanced)	73.00*** (1.78)	74.22* (2.27)	70.58*** (1.89)	70.81*** (2.00)	25.00 (3.32)	83.61*** (0.51)	61.16*** (1.29)	62.27*** (1.57)	61.66*** (1.40)	31.80*** (1.70)
	FIM (Enhanced)	63.95*** (2.68)	64.31*** (2.53)	64.52*** (2.57)	63.83*** (2.63)	28.94*** (2.45)	81.25*** (0.65)	61.19*** (0.93)	66.16*** (1.29)	62.70*** (1.07)	24.98*** (2.20)
	AT (Enhanced)	69.10*** (3.45)	68.51*** (3.59)	68.21*** (3.44)	68.28*** (3.48)	28.87*** (3.79)	84.66*** (0.49)	63.41*** (1.29)	64.63*** (1.75)	63.97*** (1.47)	29.93*** (1.36)
	MRAT (Enhanced)	71.75*** (2.27)	71.65*** (2.51)	70.02*** (2.33)	70.28*** (2.41)	25.60* (2.26)	86.80*** (0.57)	64.97*** (1.99)	60.49*** (1.52)	62.07*** (1.72)	33.56*** (2.38)
	FAT (Enhanced)	69.40*** (3.68)	68.95*** (3.76)	69.07*** (3.85)	68.91*** (3.80)	26.19* (3.59)	83.57*** (0.52)	61.32*** (1.23)	62.63*** (1.60)	61.90*** (1.37)	31.04*** (2.13)
	ARText (Enhanced)	69.35*** (2.35)	68.79*** (2.46)	68.60*** (2.40)	68.62*** (2.40)	24.70 (3.45)	85.71*** (0.40)	64.84*** (0.78)	64.64*** (0.78)	64.73*** (0.70)	28.42*** (1.38)
	ARDEL (Enhanced)	69.65*** (3.72)	69.10*** (3.86)	69.01*** (3.92)	68.98*** (3.87)	28.87*** (3.79)	87.38*** (0.46)	64.86*** (2.35)	57.43*** (1.49)	59.16*** (1.88)	29.93*** (1.36)
	EnsSel (Enhanced)	72.10*** (2.38)	71.60*** (2.48)	71.26*** (2.50)	71.34*** (2.47)	27.14*** (2.45)	85.41*** (0.50)	64.70*** (1.11)	65.37*** (1.24)	65.01*** (1.14)	26.50*** (1.20)
	Ours (MC)	75.60 (2.44)	75.39 (2.61)	74.46 (2.44)	74.72 (2.49)	23.38 (3.95)	<b>89.46</b> <b>(0.58)</b>	<b>74.17</b> <b>(1.43)</b>	<b>74.16</b> <b>(1.54)</b>	<b>74.15</b> <b>(1.40)</b>	<b>21.75</b> <b>(1.34)</b>
	Ours (LB)	<b>76.00</b> <b>(2.34)</b>	<b>75.79</b> <b>(2.48)</b>	<b>74.91</b> <b>(2.39)</b>	<b>75.16</b> <b>(2.42)</b>	<b>23.08</b> <b>(3.89)</b>	89.45 (0.60)	74.15 (1.48)	74.09 (1.55)	74.10 (1.42)	21.89 (1.29)

## R.2.2 Results of Experiment 2.2 on the ETHOS and White Supremacist Datasets (Ablation Analysis in Defending Known and New Attacks)

Table R3 shows the results of ablation analysis in defending known attacks and new attacks on the ETHOS and White Supremacist datasets. The general conclusions are similar to those of the PHEME dataset in the manuscript. Generally speaking, the elimination of any component leads to a significant performance decrease, proving the effectiveness of each component.

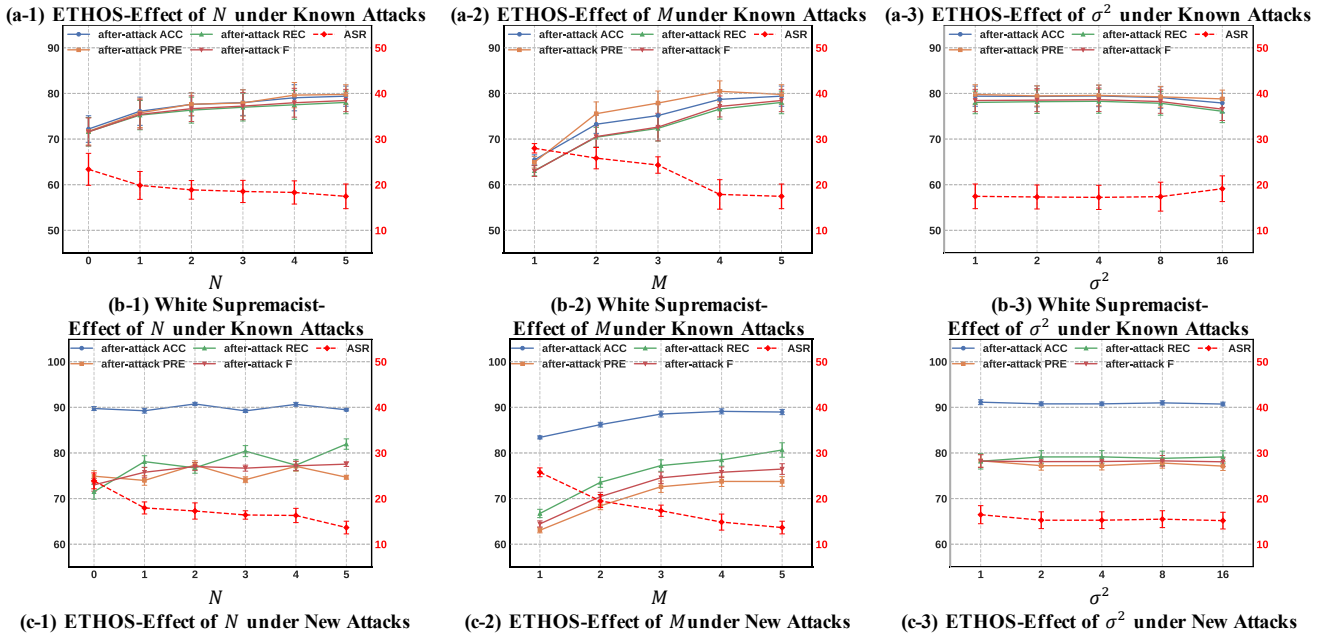
**Table R3. Results of Ablation Analysis in Defending Known and New Attacks**

Attack Scenario	Method	ETHOS Dataset				White Supremacist Dataset				ASR $\downarrow$ (%)		
		Performance after attack $\uparrow$ (%)				Performance after attack $\uparrow$ (%)						
		Accuracy	Precision	Recall	F1-score							
Known Attacks (DW, TF, TR)	Ours w/o ME	BERT	62.10*** (1.65)	61.46*** (2.17)	58.76*** (1.76)	57.73*** (2.02)	36.30*** (1.80)	83.41*** (0.33)	63.06*** (0.57)	66.74*** (0.91)	64.45*** (0.67)	25.76*** (0.97)
		DistilBERT	65.45*** (1.10)	64.93*** (1.28)	63.08*** (1.13)	62.99*** (1.19)	27.98*** (1.03)	83.80*** (0.47)	64.70*** (0.71)	70.07*** (0.88)	66.60*** (0.78)	19.77*** (0.85)
		RoBERTa	70.05*** (1.28)	70.14*** (1.41)	67.90*** (1.41)	68.06*** (1.48)	22.83*** (1.70)	84.86*** (0.42)	66.54*** (0.71)	72.46*** (0.95)	68.68*** (0.80)	19.27*** (1.12)
		XLNet	68.20*** (1.54)	69.09*** (1.82)	65.24*** (1.71)	64.96*** (1.93)	28.44*** (1.82)	85.58*** (0.46)	67.16*** (0.81)	71.88*** (1.00)	69.01*** (0.87)	22.08*** (1.28)
		ALBERT	70.10*** (1.65)	71.91*** (2.26)	67.03*** (1.70)	66.84*** (1.87)	24.58*** (2.10)	86.05*** (0.35)	65.64*** (0.86)	65.42*** (0.97)	65.52*** (0.89)	30.07*** (1.13)
	Ours w/o prior	Ours w/o prior	76.90** (2.49)	79.13 (2.21)	74.45*** (2.90)	74.88*** (3.04)	22.72*** (3.03)	90.74** (0.19)	77.46* (0.53)	75.74*** (0.83)	76.55*** (0.55)	19.69*** (1.07)
		Ours w/o data	77.85* (2.21)	79.70 (1.87)	75.62** (2.59)	76.12** (2.67)	21.29*** (3.03)	90.77* (0.25)	77.38* (0.67)	77.48 (1.12)	77.41* (0.69)	17.69* (1.16)
		Ours w/ FEL	77.25** (2.24)	79.09 (2.09)	74.97*** (2.59)	75.45*** (2.66)	21.88*** (3.00)	90.51*** (0.21)	76.72*** (0.53)	76.95* (1.09)	76.82*** (0.66)	18.11** (1.07)
	Ours w/ CBW-D	Ours w/ CBW-D	78.00* (2.00)	79.45 (1.98)	75.93** (2.24)	76.45* (2.28)	20.91*** (2.83)	90.94 (0.30)	77.94 (0.85)	76.77** (0.90)	77.32* (0.61)	18.24** (1.76)
		Ours w/ Prob-prior	78.05* (1.93)	78.78 (1.79)	76.35* (2.22)	76.81* (2.23)	20.16** (2.06)	90.75* (0.33)	77.32* (0.89)	77.60 (1.06)	77.44* (0.74)	17.19 (0.95)
		Ours w/ ES	77.90* (2.15)	79.33 (1.93)	75.84** (2.48)	76.34* (2.57)	19.79* (2.99)	90.83 (0.53)	77.71 (1.42)	76.01*** (1.45)	76.80** (1.30)	19.23*** (1.40)
	Ours w/o IAT	Ours w/o IAT	77.95 (2.67)	80.42 (2.93)	75.50** (2.86)	76.04** (3.02)	21.03*** (3.45)	87.69*** (3.43)	71.58*** (3.43)	71.37*** (5.40)	69.91*** (4.17)	23.58*** (1.33)
		Ours w/ AT	77.75* (1.89)	77.74** (1.90)	76.61 (2.08)	76.90* (2.07)	19.61** (2.28)	87.01*** (0.53)	70.27*** (0.86)	76.98* (1.04)	72.80*** (0.90)	17.28 (0.66)
		Ours (MC)	79.30 (2.36)	79.68 (2.32)	77.92 (2.62)	78.33 (2.59)	17.86 (3.08)	91.11 (0.51)	78.22 (1.30)	78.11 (1.67)	78.14 (1.34)	16.62 (1.94)
	Ours (LB)	<b>79.40</b> (2.21)	<b>79.78</b> (2.13)	<b>78.03</b> (2.48)	<b>78.45</b> (2.44)	<b>17.45</b> (2.70)	<b>91.13</b> (0.54)	<b>78.28</b> (1.37)	<b>78.18</b> (1.70)	<b>78.21</b> (1.40)	<b>16.47</b> (1.98)	
New Attacks (ED)	Ours w/o ME	BERT	60.00*** (1.41)	58.62*** (1.82)	56.83*** (1.44)	55.86*** (1.58)	38.60*** (1.32)	77.12*** (0.40)	56.89*** (0.39)	61.07*** (0.57)	57.60*** (0.48)	33.42*** (0.70)
		DistilBERT	53.25*** (1.65)	51.12*** (1.80)	51.02*** (1.64)	50.61*** (1.70)	41.59*** (1.93)	75.12*** (0.50)	53.39*** (0.64)	55.37*** (1.03)	53.39*** (0.77)	38.76*** (1.24)
		RoBERTa	53.80*** (1.99)	51.66*** (2.17)	51.49*** (1.95)	51.04*** (1.99)	42.70*** (2.05)	80.64*** (0.37)	61.49*** (0.39)	67.74*** (0.56)	63.15*** (0.47)	24.88*** (0.52)
		XLNet	65.60*** (2.23)	65.21*** (2.64)	63.14*** (2.30)	63.00*** (2.44)	31.07*** (2.28)	80.80*** (0.36)	61.13*** (0.70)	65.64*** (1.18)	62.54*** (0.83)	29.71*** (1.57)
		ALBERT	62.95*** (1.96)	62.44*** (2.52)	59.80*** (2.05)	59.04*** (2.28)	34.59*** (2.10)	79.28*** (0.53)	54.47*** (0.67)	55.55*** (0.83)	54.81*** (0.73)	42.84*** (1.00)
	Ours w/o prior	Ours w/o prior	72.50*** (2.48)	73.46** (2.77)	70.11*** (2.68)	70.32*** (2.88)	25.52* (3.33)	89.03* (0.53)	72.98* (1.42)	71.38*** (1.57)	72.13*** (1.45)	23.91*** (1.31)
		Ours w/o data	74.40* (2.64)	75.23 (2.88)	72.30** (2.85)	72.64** (3.00)	24.42 (3.34)	88.99** (0.32)	73.03** (0.79)	73.53 (1.38)	73.27* (1.02)	22.42 (0.68)
		Ours w/ FEL	72.90*** (2.20)	73.74* (2.53)	70.63*** (2.33)	70.89*** (2.46)	25.28 (3.38)	88.64*** (0.51)	72.15*** (1.28)	72.42** (1.81)	72.27*** (1.48)	22.90** (0.89)
	Ours w/ CBW-D	Ours w/ CBW-D	73.85** (2.54)	74.66 (2.78)	71.71*** (2.76)	72.01*** (2.92)	24.24 (2.93)	89.11 (0.58)	73.26 (1.46)	72.59** (1.47)	72.91* (1.41)	22.91* (1.32)
		Ours w/ Prob-	73.95* (2.48)	73.99* (2.48)	72.37** (2.48)	72.66** (2.48)	25.31* (2.48)	88.67*** (0.54)	72.33*** (1.37)	73.22 (1.70)	72.74** (1.40)	22.53* (1.98)

	prior	(2.48)	(2.66)	(2.68)	(2.73)	(2.66)	(0.53)	(1.24)	(1.67)	(1.35)	(0.49)
Ours	w/ ES	73.35*** (2.06)	73.60** (2.17)	71.52*** (2.29)	71.81*** (2.35)	24.37 (3.31)	89.23 (0.59)	73.54 (1.49)	72.20*** (1.67)	72.81** (1.45)	24.07*** (2.21)
	w/o IAT	74.75 (2.67)	75.14 (2.85)	72.95* (2.87)	73.30* (2.94)	24.39 (3.56)	86.12*** (0.64)	66.34*** (1.39)	66.98*** (1.37)	66.64*** (1.34)	27.08*** (2.28)
	w/ AT	74.15* (2.66)	73.76* (2.73)	73.34 (2.81)	73.43* (2.78)	25.11* (1.82)	84.47*** (0.83)	66.59*** (1.23)	73.79 (1.59)	68.99*** (1.36)	22.72* (0.89)
	(MC)	75.60 (2.44)	75.39 (2.61)	74.46 (2.44)	74.72 (2.49)	23.38 (3.95)	89.46 (0.58)	74.17 (1.43)	74.16 (1.43)	74.15 (1.54)	21.75 (1.34)
	(LB)	76.00 (2.34)	75.79 (2.48)	74.91 (2.39)	75.16 (2.42)	23.08 (3.89)	89.45 (0.60)	74.15 (1.48)	74.09 (1.55)	74.10 (1.42)	21.89 (1.29)

### R.2.3 Results of Experiment 2.3 on the ETHOS and White Supremacist Datasets (Sensitivity Analysis in Defending Known and New Attacks)

Figure R1 shows the results of sensitivity analysis in defending known attacks and new attacks on the ETHOS and White Supremacist datasets. The general conclusions are similar to that of the PHEME dataset in the manuscript. First, increasing either the number of generated samples ( $N$ ) or the number of base detectors ( $M$ ) leads to improved after-attack performance and reduced ASR. As the White Supremacist dataset is highly imbalanced (with a ratio of 1:7.6), the results exhibit certain fluctuations; however, the overall trend shows an increase in F1-score and a decrease in ASR. Second,  $\sigma^2$  of the log-normal distribution does not significantly affect the performance in both scenarios.



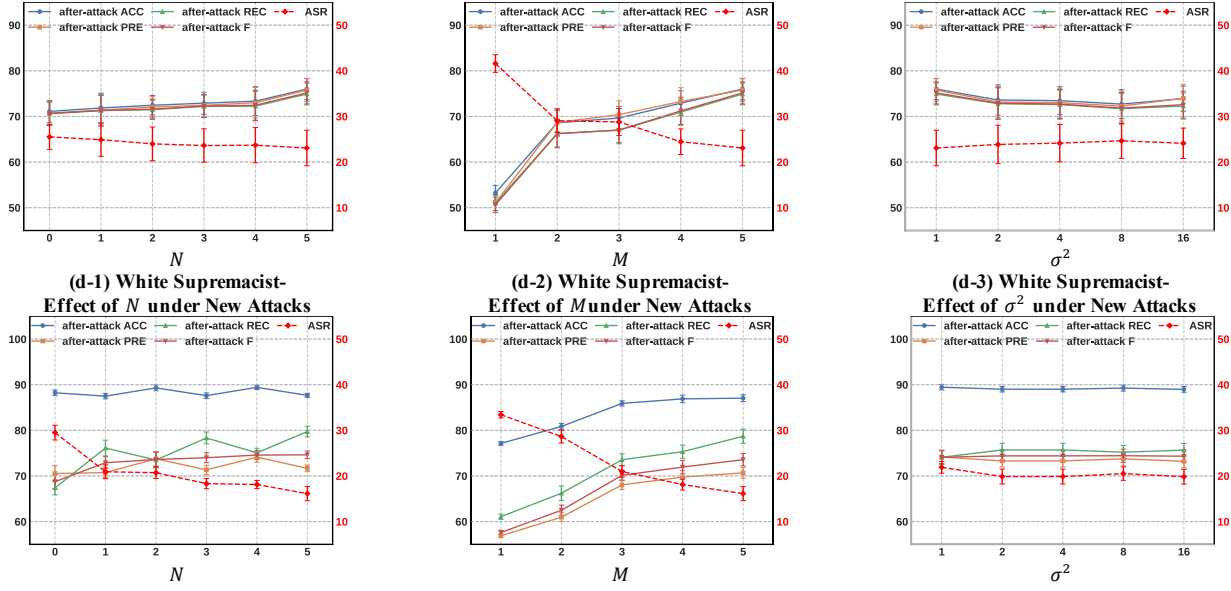


**Figure R1. Results of Sensitivity Analysis in Defending Known and New Attacks**

## Appendix S: Details of Enhancements of Baselines

For passive defense baselines, since both LLM-puri and Det&Res can generate samples, we used their own processes for sample generation. However, they lack multiple base detectors and the aggregation process. Thus, we introduced the same five base detectors and the aggregation was then performed using the CBW-D method. We also updated the base detectors for the passive defense baselines using AT (Goodfellow et al. 2015) to maintain fairness.

For random noise-based methods (SAFER, MASKFil), which inherently generate multiple samples, we similarly employed the five base detectors and used CBW-D for aggregation. As both methods involve parameter updating, we adopted their own training procedures.

For adversarial training-based methods (AT, MRAT, FAT), the enhancement process followed the same procedure as the regularization-based methods described in the manuscript.

For ensemble model-based methods (ARText, ARDEL, EnsSel), sample generation in ARTtext and EnsSel again adopted SAFER, whereas ARDEL followed its own procedure, employing random word masking for sample generation. We used the same five base detectors but retained their own aggregation strategies for prediction. All the three methods involve AT, so we followed their own training methods.

## Appendix T: Details of Variants in Ablation Study

### Variants in examine the two-dimensional ensemble (Design Component 1)

- (1) Ours w/o ME: In this variant, we used only one detector (BERT, DistilBERT, RoBERTa, XLNet, or ALBERT), and thus performed aggregation only along samples. Specifically, for each input sample, we obtained a one-dimensional prediction vector consisting of the predicted probabilities for the original sample  $x_0$  and its generated samples  $\hat{x}_1, \hat{x}_2, \dots, \hat{x}_N$ . In this setting, as our variance-based prior cannot be applied, the predictions were aggregated using equal weights.

### Variants in examine the weight assignment method (Design Component 2)

- (1) Ours w/o prior: In this variant, we removed the variance-based prior. Hence, the weight assignor was trained without domain knowledge and thus was optimized directly based on data.
- (2) Ours w/o data: In this variant, we removed the data-driven refinement process. Specifically, the assigned weights were directly drawn from the prior distribution (i.e.,  $p(\tilde{w}_{m,n})$ ).
- (3) Ours w/ FEL: In our context, the samples  $\hat{x}_1, \hat{x}_2, \dots, \hat{x}_N$  were generated at runtime, and thus their weights cannot be predetermined. Therefore, we replaced our weight assignment method with an equal-weighting scheme. Specifically, all predictions were assigned equal weights (i.e.,  $w_{m,n} = \frac{1}{M(N+1)}, \forall m, n$ ).
- (4) Ours w/ CBW-D: In this variant, we replaced our weight assignment method with the dynamic CBW-D weighting method. Specifically, higher weights were assigned to predictions with larger margins. The weight for each prediction was computed as  $w_{m,n} = |p_{m,n} - (1 - p_{m,n})|^\gamma, \forall m, n$ , where  $\gamma$  is a hyperparameter and is set to 3 following (Dubey et al. 2019).
- (5) Ours w/ ES: In this variant, for each input sample (including both the original sample  $x_0$  and its generated samples  $\hat{x}_1, \hat{x}_2, \dots, \hat{x}_N$ ), we performed ensemble selection across detectors. Specifically, for each sample, we chose the detector that produced the highest predictive probability. The selected predictions for all samples are then aggregated using an equal-weight average.
- (6) Ours w/ Prob-prior: we replaced our variance-based prior with a probability-based prior. A larger gap indicated higher reliability and thus gets a larger weight. Specifically, the parameter  $\psi_{m,n}$  of the prior distribution was computed by  $\psi_{m,n} = |p_{m,n} - (1 - p_{m,n})|^\gamma, \forall m, n$ , where  $\gamma$  is a hyperparameter and is set to 3.

### Variants in examine the Iterative Adversarial Training (IAT) Strategy (Design Component 3)

- (1) Ours w/o IAT: In this variant, we removed the IAT component. Consequently, the base detector was trained using a standard training procedure, without incorporating adversarial samples into the training set. Meanwhile, the weight assignor was learned via variational inference, following the same setting as in ARHOCD.
- (2) Ours w/ AT: In this variant, we replaced the IAT component with traditional adversarial training. Consequently, the base detector was trained using AT (Goodfellow et al. 2015), but did not interact with the weight assignor. Meanwhile, the weight assignor was also learned via variational inference, following the same setting as in ARHOCD, but without interacting with the base detectors.

## Appendix U: Results of the Accuracy Comparison without Updating Base Detectors

In this setting, the defenders do not update the parameters of base detectors to reduce computational costs and ensure compatibility with existing systems. In such cases, we disabled our training for the base detectors and only updates weight assignor. Since defending against new attacks is more critical, we

restricted our evaluation to this scenario in this section.

We first compared our method with baselines in Experiment 3.1. Since regularization-based and adversarial training baselines require updating the base detectors, and EnsSel modifies the training process to obtain predictive uncertainty, these baselines were excluded from this setting. We enhanced other baselines with the same principle as in the manuscript.

In Experiment 3.2, we conducted an ablation analysis to evaluate the effectiveness of the Design Component 1 and Design Component 2 of our method. The variants include Ours w/o ME, Ours w/o prior, Ours w/o data, Ours w/ FEL, Ours w/ CBW-D, Ours w/ ES, and Ours w/ Prob-prior, consistent with those examined in Experiment 2.2 of the manuscript. Since IAT (Design Component 3) is not applied in this setting, the variants Ours w/o IAT and Ours w/ AT are excluded from the analysis.

In Experiment 3.3, we further investigated the sensitivity of key parameters in our method, including the number of generated samples, the number of base detectors, and the  $\sigma^2$  of the log-normal distribution.

### U.1 Results of Experiment 3.1 (Comparison with Baselines)

Table U2 shows the comparison results with baselines in defending against new attacks on the ETHOS, PHEME and White Supremacist datasets. Across all datasets, our method consistently outperforms the enhanced baselines, achieving the highest after-attack F1-scores and the lowest ASRs. For instance, on the ETHOS dataset, compared with the best-performing baseline (SAFER (Enhanced)), Ours (MC) improves after-attack accuracy from 69.50% to 75.40% and F1-score from 68.78% to 73.90%, while reducing the ASR from 27.50% to 23.49%, demonstrating its superior robustness to adversarial perturbations. On the highly imbalanced dataset White Supremacist (with a ratio of 1:7.6), Ours (MC) also achieves the highest after-attack F1-score of 66.78% and the lowest ASR of 26.96%. These results demonstrate that our method has strong robustness against adversarial attacks.

**Table U2. Results of Comparison with Baselines**

Dataset	Method	Performance after attack <sup>†</sup> (%)				ASR <sup>↓</sup> (%)
		Accuracy	Precision	Recall	F1-score	
ETHOS Dataset	LLM-puri (Enhanced)	68.75*** (3.01)	72.14** (3.44)	64.98*** (3.43)	63.94*** (4.28)	32.76*** (3.20)
	Det&Res (Enhanced)	69.75*** (2.31)	69.20*** (2.40)	68.45*** (2.51)	68.60*** (2.53)	28.28** (3.54)
	SAFER (Enhanced)	69.50*** (2.65)	68.95*** (2.75)	68.80*** (2.88)	68.78*** (2.82)	27.50** (3.41)

	MASKFil (Enhanced)	69.10*** (2.77)	69.13*** (3.20)	66.94*** (2.92)	67.02*** (3.09)	30.17*** (3.18)
	ARText (Enhanced)	67.00*** (3.09)	66.41*** (3.13)	66.37*** (3.16)	66.33*** (3.14)	30.51*** (2.95)
	ARDEL (Enhanced)	67.65*** (3.03)	66.98*** (3.12)	66.71*** (3.10)	66.77*** (3.10)	27.50** (3.41)
	Ours (MC)	<b>75.40 (2.80)</b>	<b>76.04 (3.06)</b>	<b>73.52 (2.95)</b>	<b>73.90 (3.05)</b>	<b>23.49 (3.74)</b>
	Ours (LB)	74.75 (2.67)	75.14 (2.85)	72.95 (2.87)	73.30 (2.94)	24.39 (3.56)
PHEME Dataset	LLM-puri (Enhanced)	77.80*** (1.31)	77.20 (1.53)	74.13*** (1.49)	75.03*** (1.53)	20.96*** (1.78)
	Det&Res (Enhanced)	74.47*** (1.06)	73.16*** (1.26)	70.64*** (1.18)	71.34*** (1.23)	23.97*** (1.56)
	SAFER (Enhanced)	73.55*** (1.25)	72.12*** (1.52)	69.57*** (1.34)	70.24*** (1.41)	25.68*** (1.19)
	MASKFil (Enhanced)	73.98*** (1.25)	72.77*** (1.49)	69.76*** (1.44)	70.50*** (1.50)	25.18*** (1.47)
	ARText (Enhanced)	71.49*** (1.25)	69.70*** (1.48)	67.12*** (1.49)	67.69*** (1.55)	25.68*** (1.19)
	ARDEL (Enhanced)	73.73*** (1.39)	72.11*** (1.59)	70.23*** (1.55)	70.80*** (1.58)	25.68*** (1.19)
	Ours (MC)	<b>79.30 (0.98)</b>	<b>78.06 (1.06)</b>	<b>77.20 (1.14)</b>	<b>77.56 (1.10)</b>	16.89 (1.29)
	Ours (LB)	79.29 (1.00)	78.04 (1.07)	77.19 (1.16)	77.55 (1.12)	<b>16.80 (1.32)</b>
White Supremacist Dataset	LLM-puri (Enhanced)	<b>88.62*** (0.57)</b>	<b>71.06*** (3.05)</b>	59.41*** (1.37)	62.03*** (1.82)	38.62*** (1.63)
	Det&Res (Enhanced)	83.48*** (0.84)	62.63*** (1.40)	65.54** (1.58)	63.78*** (1.47)	28.50* (1.40)
	SAFER (Enhanced)	82.17*** (0.87)	61.72*** (1.40)	65.93* (1.76)	63.16*** (1.56)	28.43* (1.65)
	MASKFil (Enhanced)	84.64*** (0.82)	63.41*** (1.59)	64.55*** (1.53)	63.92*** (1.54)	29.43*** (1.55)
	ARText (Enhanced)	81.12*** (0.96)	61.04*** (1.30)	65.98 (1.79)	62.52*** (1.50)	28.16 (1.46)
	ARDEL (Enhanced)	87.34*** (0.38)	62.26*** (2.39)	54.38*** (0.79)	55.25*** (1.15)	28.39* (1.63)
	Ours (MC)	86.21 (0.61)	66.52 (1.32)	<b>67.08 (1.28)</b>	<b>66.78 (1.24)</b>	<b>26.96 (2.35)</b>
	Ours (LB)	86.12 (0.64)	66.34 (1.39)	66.98 (1.37)	66.64 (1.34)	27.08 (2.28)

## U.2 Results of Experiment 3.2 (Ablation Analysis)

Table U3 shows the results of ablation analysis on defending against new attacks across the ETHOS, PHEME and White Supremacist datasets. We find that removing or replacing any key component leads to reduced performance across all datasets. First, using a single detector without model ensemble greatly degrades results. For instance, using only a BERT lowers the after-attack F1-score from 77.56% to 61.92% and raises the ASR from 16.80% to 31.38% on the PHEME dataset. Second, removing the prior (Ours w/o prior) or replacing it with probability-based prior (Ours w/ Prob-prior) leads to worse performance. Removing the posterior refinement (Ours w/o data) also performs worse. For instance, the after-attack F1-score reduces from 77.56% to 76.79% without domain knowledge, and to 76.33% without posterior refinement on the PHEME dataset. Third, the alternative weighting methods (Ours w/ FEL, Ours w/ CBW-D and Ours w/ ES) all perform worse. For instance, the after-attack F1-score drops from 77.56% to 75.82%, and the ASR rises from 16.80% to 18.48% under Ours w/ FEL on the PHEME dataset.

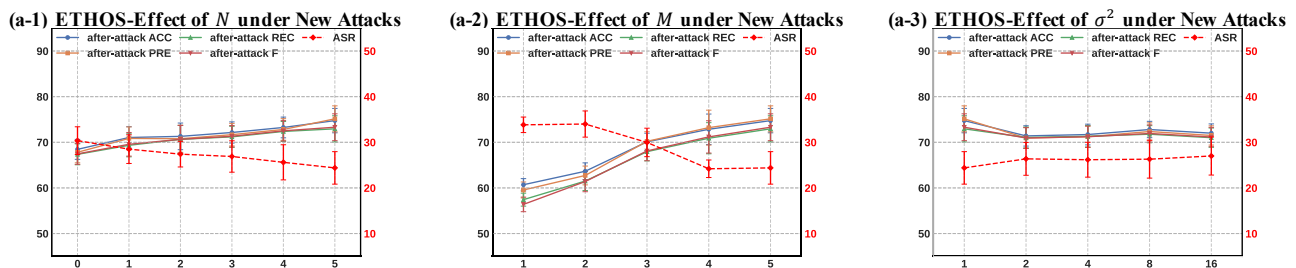
**Table U3. Results of Ablation Analysis**

Dataset	Method	Performance after attack <sup>†</sup> (%)				ASR <sup>↓</sup> (%)	
		Accuracy	Precision	Recall	F1-score		
ETHOS Dataset	Ours w/o ME	BERT	63.95*** (1.43)	63.67*** (1.64)	60.85*** (1.70)	60.17*** (2.06)	34.85*** (1.83)
		DistilBERT	60.70*** (1.34)	59.55*** (1.75)	57.43*** (1.42)	56.39*** (1.60)	33.83*** (1.70)
		RoBERTa	59.75*** (1.29)	58.36*** (1.72)	56.34*** (1.32)	55.06*** (1.49)	39.37*** (1.31)

		XLNet	70.50*** (1.05)	71.56*** (1.28)	67.80*** (1.11)	67.82*** (1.21)	25.82 (0.73)
		ALBERT	62.35*** (2.18)	61.50*** (2.73)	59.49*** (2.21)	58.95*** (2.36)	32.93*** (2.71)
	Ours w/o prior		73.65 (2.21)	75.34 (2.55)	71.06* (2.35)	71.31* (2.53)	26.85* (3.38)
	Ours w/o data		73.40 (2.46)	75.39 (2.77)	70.65* (2.67)	70.83** (2.93)	26.73* (3.32)
	Ours w/ FEL		72.90* (1.94)	74.69 (2.33)	70.19** (2.06)	70.36** (2.22)	27.49** (3.26)
	Ours w/ CBW-D		72.85* (2.18)	75.01 (1.83)	70.46** (2.04)	70.63** (2.24)	26.90* (3.78)
	Ours w/ Prob-prior		73.70 (1.45)	75.07 (1.84)	71.26* (1.52)	71.55* (1.62)	26.93* (3.15)
	Ours w/ ES		72.20** (2.09)	73.68 (2.24)	69.53*** (2.34)	69.64*** (2.56)	27.87** (3.29)
	Ours (MC)		<b>75.40 (2.80)</b>	<b>76.04 (3.06)</b>	<b>73.52 (2.95)</b>	<b>73.90 (3.05)</b>	<b>23.49 (3.74)</b>
	Ours (LB)		74.75 (2.67)	75.14 (2.85)	72.95 (2.87)	73.30 (2.94)	24.39 (3.56)
PHEME Dataset	Ours w/o ME	BERT	63.31*** (0.71)	61.89*** (0.75)	62.49*** (0.81)	61.92*** (0.75)	31.38*** (0.86)
		DistilBERT	61.80*** (0.66)	60.60*** (0.65)	61.20*** (0.69)	60.54*** (0.67)	31.69*** (0.83)
		RoBERTa	69.19*** (0.62)	66.84** (0.71)	65.97*** (0.74)	66.26*** (0.74)	27.29*** (0.77)
		XLNet	68.01*** (0.81)	65.46*** (0.93)	64.34*** (0.88)	64.65*** (0.90)	27.96*** (0.97)
		ALBERT	63.09*** (1.02)	60.87*** (1.09)	61.07*** (1.13)	60.94*** (1.10)	33.41*** (1.13)
	Ours w/o prior		78.55* (1.19)	77.19* (1.32)	76.49 (1.20)	76.79 (1.25)	17.44 (1.37)
	Ours w/o data		78.52** (0.78)	77.51 (0.89)	75.66*** (0.88)	76.33*** (0.88)	18.04** (1.34)
	Ours w/ FEL		78.13*** (0.74)	77.12** (0.84)	75.13*** (0.83)	75.82*** (0.84)	18.48*** (1.28)
	Ours w/ CBW-D		77.74*** (0.75)	76.75*** (0.86)	74.60*** (0.86)	75.32*** (0.87)	18.87*** (1.06)
	Ours w/ Prob-prior		78.29** (1.05)	76.91** (1.15)	76.23* (1.13)	76.52** (1.13)	17.90* (1.30)
	Ours w/ ES		77.13*** (1.37)	75.85*** (1.50)	74.27*** (1.61)	74.84*** (1.59)	19.42*** (1.19)
	Ours (MC)		<b>79.30 (0.98)</b>	<b>78.06 (1.06)</b>	<b>77.20 (1.14)</b>	<b>77.56 (1.10)</b>	16.89 (1.29)
	Ours (LB)		79.29 (1.00)	78.04 (1.07)	77.19 (1.16)	77.55 (1.12)	<b>16.80 (1.32)</b>
White Suprema cist Dataset	Ours w/o ME	BERT	73.91*** (0.45)	51.44*** (0.58)	52.27*** (0.91)	51.04*** (0.69)	41.75*** (1.17)
		DistilBERT	68.54*** (0.47)	51.03*** (0.49)	52.00*** (0.96)	49.39*** (0.61)	42.30*** (1.24)
		RoBERTa	81.26*** (0.42)	57.63*** (0.78)	59.13*** (1.01)	58.22*** (0.87)	33.38*** (1.36)
		XLNet	81.30*** (0.47)	51.61*** (0.86)	51.43*** (0.78)	51.48*** (0.81)	44.99*** (0.94)
		ALBERT	72.37*** (0.50)	53.74*** (0.46)	56.79*** (0.83)	53.25*** (0.59)	36.39*** (1.02)
	Ours w/o prior		87.41*** (0.49)	67.64** (1.46)	63.54*** (1.13)	65.15*** (1.21)	30.66*** (1.57)
	Ours w/o data		87.20*** (0.51)	67.52** (1.43)	64.72*** (1.28)	65.91 (1.30)	29.37*** (1.83)
	Ours w/ FEL		86.98*** (0.47)	66.92 (1.33)	64.27*** (1.23)	65.40** (1.23)	29.69*** (1.99)
	Ours w/ CBW-D		87.26*** (0.49)	67.38* (1.42)	63.82*** (1.16)	65.27** (1.24)	30.30*** (2.01)
	Ours w/ Prob-prior		85.64* (0.67)	65.23** (1.11)	65.79** (0.76)	65.48** (0.86)	28.46* (1.37)
	Ours w/ ES		<b>87.98*** (0.49)</b>	<b>68.35** (2.15)</b>	60.55*** (1.69)	62.83*** (1.95)	35.29*** (1.74)
	Ours (MC)		86.21 (0.61)	66.52 (1.32)	<b>67.08 (1.28)</b>	<b>66.78 (1.24)</b>	<b>26.96 (2.35)</b>
	Ours (LB)		86.12 (0.64)	66.34 (1.39)	66.98 (1.37)	66.64 (1.34)	27.08 (2.28)

### U.3 Results of Experiment 3.3 (Sensitivity Analysis)

Figure U1 shows the results of sensitivity analysis in defending new attacks across the ETHOS, PHEME and White Supremacist datasets. The general conclusions are similar to those of the Experiment 2.3 in the manuscript.



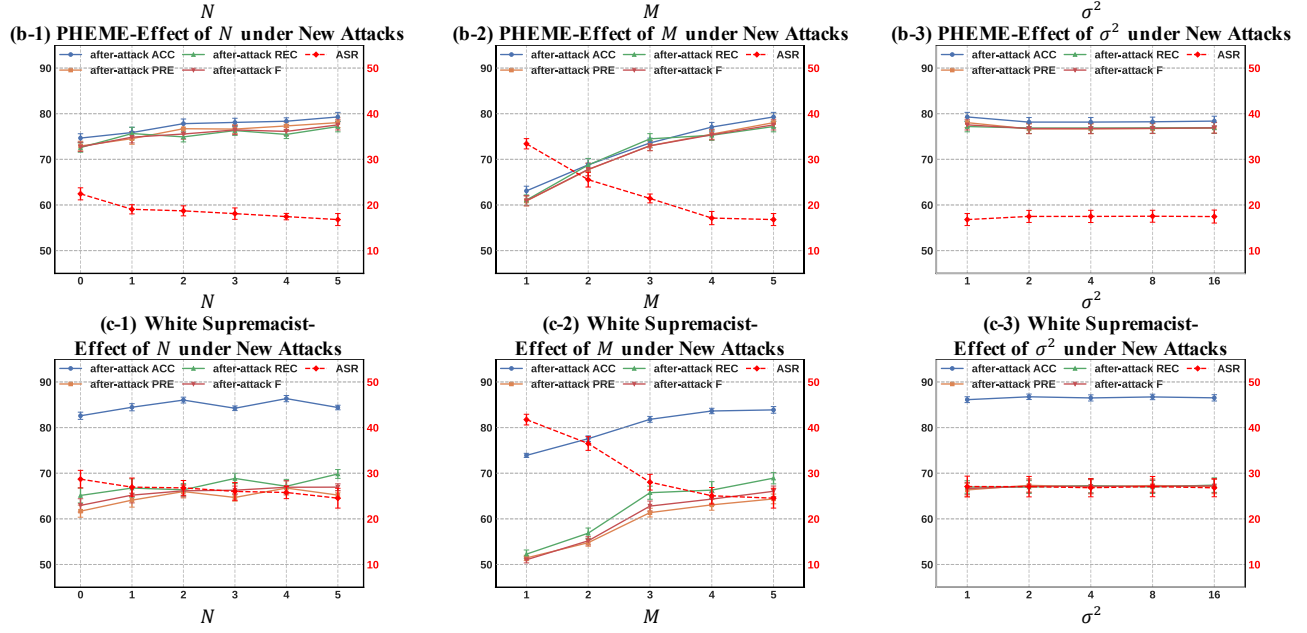


**Figure U1. Results of Sensitivity Analysis**

## Appendix V: Performance Evaluation of Our Method on Other Types of Data

Our LLM-SGA framework is designed for textual data. However, our two-dimensional ensemble (Design Component 1), Bayesian weight assignment method (Design Component 2) and iterative adversarial training strategy (Design Component 3) can be applied to other data types. In this section, we will demonstrate the effectiveness of these three design components in image classification. The task is malware detection, where adversarial attacks are also prevalent and can enable attackers to achieve malicious goals such as unauthorized access, data leakage, and blackmailing (Yan et al. 2023).

Specifically, we applied the three novel design components to a malware image dataset<sup>7</sup> (short for Malware dataset). The Malware dataset is a widely recognized benchmark for malware detection, comprising 24,380 images labeled as malicious or benign. As malware samples are originally binary files, this dataset follows the common practice (Bozkir et al. 2019) by converting all binaries into RGB images using a bin2png tool, thereby providing a more informative data representation. Details of the dataset split are provided in Table V1.

<sup>7</sup> <https://www.kaggle.com/datasets/tashiee/malebin-rgb-malware-binary-dataset>

Notably, our method consists of a sample generation method and three design components. Since the LLM-based sample generation method cannot be directly applied to image data, we generated input variants by adding Gaussian random noise to pixel values. For design component 1, we selected 3 widely used models including CNN, VGG, ResNet as the base detectors. The detailed specifications of these base detectors are provided in Table V2. By combining variant sample generation and model ensemble, we obtained a two-dimensional matrix of predictive probabilities for each input. This enabled us to apply the weight assignment method and adversarial training strategy in the same manner as in textual data.

**Table V1. Statistics of the Malware Dataset**

Dataset	#Samples	Train	Validation	Test
Malware	24,380	Normal: 8533/ Malicious :8533	Normal: 1219/ Malicious:1219	Normal: 2438/ Malicious :2438

**Table V2. Details of the Specifications of the Base Detectors**

Model	Layer	Module	Output Channels	Description
CNN	1	Depthwise Separable Conv	32	$3 \times 3$ conv + BN + ReLU
	2	Fire Module 1	64	$1 \times 1$ squeeze + $1 \times 1$ & $3 \times 3$ expand
	3	CBAM 1	64	Channel & spatial attention
	4	MaxPool	64	Downsampling
	5	Depthwise Separable Conv	128	$3 \times 3$ conv + BN + ReLU
	6	Fire Module 2	128	$1 \times 1$ squeeze + $1 \times 1$ & $3 \times 3$ expand
	7	CBAM 2	128	Channel & spatial attention
	8	MaxPool	128	Downsampling
	9	Depthwise Separable Conv	256	$3 \times 3$ conv
	10	Global AvgPool + Dropout	256	Feature aggregation + regularization
	11	Fully Connected	num_classes	Classification output
VGG	1	VGGBlock 1 + CBAM	64	$2 \times 3 \times 3$ conv + BN + ReLU, channel & spatial attention, MaxPool
	2	VGGBlock 2 + CBAM	128	$2 \times 3 \times 3$ conv + BN + ReLU, channel & spatial attention, MaxPool
	3	VGGBlock 3 + CBAM	128	$2 \times 3 \times 3$ conv + BN + ReLU, channel & spatial attention, MaxPool
	4	Global AvgPool	128	Feature aggregation
	5	Fully Connected	num_classes	Classification output
ResNet	1	Conv1 + BN + ReLU	32	$3 \times 3$ conv, stride 1, padding 1
	2	Layer1: $2 \times$ BasicBlock + CBAM	32	Residual block $\times 2$ , channel & spatial attention, stride 1
	3	Layer2: $2 \times$ BasicBlock + CBAM	64	Residual block $\times 2$ , channel & spatial attention, stride 2
	4	Layer3: $2 \times$ BasicBlock + CBAM	128	Residual block $\times 2$ , channel & spatial attention, stride 2
	5	Global AvgPool	128	Feature aggregation
	6	Fully Connected	num_classes	Classification output

We selected two classic adversarial attack methods: FGSM (Goodfellow et al. 2015) and Projected

Gradient Descent (PGD, (Madry et al. 2018)), to generate adversarial samples. Specifically, FGSM perturbs the input once in the direction of the gradient to maximize the model’s loss, while PGD extends this approach by iteratively applying small perturbations and projecting the perturbed input back into a constrained range to avoid large distortions.

We examined the effectiveness of our design components in two scenarios: defending known and new attacks. During adversarial training, adversarial samples were generated using FGSM. Accordingly, when defending against known attacks, we generated adversarial samples with FGSM from  $D^{\text{test}}$ , denoted as  $D_{\text{FGSM}}^{\text{test}}$ ; When defending against new attacks, we generated adversarial samples with PGD from  $D^{\text{test}}$ , denoted as  $D_{\text{PGD}}^{\text{test}}$ . Our method was evaluated on  $D_{\text{FGSM}}^{\text{test}}$  and  $D_{\text{PGD}}^{\text{test}}$ .

For both scenarios, we conducted an ablation analysis to evaluate the contribution of each key design component in our method. First, to examine the two-dimensional ensemble (Design Component 1), we evaluated Ours w/o ME. Second, to examine the weight assignment method (Design Component 2), we evaluated Ours w/o prior, Ours w/o data, Ours w/ FEL, Ours w/ CBW-D, Ours w/ ES, and Ours w/ Prob-prior. Third, to examine the contribution of IAT (Design Component 3), we evaluated Ours w/o IAT and Ours w/ AT. These variants are the same as those detailed in Appendix T.

Table V3 shows the results of ablation analysis in defending known and new attacks on the Malware dataset. The general conclusions are similar to those observed on the text datasets. Three observations are reached. First, using a single detector without model ensemble greatly degrades performance. For instance, when defending known attacks, using only CNN lowers the after-attack F1-score from 91.28% to 82.03%, showing lower robustness. Second, removing the variance-based prior (Ours w/o prior), or replacing it with probability-based prior (Ours w/ Prob-prior) degrades performance. Removing the data-driven refinement process (Ours w/o data) also worsens performance. Meanwhile, alternative weighting methods, including Ours w/ FEL, Ours w/ CBW-D, and Ours w/ ES, exhibit inferior robustness. For instance, when defending new attacks, Ours w/ FEL increases the ASR from 21.87% to 23.87%. Finally, removing IAT (Ours w/o IAT) or replacing it with AT (Ours w/ AT) notably reduces robustness. For instance, when removing IAT,

the ASR increases from 8.71% to 29.87% for known attacks, and from 21.87% to 62.95% for new attacks. Overall, the elimination of any design component leads to a significant performance decrease, proving the effectiveness of each design component.

**Table V3. Results of Ablation Analysis in Defending Known and New Attacks**

Attack Scenario	Method	Performance after attack <sup>†</sup> (%)				ASR <sub>↓</sub> (%)
		Accuracy	Precision	Recall	F1-score	
Known Attacks (FGSM)	Ours	82.12 *** (1.74)	82.73 *** (1.54)	82.12 *** (1.74)	82.03 *** (1.78)	17.88 *** (1.74)
	w/o	79.69 *** (0.34)	80.23 *** (0.38)	79.69 *** (0.34)	79.60 *** (0.34)	20.31 *** (0.34)
	ME	76.60 *** (0.58)	76.76 *** (0.60)	76.60 *** (0.58)	76.57 *** (0.58)	23.40 *** (0.58)
	Ours w/o prior	90.94 *** (0.19)	91.01 *** (0.19)	90.94 *** (0.19)	90.94 *** (0.19)	9.06 *** (0.19)
	Ours w/o data	89.69 *** (0.26)	89.83 *** (0.24)	89.69 *** (0.26)	89.68 *** (0.26)	10.31 *** (0.26)
	Ours w/ FEL	87.99 *** (0.52)	88.26 *** (0.46)	87.99 *** (0.52)	87.97 *** (0.53)	12.01 *** (0.52)
	Ours w/ CBW-D	89.29 *** (0.40)	89.37 *** (0.39)	89.29 *** (0.40)	89.29 *** (0.40)	10.71 *** (0.40)
	Ours w/ ES	87.08 *** (0.68)	87.17 *** (0.64)	87.08 *** (0.68)	87.07 *** (0.68)	12.92 *** (0.68)
	Ours w/ Prob-prior	91.02 ** (0.10)	91.13 *** (0.11)	91.02 ** (0.10)	91.02 ** (0.10)	8.98 ** (0.10)
	Ours w/o IAT	70.13 *** (0.86)	70.18 *** (0.84)	70.18 *** (0.84)	70.13 *** (0.86)	29.87 *** (0.86)
	Ours w/ AT	89.43 *** (0.19)	89.46 *** (0.19)	89.43 *** (0.19)	89.42 *** (0.19)	10.57 *** (0.19)
	Ours (MC)	91.27 (0.31)	91.42 (0.30)	91.27 (0.31)	91.26 (0.31)	8.73 (0.31)
	Ours (LB)	<b>91.29 (0.30)</b>	<b>91.44 (0.30)</b>	<b>91.29 (0.30)</b>	<b>91.28 (0.31)</b>	<b>8.71 (0.30)</b>
New Attacks (PGD)	Ours	47.54 *** (1.98)	47.28 *** (2.18)	47.54 *** (1.98)	46.25 *** (2.02)	52.46 *** (1.98)
	w/o	69.10 *** (0.64)	69.25 *** (0.68)	69.10 *** (0.64)	69.04 *** (0.62)	30.90 *** (0.64)
	ME	74.16 *** (0.71)	74.19 *** (0.72)	74.16 *** (0.71)	74.15 *** (0.71)	25.84 *** (0.71)
	Ours w/o prior	76.25 *** (0.41)	76.99 *** (0.44)	76.25 *** (0.41)	76.08 *** (0.42)	23.75 *** (0.41)
	Ours w/o data	76.94 *** (0.23)	77.91 *** (0.33)	76.94 *** (0.23)	76.73 *** (0.24)	23.06 *** (0.23)
	Ours w/ FEL	76.13 *** (0.43)	77.08 *** (0.46)	76.13 *** (0.43)	75.92 *** (0.45)	23.87 *** (0.43)
	Ours w/ CBW-D	76.96 *** (0.59)	77.35 *** (0.62)	76.96 *** (0.59)	76.88 *** (0.59)	23.04 *** (0.59)
	Ours w/ ES	75.65 *** (0.91)	75.85 *** (0.96)	75.65 *** (0.91)	75.61 *** (0.91)	24.35 *** (0.91)
	Ours w/ Prob-prior	77.59 *** (0.27)	78.61 *** (0.28)	77.59 *** (0.27)	77.38 *** (0.28)	22.41 *** (0.27)
	Ours w/o IAT	37.05 *** (0.56)	37.09 *** (0.56)	37.13 *** (0.55)	37.03 *** (0.57)	62.95 *** (0.56)
	Ours w/ AT	57.78 *** (0.67)	57.82 *** (0.68)	57.78 *** (0.67)	57.73 *** (0.66)	42.22 *** (0.67)
	Ours (MC)	<b>78.14 (0.45)</b>	<b>79.26 (0.45)</b>	<b>78.14 (0.45)</b>	<b>77.92 (0.46)</b>	<b>21.87 (0.45)</b>
	Ours (LB)	77.75 (0.45)	79.16 (0.46)	77.75 (0.45)	77.48 (0.46)	21.85 (0.45)

## Appendix W: Adversarial Sample Detection

Adversarial sample detection aims to identify whether an input sample is clean or adversarial. In contrast, robustness enhancement method focuses on making the model still perform well even if the input is adversarial. Prior studies have shown that adversarial samples are often difficult to identify, making the approach of adversarial sample detection challenging (Carlini and Wagner 2017).

We also empirically verify this in our study. We trained a BERT-based adversarial attack detector to distinguish adversarial samples from clean samples. Specifically, we constructed the training set using clean samples (i.e.,  $D^{\text{train}}$ ) together with the same number of adversarial samples generated by DeepWordBug

TFAdjusted, and TREPAT (i.e., random sampled from  $D_{DTT}^{\text{train}}$ , as defined in Section 6.3 of the manuscript; that is, adversarial samples generated from the training set). All clean samples were labeled as 0, and all adversarial samples were labeled as 1. The training process followed a standard text binary classification setup, where the adversarial attack detector was trained by minimizing the cross-entropy loss between the predicted probabilities and the assigned labels. After training, the trained adversarial attack detector was used to detect the adversarial samples in the test set.

We report the accuracy of the trained adversarial attack detector on adversarial samples generated by character-level attack (DeepWordBug), word-level attack (TFAdjusted), sentence-level attack (TREPAT), and multi-level attack (ExplainDrive) across the three datasets in Table W1. Two observations can be found.

First, character-level attacks are comparatively easier to detect. Specifically, for adversarial samples generated by DeepWordBug, the adversarial attack detector achieves detection accuracies of 94.00%, 94.87%, and 93.80% on the ETHOS, PHEME, and White Supremacist datasets, respectively. Character-level attacks involve minor perturbations such as misspellings, character substitutions, or visually similar symbols. These small and localized changes are easier for the detector to capture.

Second, other types of attacks including word-level attacks, sentence-level attacks, and multi-level attacks, pose a significantly greater challenge. For instance, when confronted with adversarial samples generated by TREPAT, the detection accuracy drops sharply to 36.00%, 44.95%, and 41.72% on the ETHOS, PHEME, and White Supremacist datasets, respectively. These results show the difficulty of detecting adversarial samples, and thus the limitation of this approach.

**Table W1. Accuracy (%) of Adversarial Attack Detector Under Different Attack Types**

Dataset	ETHOS	PHEME	White Supremacist
Character-level	94.00	94.87	93.80
Word-level	72.00	59.25	74.44
Sentence-level	36.00	44.95	41.72
Multi-level	48.00	57.39	75.22

## Appendix X: Experimental Configuration and Computational Efficiency

We conducted all experiments on an Ubuntu 20.04 system equipped with powerful hardware to

accelerate deep learning tasks. The detailed CPU, GPU, hardware, and software configurations are summarized in Tables X1–X3.

**Table X1. The CPU and GPU Configurations**

Item	Value
CPU Type	Intel(R) Xeon(R) Gold 6326 CPU @ 2.90GHz
CPU Cores	16 Cores, 3.341GHz
Graphic Card	4 ×NVIDIA GeForce GTX 4090
Graphic Memory	24 GB each
Main Memory	503GB

**Table X2. The Hardware Configurations**

Storage Devices	Capacity	Type
SSD Disk	894.3G	SAMSUNG_MZ7LH960HAJR
Disk Array	2 × 14.6TB	ST16000NM000J

**Table X3. The Software Configurations**

Software	Version
OS	Ubuntu 20.04
Anaconda	2021.05
Python	Python 3.11
CUDA	12.0
Torch	2.6.0

To assess the computational efficiency of our method, we evaluated the runtime required to process samples from the ETHOS, PHEME, and White Supremacist datasets using our ARHOCD. For each test sample, we used LLaMA to generate 5 samples with the same meaning, which were then processed by the trained base detectors and the weight assignor to produce the final prediction. The results are shown in Table X4. With a batch size of 8, the total runtime per test sample is about 2.88, 2.72, 2.44 seconds for the ETHOS, PHEME and White Supremacist datasets, respectively. Of this, the process of calling LLM to generate samples requires about 2.47, 2.23, and 2.27 seconds, respectively. While this may introduce response latency in practical applications, the rapid advancements in LLMs are expected to improve response speed in the near future, thereby enhancing the efficiency of sample generation. The runtime efficiency can also be improved through engineering optimizations, such as parallel processing, which can reduce run time without compromising performance.

**Table X4. Efficiency of Our Method**

Datasets	Average Per-Sample Runtime	Call LLM for Samples Generation
ETHOS	2.88 s	2.47 s
PHEME	2.72 s	2.23 s

White Supremacist	2.44 s	2.27 s
-------------------	--------	--------

Note: “s” denotes seconds.

## Appendix Y: Case Study

In this section, we first selected several adversarial samples to illustrate why our approach is effective (details in Y.1). Then, we examined how our detector behaves across different attack types and different topics (details in Y.2-3). Finally, we analyzed the distribution of correctly and incorrectly predicted samples across different attack types and topics (details in Y.4-5).

### Y.1 Case Study with Specific Examples

We randomly selected several adversarial samples to examine why our approach is effective. The selected adversarial samples are shown in Table Y1-Y3.

Specifically, for each dataset, we randomly selected three adversarial samples of different types (i.e., character-level, word-level, and sentence-level attacks). In Table Y1-Y3, the differences between the adversarial and clean samples are highlighted in bold. We also present the samples generated by LLaMA, where the number of generated samples is set to five in our experiments. After sample generation, the original input ( $x_0$ ) and the generated samples ( $\hat{x}_1, \hat{x}_2, \dots, \hat{x}_5$ ) were fed into the base detectors, producing a two-dimensional matrix of predictive probabilities with dimensions  $5 \times 6$ . The trained weight assignor then took this probability matrix as input and produced a corresponding two-dimensional matrix of assigned weights with the same dimensions. Finally, these weights were used to aggregate the predictive probabilities to obtain the final output. Both the probability matrix, the weight matrix and the final output are also presented. Take the first adversarial sample in Table Y1 as an example. The clean sample, which is labeled as hate speech, is “but women aren’t people, so it’s fine!”. The corresponding adversarial sample generated by DeepWordBug only changes “women” to “womEen”. Notably, all generated samples correct this misspelling while preserving the original meaning of the sentence, such as “Women aren’t people, so it is all right.” Four key observations are reached.

First, more accurate predictive probabilities correspond to higher weights. Notably, the ground-truth label is hate speech (i.e., the positive class). Therefore, a larger value in the probability matrix indicates a

smaller Brier Score and thus a more accurate prediction. For example, in the first case of Table Y1, the predictive probability produced by model 1 (i.e., the base detector with index 1 in the matrix; the same below) on the first sample is 0.03, which is highly inaccurate, yielding a Brier Score of  $(1 - 0.03)^2 = 0.9409$ . Its assigned weight is therefore only 0.0196. In contrast, the predictive probability of the base model 3 on the sample 2 (i.e., the sample with index 2 in the matrix; the same below) is 0.99, which is highly accurate with a Brier Score of  $(1 - 0.99)^2 = 0.0001$ , and its assigned weight increases to 0.0624. We further evaluate this relationship by computing the Pearson correlation between each prediction's Brier Score and its assigned weights (denoted as Pearson<sup>1</sup> in the table), which yields a value of -0.8495. Similar patterns are observed in other examples, confirming that more accurate predictive probabilities consistently receive higher weights.

Second, samples that are easier to predict are assigned higher weights. For the probability matrix, we compute the average Brier Score of each column. A smaller mean value means the sample is easier to predict, and thus has a higher predictability. We can see the samples' predictability varies. For instance, in the first case of Table Y1, sample 0 has an average Brier Score of 0.7331, whereas sample 3 has 0.1507. We also compute the total assigned weight for each sample (i.e., the sum of each column in the weight matrix). We find samples with higher predictability are assigned higher weight. For instance, note that sample 3's average Brier Score (0.1507) is much lower than sample 0's (0.7331). The total weight assigned for sample 3 is 0.2185, whereas that for sample 0 is 0.1507. We also examine this relationship by computing the Pearson correlation between the sample's average Brier Score and its assigned weights (denoted as Pearson<sup>2</sup> in the table), yielding a value of -0.9905, indicating the higher weights are associated with lower Brier Score and thus more accurate predictions. Similar patterns are observed in other examples, confirming that samples with higher predictability are assigned higher weight.

Third, models with stronger capability are assigned higher weights. For the probability matrix, we computed the average Brier Score of each row. A smaller mean value means the model is easy to be predicted, and thus has a stronger capability. We can see the model' capability varies. For instance, in the

first case of Table Y1, model 2 has an average Brier Score of 0.6401, whereas model 3 has 0.0713. We also compute the total assigned weight for each model (i.e., the sum of each row in the weight matrix). We find models with stronger capability are assigned higher weight. For instance, note that model 3's average Brier Score (0.0713) is much lower than model 2's (0.6401). The total weight assigned for model 3 is 0.2906, whereas that for model 2 is only 0.1465. We also examine this relationship by computing the Pearson correlation between the model's average Brier Score and its assigned weights (denoted as Pearson<sup>3</sup> in the table), yielding a value of -0.9606, indicating the higher weights are associated with lower Brier Score and thus more accurate predictions. Similar patterns are observed in other examples, confirming that models with stronger capability are assigned higher weight.

Fourth, in all cases, our ARHOCD consistently produced the correct detection. For instance, in the first case, by weighted averaging all the predictive probabilities, we obtain an average value of 0.6711, which is larger than the threshold 0.5. Hence, the initial input is classified as positive (hate speech). The correct prediction is due to the fact that, while different base detectors may have different capacity in predicting different samples, our ARHOCD can assign higher weight to more accurate predictions. Across those examples, we can see that different base detectors' capacity also varies across samples. For instance, in the first case, model 3 (i.e., a RoBERTa) achieves the best performance, while on the second one, model 4 (i.e., an XLNet) achieves the best performance. Hence, different base detectors have their advantages in specific samples and there is no base detector outperforms all others. This also demonstrates the advantage of ensemble learning approach which dynamically assigns weight to reflect their capacity in different samples. This inspires that future studies can employ the complementary advantage of ensemble learning to address difficult tasks where one single model struggles to fit all settings.

**Table Y1. Selected Adversarial Samples from the ETHOS Dataset**

ETHOS-known attack (generated by DeepWordbug, character-level insertion)	
Clean Sample	but <b>women</b> aren't people, so it's fine! <b>(Ground Truth:</b> Hate)
Adversarial Sample	but <b>womEen</b> aren't people, so it's fine!
Generated Sample	However, women cannot be counted as people, so it's perfectly fine! Women aren't people, so it is all right. Women aren't considered people, so it's acceptable.

	But women don't count as people, so it's alright. But women aren't people, thus it is fine!
<b>Visualization</b> (Pearson <sup>1</sup> = <b>-0.8495</b> ; Pearson <sup>2</sup> = <b>-0.9905</b> ; Pearson <sup>3</sup> = <b>-0.9606</b> )	<p><b>Two-Dimensional Matrix of Probabilities</b></p> <p><b>Two-Dimensional Matrix of Assigned Weights</b></p>
	<b>Aggregated Prediction</b> : Weighted Probability: 0.6711 <b>Predictive Lable</b> : Hate
<b>ETHOS-known attack (generated by TREPAT, sentence-level)</b>	
<b>Clean Sample</b>	how is it to have a kid acting like a sloth or like a pug dog? isn't it hard? in your place i'd put it in a dedicated institute for problematics and pay a visit each year at max <b>(Ground Truth: Hate)</b>
<b>Adversarial Sample</b>	What's it like having a child that is it to have a kid acting like a sloth or like a pug dog? isn't it hard? in your place i'd put it in a dedicated institute for problematics and pay a visit each year at max
<b>Generated Sample</b>	what is it like having a child? is it hard to have a kid that behaves like a sloth or a pug dog? if i were you, i'd send it to an institute that helps kids with problems and visit only once a year
	What's it like having a child that acts like a sloth or a pug dog? Isn't it difficult? I would send it to a special institution for problem children and visit it annually.
	What's it like to have a child like a sloth or a pug? Is it tough? I would have it placed in a specialized institution for children with problems and visit it annually.
	How is it to have a child that behaves like a sloth or a pug dog? Isn't it hard? In my place, I would have it attend a specialized school for problem children and visit it regularly.
	what is it like having a child, that is, to have a kid, acting like a sloth or a pug dog? isn't it hard? in your place, i'd put it in a dedicated institute for problematics and pay a visit once a year at max
<b>Visualization</b> (Pearson <sup>1</sup> = <b>-0.5494</b> ; Pearson <sup>2</sup> = <b>-0.6367</b> ; Pearson <sup>3</sup> = <b>-0.9995</b> )	<p><b>Two-Dimensional Matrix of Probabilities</b></p> <p><b>Two-Dimensional Matrix of Assigned Weights</b></p>
	<b>Aggregated Prediction</b> : Weighted Probability: 0.5350 <b>Predictive Lable</b> : Hate
<b>ETHOS-new attack (generated by ExplainDrive, word-level replacement)</b>	
<b>Clean Sample</b>	throwing stones to <b>paraplegic</b> kids is my favourite hobby <b>(Ground Truth: Hate)</b>

<b>Adversarial Sample</b>	throwing stones to <b>bedridden</b> kids is my favourite hobby																																																																																																																												
<b>Generated Sample</b>	Bedridden kids love having stones thrown at them by me.																																																																																																																												
	My hobby is to throw stones at kids who are confined to their beds.																																																																																																																												
	Throwing stones to kids who are bedridden is one of my favourite hobbies.																																																																																																																												
	My favorite hobby is throwing stones at kids who are bedridden.																																																																																																																												
	I enjoy throwing stones at kids who are lying in bed as a favorite pastime.																																																																																																																												
<b>Visualization</b> (Pearson <sup>1</sup> = <b>-0.8112</b> ; Pearson <sup>2</sup> = <b>-0.9827</b> ; Pearson <sup>3</sup> = <b>-0.9157</b> )	<b>Two-Dimensional Matrix of Probabilities</b>			<b>Two-Dimensional Matrix of Assigned Weights</b>																																																																																																																									
	<table border="1"> <thead> <tr> <th>Model Index</th> <th>0</th> <th>1</th> <th>2</th> <th>3</th> <th>4</th> <th>5</th> <th>Avg Brier Score</th> </tr> </thead> <tbody> <tr> <td>1</td> <td>0.09</td> <td>0.37</td> <td>0.12</td> <td>0.05</td> <td>0.06</td> <td>0.04</td> <td>0.7853</td> </tr> <tr> <td>2</td> <td>0.08</td> <td>0.67</td> <td>0.50</td> <td>0.05</td> <td>0.04</td> <td>0.14</td> <td>0.6263</td> </tr> <tr> <td>3</td> <td>0.88</td> <td>0.98</td> <td>0.63</td> <td>0.79</td> <td>0.84</td> <td>0.05</td> <td>0.1885</td> </tr> <tr> <td>4</td> <td>0.74</td> <td>0.44</td> <td>0.87</td> <td>0.97</td> <td>0.92</td> <td>0.43</td> <td>0.1218</td> </tr> <tr> <td>5</td> <td>0.40</td> <td>0.29</td> <td>0.17</td> <td>0.08</td> <td>0.09</td> <td>0.25</td> <td>0.6306</td> </tr> <tr> <td></td> <td>0.4214</td> <td>0.2676</td> <td>0.3716</td> <td>0.5389</td> <td>0.5342</td> <td>0.6894</td> <td></td> </tr> </tbody> </table>			Model Index	0	1	2	3	4	5	Avg Brier Score	1	0.09	0.37	0.12	0.05	0.06	0.04	0.7853	2	0.08	0.67	0.50	0.05	0.04	0.14	0.6263	3	0.88	0.98	0.63	0.79	0.84	0.05	0.1885	4	0.74	0.44	0.87	0.97	0.92	0.43	0.1218	5	0.40	0.29	0.17	0.08	0.09	0.25	0.6306		0.4214	0.2676	0.3716	0.5389	0.5342	0.6894		<table border="1"> <thead> <tr> <th>Model Index</th> <th>0</th> <th>1</th> <th>2</th> <th>3</th> <th>4</th> <th>5</th> <th>Row Sum</th> </tr> </thead> <tbody> <tr> <td>1</td> <td>-0.0237</td> <td>0.0265</td> <td>0.0251</td> <td>0.0227</td> <td>0.0225</td> <td>0.0157</td> <td>0.1361</td> </tr> <tr> <td>2</td> <td>-0.0282</td> <td>0.0309</td> <td>0.0293</td> <td>0.0269</td> <td>0.0267</td> <td>0.0189</td> <td>0.1609</td> </tr> <tr> <td>3</td> <td>-0.0499</td> <td>0.0559</td> <td>0.0509</td> <td>0.0477</td> <td>0.0477</td> <td>0.0302</td> <td>0.2823</td> </tr> <tr> <td>4</td> <td>-0.0474</td> <td>0.0534</td> <td>0.0486</td> <td>0.0447</td> <td>0.0447</td> <td>0.0284</td> <td>0.2672</td> </tr> <tr> <td>5</td> <td>-0.0267</td> <td>0.0292</td> <td>0.0278</td> <td>0.0264</td> <td>0.0261</td> <td>0.0173</td> <td>0.1534</td> </tr> <tr> <td></td> <td>0.1759</td> <td>0.1958</td> <td>0.1817</td> <td>0.1684</td> <td>0.1677</td> <td>0.1104</td> <td></td> </tr> <tr> <td></td> <td>Col Sum</td> <td>1</td> <td>2</td> <td>3</td> <td>4</td> <td>5</td> <td>Row Sum</td> </tr> </tbody> </table>			Model Index	0	1	2	3	4	5	Row Sum	1	-0.0237	0.0265	0.0251	0.0227	0.0225	0.0157	0.1361	2	-0.0282	0.0309	0.0293	0.0269	0.0267	0.0189	0.1609	3	-0.0499	0.0559	0.0509	0.0477	0.0477	0.0302	0.2823	4	-0.0474	0.0534	0.0486	0.0447	0.0447	0.0284	0.2672	5	-0.0267	0.0292	0.0278	0.0264	0.0261	0.0173	0.1534		0.1759	0.1958	0.1817	0.1684	0.1677	0.1104			Col Sum	1	2	3	4	5
Model Index	0	1	2	3	4	5	Avg Brier Score																																																																																																																						
1	0.09	0.37	0.12	0.05	0.06	0.04	0.7853																																																																																																																						
2	0.08	0.67	0.50	0.05	0.04	0.14	0.6263																																																																																																																						
3	0.88	0.98	0.63	0.79	0.84	0.05	0.1885																																																																																																																						
4	0.74	0.44	0.87	0.97	0.92	0.43	0.1218																																																																																																																						
5	0.40	0.29	0.17	0.08	0.09	0.25	0.6306																																																																																																																						
	0.4214	0.2676	0.3716	0.5389	0.5342	0.6894																																																																																																																							
Model Index	0	1	2	3	4	5	Row Sum																																																																																																																						
1	-0.0237	0.0265	0.0251	0.0227	0.0225	0.0157	0.1361																																																																																																																						
2	-0.0282	0.0309	0.0293	0.0269	0.0267	0.0189	0.1609																																																																																																																						
3	-0.0499	0.0559	0.0509	0.0477	0.0477	0.0302	0.2823																																																																																																																						
4	-0.0474	0.0534	0.0486	0.0447	0.0447	0.0284	0.2672																																																																																																																						
5	-0.0267	0.0292	0.0278	0.0264	0.0261	0.0173	0.1534																																																																																																																						
	0.1759	0.1958	0.1817	0.1684	0.1677	0.1104																																																																																																																							
	Col Sum	1	2	3	4	5	Row Sum																																																																																																																						
Weighted Probability: 0.5008																																																																																																																													
Predictive Label: Hate																																																																																																																													

**Table Y2. Selected Adversarial Samples from the PHEME Dataset**

<b>PHEME-known attack (generated by TREPAT, sentence-level)</b>		
<b>Clean Sample</b>	<b>afp map of the region northeast of paris</b> where wednesday's massacre suspects are cornered with hostage <b>(Ground Truth: Rumor)</b>	
<b>Adversarial Sample</b>	<b>afp map of the north - eastern area around Paris</b> where wednesday's massacre suspects are cornered with hostage	
<b>Generated Sample</b>	An AFP map of the North Eastern area in Paris where Wednesday's massacre suspects are being cornered with hostages. map of the northeastern area around Paris where the suspects from Wednesday's event are being held hostage According to an afp map of the north-eastern area around Paris, Wednesday's massacre suspects are cornered with a hostage. The afp map of the north-eastern Paris region indicates that the suspects of Wednesday's massacre are being held hostage in a corner. A map by AFP of the North Eastern area around Paris where Wednesday's massacre suspects are being cornered with hostages.	
<b>Visualization</b>	<b>Two-Dimensional Matrix of Probabilities</b>	<b>Two-Dimensional Matrix of Assigned Weights</b>

$(\text{Pearson}^1 = -0.7137;$ $\text{Pearson}^2 = -0.7296;$ $\text{Pearson}^3 = -0.9963)$		
	<b>Aggregated Prediction</b> : Weighted Probability: 0.7182 <b>Predictive Lable</b> : Rumor	
<b>PHEME-known attack (generated by DeepWordBug, character-level insert)</b>		
Clean Sample	update: french police in <b>standoff</b> with attack suspects, hostage believed taken	
Adversarial Sample	update: french police in a <b>stand - off</b> with attack suspects, hostage believed taken	
Generated Sample	French police are involved in a standoff with suspects who allegedly carried out an attack, with a hostage reportedly taken.	
	French police are in a standoff with suspects who attacked, a hostage is believed to have been taken.	
	French police are engaged in a standoff with the attack suspects, who are believed to have a hostage.	
	France police are in a standoff situation with the suspected attackers and it's believed a hostage has been taken.	
	French police are in a standoff with suspects in an attack, a hostage is believed to have been taken.	
<b>Visualization</b> $(\text{Pearson}^1 = -0.5168;$ $\text{Pearson}^2 = -0.8322;$ $\text{Pearson}^3 = -0.8270)$	<b>Two-Dimensional Matrix of Probabilities</b> 	
	<b>Two-Dimensional Matrix of Assigned Weights</b> 	
Aggregated Prediction	Weighted Probability: 0.6330 <b>Predictive Lable</b> : Rumor	
<b>PHEME-new attack (generated by ExplainDrive, word-level replacement)</b>		
Clean Sample	the man at the <b>centre</b> of the has been named as man haron monis <b>(Ground Truth: Rumor)</b>	
Adversarial Sample	the man at the <b>focused</b> of the has been named as man haron monis	
Generated Sample	the man at the center of the has been named man haron monis a man at the center of the has been named as man haron monis the man in the spotlight has been named man haron monis man haron monis is now centre of scrutiny the man at the centre of the has been named as man haron monis	
	<b>Two-Dimensional Matrix of Probabilities</b>	
	<b>Two-Dimensional Matrix of Assigned Weights</b>	

<b>Visualization</b> (Pearson <sup>1</sup> = <b>-0.6995</b> ; Pearson <sup>2</sup> = <b>-0.6691</b> ; Pearson <sup>3</sup> = <b>-0.9762</b> )												
	1	0.19	0.99	0.72	0.01	0.15	1.00	0.4057	0.3829	0.2101	0.2122	0.1653
	2	0.30	0.90	0.65	0.11	0.07	0.96	0.6961	0.242	0.0332	0.0311	0.0273
	3	0.06	0.08	0.17	0.53	0.06	0.20	0.2583	0.0261	0.0345	0.0332	0.0344
	4	0.67	0.48	0.46	0.79	0.26	0.45	0.2021	0.0334	0.0455	0.0434	0.0450
	5	0.54	0.99	0.95	0.91	0.00	0.99	0.4695	0.2258	0.2353	0.4075	0.8060
<b>Aggregated Prediction</b>		Weighted Probability: 0.5577 Predictive Label: Rumor										

**Table Y3. Selected Adversarial Samples from the White Supremacist Dataset**

White Supremacist-known attack (generated by TREPAT, sentence-level)																													
Clean Sample	the jews say they are the chosen ones the blacks say they are the original hebreus Israelites. <b>our worst enemies want to be us and we refuse to accept that we are his ! ... and so it goes ..</b> <b>(Ground Truth: Hate)</b>																												
Adversarial Sample	the jews say they are the chosen ones the blacks say they are the original hebreus Israelites. <b>we refuse to accept that we are his !wont buy into the ideaoes ..</b>																												
Generated Sample	Jews say they're the chosen ones, but blacks say they're the original Hebrews or Israelites. We don't accept this label. Jews claim they're the chosen people, but blacks claim they're the original Hebrews or Israelites. We don't want to be identified with this. They claim to be the chosen ones, but the blacks say they are the original Hebrews, or Israelites. We won't accept the idea that we are his. Jews say they are chosen, but the black community argues that they are the original Hebrews or Israelites. We are not going to buy into the idea that we are his chosen ones! The Jews claim to be the chosen ones, but the blacks argue they are the original Hebrews or Israelites. We won't accept being labeled like this.																												
Visualization (Pearson <sup>1</sup> = <b>-0.5427</b> ; Pearson <sup>2</sup> = <b>-0.7037</b> ; Pearson <sup>3</sup> = <b>-0.9262</b> )	<b>Two-Dimensional Matrix of Probabilities</b> 						<b>Two-Dimensional Matrix of Assigned Weights</b> 																						
<b>Aggregated Prediction</b>		Weighted Probability: 0.6261 Predictive Label: Hate																											
White Supremacist-known attack (generated by DeepWordBug, character-level replacement)																													
Clean Sample	those evil <b>whites</b> . <b>(Ground Truth: Hate)</b>																												
Adversarial Sample	those evil <b>whiCes</b> .																												

Generated Sample	those evil whites.																																																																																																												
	those wicked whites.																																																																																																												
	those evil white people.																																																																																																												
	those evil whiCes.																																																																																																												
	those evil whites.																																																																																																												
Visualization (Pearson <sup>1</sup> = <b>-0.7094</b> ; Pearson <sup>2</sup> = <b>-0.8752</b> ; Pearson <sup>3</sup> = <b>-0.9999</b> )	<b>Two-Dimensional Matrix of Probabilities</b>																																																																																																												
	<table border="1"> <thead> <tr> <th colspan="6">Model Index</th> <th colspan="6">Sample Index</th> </tr> <tr> <th>0</th><th>1</th><th>2</th><th>3</th><th>4</th><th>5</th> <th>0</th><th>1</th><th>2</th><th>3</th><th>4</th><th>5</th> </tr> </thead> <tbody> <tr> <td>0.57</td><td>0.78</td><td>0.67</td><td>0.93</td><td>0.57</td><td>0.78</td> <td>0.0954</td><td></td><td></td><td></td><td></td><td></td> </tr> <tr> <td>0.06</td><td>0.93</td><td>0.77</td><td>0.92</td><td>0.06</td><td>0.93</td> <td>0.3031</td><td></td><td></td><td></td><td></td><td></td> </tr> <tr> <td>1.00</td><td>0.96</td><td>0.78</td><td>0.95</td><td>1.00</td><td>0.96</td> <td>0.0090</td><td></td><td></td><td></td><td></td><td></td> </tr> <tr> <td>0.06</td><td>0.83</td><td>0.70</td><td>0.84</td><td>0.06</td><td>0.83</td> <td>0.3244</td><td></td><td></td><td></td><td></td><td></td> </tr> <tr> <td>0.00</td><td>0.99</td><td>1.00</td><td>0.97</td><td>0.00</td><td>0.99</td> <td>0.3314</td><td></td><td></td><td></td><td></td><td></td> </tr> <tr> <td>0.5873</td><td>0.0162</td><td>0.0606</td><td>0.0083</td><td>0.5873</td><td>0.0162</td> <td>Avg Brier Score</td><td></td><td></td><td></td><td></td><td></td> </tr> <tr> <td>0</td><td>1</td><td>2</td><td>3</td><td>4</td><td>5</td> <td></td><td></td><td></td><td></td><td></td><td></td> </tr> </tbody> </table>		Model Index						Sample Index						0	1	2	3	4	5	0	1	2	3	4	5	0.57	0.78	0.67	0.93	0.57	0.78	0.0954						0.06	0.93	0.77	0.92	0.06	0.93	0.3031						1.00	0.96	0.78	0.95	1.00	0.96	0.0090						0.06	0.83	0.70	0.84	0.06	0.83	0.3244						0.00	0.99	1.00	0.97	0.00	0.99	0.3314						0.5873	0.0162	0.0606	0.0083	0.5873	0.0162	Avg Brier Score						0	1	2	3	4	5					
Model Index						Sample Index																																																																																																							
0	1	2	3	4	5	0	1	2	3	4	5																																																																																																		
0.57	0.78	0.67	0.93	0.57	0.78	0.0954																																																																																																							
0.06	0.93	0.77	0.92	0.06	0.93	0.3031																																																																																																							
1.00	0.96	0.78	0.95	1.00	0.96	0.0090																																																																																																							
0.06	0.83	0.70	0.84	0.06	0.83	0.3244																																																																																																							
0.00	0.99	1.00	0.97	0.00	0.99	0.3314																																																																																																							
0.5873	0.0162	0.0606	0.0083	0.5873	0.0162	Avg Brier Score																																																																																																							
0	1	2	3	4	5																																																																																																								
<b>Two-Dimensional Matrix of Assigned Weights</b>																																																																																																													
<table border="1"> <thead> <tr> <th colspan="6">Model Index</th> <th colspan="6">Sample Index</th> </tr> <tr> <th>0</th><th>1</th><th>2</th><th>3</th><th>4</th><th>5</th> <th>0</th><th>1</th><th>2</th><th>3</th><th>4</th><th>5</th> </tr> </thead> <tbody> <tr> <td>0.0139</td><td>0.0437</td><td>0.0410</td><td>0.0437</td><td>0.0139</td><td>0.0437</td> <td>0.2000</td><td></td><td></td><td></td><td></td><td></td> </tr> <tr> <td>-0.0133</td><td>0.0385</td><td>0.0365</td><td>0.0388</td><td>0.0133</td><td>0.0385</td> <td>0.1788</td><td></td><td></td><td></td><td></td><td></td> </tr> <tr> <td>-0.0182</td><td>0.0590</td><td>0.0555</td><td>0.0594</td><td>0.0182</td><td>0.0590</td> <td>0.2692</td><td></td><td></td><td></td><td></td><td></td> </tr> <tr> <td>-0.0124</td><td>0.0352</td><td>0.0334</td><td>0.0354</td><td>0.0124</td><td>0.0352</td> <td>0.1640</td><td></td><td></td><td></td><td></td><td></td> </tr> <tr> <td>-0.0139</td><td>0.0405</td><td>0.0384</td><td>0.0407</td><td>0.0139</td><td>0.0405</td> <td>0.1880</td><td></td><td></td><td></td><td></td><td></td> </tr> <tr> <td>0.0716</td><td>0.2170</td><td>0.2048</td><td>0.2179</td><td>0.0716</td><td>0.2170</td> <td>Row Sum</td><td></td><td></td><td></td><td></td><td></td> </tr> <tr> <td>0</td><td>1</td><td>2</td><td>3</td><td>4</td><td>5</td> <td></td><td></td><td></td><td></td><td></td><td></td> </tr> </tbody> </table>		Model Index						Sample Index						0	1	2	3	4	5	0	1	2	3	4	5	0.0139	0.0437	0.0410	0.0437	0.0139	0.0437	0.2000						-0.0133	0.0385	0.0365	0.0388	0.0133	0.0385	0.1788						-0.0182	0.0590	0.0555	0.0594	0.0182	0.0590	0.2692						-0.0124	0.0352	0.0334	0.0354	0.0124	0.0352	0.1640						-0.0139	0.0405	0.0384	0.0407	0.0139	0.0405	0.1880						0.0716	0.2170	0.2048	0.2179	0.0716	0.2170	Row Sum						0	1	2	3	4	5						
Model Index						Sample Index																																																																																																							
0	1	2	3	4	5	0	1	2	3	4	5																																																																																																		
0.0139	0.0437	0.0410	0.0437	0.0139	0.0437	0.2000																																																																																																							
-0.0133	0.0385	0.0365	0.0388	0.0133	0.0385	0.1788																																																																																																							
-0.0182	0.0590	0.0555	0.0594	0.0182	0.0590	0.2692																																																																																																							
-0.0124	0.0352	0.0334	0.0354	0.0124	0.0352	0.1640																																																																																																							
-0.0139	0.0405	0.0384	0.0407	0.0139	0.0405	0.1880																																																																																																							
0.0716	0.2170	0.2048	0.2179	0.0716	0.2170	Row Sum																																																																																																							
0	1	2	3	4	5																																																																																																								
Aggregated Prediction: Weighted Probability: 0.8095 Predictive Lable: Hate																																																																																																													
White Supremacist-known attack (generated by TFAdjusted, word-level replacement)																																																																																																													
Clean Sample	may they be put away for good.																																																																																																												
Adversarial Sample	may they <b>worden</b> put away for good.																																																																																																												
Generated Sample	they will be put away once and for all.																																																																																																												
	they have to be placed away for good.																																																																																																												
	should they be put away for good.																																																																																																												
	may they be put away for good forever.																																																																																																												
	may they be put away for good.																																																																																																												
Visualization (Pearson <sup>1</sup> = <b>-0.4956</b> ; Pearson <sup>2</sup> = <b>-0.9562</b> ; Pearson <sup>3</sup> = <b>-0.8219</b> )	<b>Two-Dimensional Matrix of Probabilities</b>																																																																																																												
	<table border="1"> <thead> <tr> <th colspan="6">Model Index</th> <th colspan="6">Sample Index</th> </tr> <tr> <th>0</th><th>1</th><th>2</th><th>3</th><th>4</th><th>5</th> <th>0</th><th>1</th><th>2</th><th>3</th><th>4</th><th>5</th> </tr> </thead> <tbody> <tr> <td>0.03</td><td>0.37</td><td>0.75</td><td>0.55</td><td>0.32</td><td>0.30</td> <td>0.4261</td><td></td><td></td><td></td><td></td><td></td> </tr> <tr> <td>0.04</td><td>0.76</td><td>0.60</td><td>0.74</td><td>0.14</td><td>0.17</td> <td>0.4394</td><td></td><td></td><td></td><td></td><td></td> </tr> <tr> <td>0.83</td><td>0.07</td><td>0.28</td><td>0.80</td><td>0.83</td><td>0.42</td> <td>0.3032</td><td></td><td></td><td></td><td></td><td></td> </tr> <tr> <td>0.04</td><td>0.07</td><td>0.45</td><td>0.91</td><td>0.57</td><td>0.50</td> <td>0.4227</td><td></td><td></td><td></td><td></td><td></td> </tr> <tr> <td>0.73</td><td>0.70</td><td>1.00</td><td>0.94</td><td>0.02</td><td>0.88</td> <td>0.1895</td><td></td><td></td><td></td><td></td><td></td> </tr> <tr> <td>0.5802</td><td>0.4520</td><td>0.2104</td><td>0.0640</td><td>0.4724</td><td>0.3580</td> <td>Avg Brier Score</td><td></td><td></td><td></td><td></td><td></td> </tr> <tr> <td>0</td><td>1</td><td>2</td><td>3</td><td>4</td><td>5</td> <td></td><td></td><td></td><td></td><td></td><td></td> </tr> </tbody> </table>		Model Index						Sample Index						0	1	2	3	4	5	0	1	2	3	4	5	0.03	0.37	0.75	0.55	0.32	0.30	0.4261						0.04	0.76	0.60	0.74	0.14	0.17	0.4394						0.83	0.07	0.28	0.80	0.83	0.42	0.3032						0.04	0.07	0.45	0.91	0.57	0.50	0.4227						0.73	0.70	1.00	0.94	0.02	0.88	0.1895						0.5802	0.4520	0.2104	0.0640	0.4724	0.3580	Avg Brier Score						0	1	2	3	4	5					
Model Index						Sample Index																																																																																																							
0	1	2	3	4	5	0	1	2	3	4	5																																																																																																		
0.03	0.37	0.75	0.55	0.32	0.30	0.4261																																																																																																							
0.04	0.76	0.60	0.74	0.14	0.17	0.4394																																																																																																							
0.83	0.07	0.28	0.80	0.83	0.42	0.3032																																																																																																							
0.04	0.07	0.45	0.91	0.57	0.50	0.4227																																																																																																							
0.73	0.70	1.00	0.94	0.02	0.88	0.1895																																																																																																							
0.5802	0.4520	0.2104	0.0640	0.4724	0.3580	Avg Brier Score																																																																																																							
0	1	2	3	4	5																																																																																																								
<b>Two-Dimensional Matrix of Assigned Weights</b>																																																																																																													
<table border="1"> <thead> <tr> <th colspan="6">Model Index</th> <th colspan="6">Sample Index</th> </tr> <tr> <th>0</th><th>1</th><th>2</th><th>3</th><th>4</th><th>5</th> <th>0</th><th>1</th><th>2</th><th>3</th><th>4</th><th>5</th> </tr> </thead> <tbody> <tr> <td>-0.0227</td><td>0.0357</td><td>0.0341</td><td>0.0360</td><td>0.0167</td><td>0.0276</td> <td>0.1728</td><td></td><td></td><td></td><td></td><td></td> </tr> <tr> <td>-0.0210</td><td>0.0323</td><td>0.0315</td><td>0.0336</td><td>0.0158</td><td>0.0261</td> <td>0.1603</td><td></td><td></td><td></td><td></td><td></td> </tr> <tr> <td>-0.0275</td><td>0.0342</td><td>0.0397</td><td>0.0494</td><td>0.0224</td><td>0.0360</td> <td>0.2093</td><td></td><td></td><td></td><td></td><td></td> </tr> <tr> <td>-0.0253</td><td>0.0379</td><td>0.0390</td><td>0.0423</td><td>0.0188</td><td>0.0314</td> <td>0.1947</td><td></td><td></td><td></td><td></td><td></td> </tr> <tr> <td>-0.0351</td><td>0.0431</td><td>0.0502</td><td>0.0603</td><td>0.0285</td><td>0.0457</td> <td>0.2629</td><td></td><td></td><td></td><td></td><td></td> </tr> <tr> <td>0.1317</td><td>0.1832</td><td>0.1946</td><td>0.2215</td><td>0.1022</td><td>0.1668</td> <td>Row Sum</td><td></td><td></td><td></td><td></td><td></td> </tr> <tr> <td>0</td><td>1</td><td>2</td><td>3</td><td>4</td><td>5</td> <td></td><td></td><td></td><td></td><td></td><td></td> </tr> </tbody> </table>		Model Index						Sample Index						0	1	2	3	4	5	0	1	2	3	4	5	-0.0227	0.0357	0.0341	0.0360	0.0167	0.0276	0.1728						-0.0210	0.0323	0.0315	0.0336	0.0158	0.0261	0.1603						-0.0275	0.0342	0.0397	0.0494	0.0224	0.0360	0.2093						-0.0253	0.0379	0.0390	0.0423	0.0188	0.0314	0.1947						-0.0351	0.0431	0.0502	0.0603	0.0285	0.0457	0.2629						0.1317	0.1832	0.1946	0.2215	0.1022	0.1668	Row Sum						0	1	2	3	4	5						
Model Index						Sample Index																																																																																																							
0	1	2	3	4	5	0	1	2	3	4	5																																																																																																		
-0.0227	0.0357	0.0341	0.0360	0.0167	0.0276	0.1728																																																																																																							
-0.0210	0.0323	0.0315	0.0336	0.0158	0.0261	0.1603																																																																																																							
-0.0275	0.0342	0.0397	0.0494	0.0224	0.0360	0.2093																																																																																																							
-0.0253	0.0379	0.0390	0.0423	0.0188	0.0314	0.1947																																																																																																							
-0.0351	0.0431	0.0502	0.0603	0.0285	0.0457	0.2629																																																																																																							
0.1317	0.1832	0.1946	0.2215	0.1022	0.1668	Row Sum																																																																																																							
0	1	2	3	4	5																																																																																																								
Aggregated Prediction	Weighted Probability: 0.5474 Predictive Lable: Hate																																																																																																												

## Y.2 Examine the Performance of Different Base Detectors on Different Attack Types

Appendix Y.1 demonstrates that different base detectors' predictive probability and assigned weight can vary substantially within one sample. Meanwhile, we also notice that one base detector may perform well on the sample while perform poorly on another. Hence, we next investigate each base detector's overall

performance under different attack types.

Specifically, for each dataset, we evaluated the accuracy of each base detector in our ARHOCD under four types of adversarial attacks: character-level attack (DeepWordBug), word-level attack (TFAdjusted), sentence-level attack (TREPAT), and multi-level attack (ExplainDrive). We also computed the average weight assigned to each base detector by averaging its weights over all samples generated by the same attack type. The accuracies and their corresponding average weights for the five base detectors under each attack are reported in Tables Y4–Y6. For each attack type, the base detector achieving the highest accuracy is highlighted in bold, and the associated average assigned weights are shown in brackets. Two observations are reached.

First, the attacks that each base detector can better defend against vary. For instance, in Table Y4, on the ETHOS Dataset, BERT can better defend against character-level attack (DeepWordBug), achieving an accuracy of 81.43%, while RoBERTa can better defend against word-level attack (TFAdjusted), with an accuracy of 84.29%. However, such pattern is dataset-specific. On the PHEME dataset, ALBERT can better defend against character-level attack (DeepWordBug) (with an accuracy of 93.33%), while the accuracy of BERT under this attack type drops to 86.67%.

Second, though the performance gap of different base detectors is relatively minor and the weight assigned for them are also comparable across samples, more accurate predictions still obtain higher weight. For instance, on the PHEME dataset under the sentence-level attack, ALBERT attains the highest accuracy (85.33%) and correspondingly receives the highest average weight (0.2092). In contrast, the other four models (BERT, DistilBERT, RoBERTa, and XLNet) obtain lower accuracies of 84.67%, 82.67%, 84.00%, and 78.00%, respectively, and are assigned lower average weights of 0.2027, 0.1982, 0.2013, and 0.1894. We also examine the Pearson correlation between accuracy and the assigned weight, and we find the values are consistently positive across different attack types. For instance, on the PHEME dataset, the Pearson correlation coefficients are 0.9688, 0.9609, 0.9551, and 0.8778 under character-level, word-level, sentence-level, and multi-level attacks, respectively. Hence, a base detector with higher accuracy tends to be assigned higher weight and vice versa. These results demonstrate the effectiveness of our Bayesian weight

assignment method.

**Table Y4. Accuracy (%) of Base Detectors Across Different Attack Types on the ETHOS Dataset**

Index	Attack types	BERT	DistilBERT	RoBERTa	XLNet	ALBERT	Pearson correlation
1	Character-level attack (DeepWordBug)	<b>81.43</b> ( <b>0.2039</b> )	75.71 (0.2012)	74.29 (0.1983)	77.14 (0.2006)	77.14 (0.1969)	0.6858
2	Word-level attack (TFAdjusted)	74.29 (0.1984)	78.57 (0.2019)	<b>84.29</b> ( <b>0.2041</b> )	80.00 (0.2036)	72.86 (0.1923)	0.8895
3	Sentence-level attack (TREPAT)	75.71 (0.1985)	74.29 (0.1991)	72.86 (0.1987)	75.71 (0.1992)	<b>80.00</b> ( <b>0.2047</b> )	0.8980
4	Multi-level attack (ExplainDrive)	70.00 (0.1971)	70.00 (0.1993)	74.29 (0.2006)	71.43 (0.1986)	<b>75.71</b> ( <b>0.2052</b> )	0.8874

Note: Values in brackets show the average weight assigned to each base detector. Same below.

**Table Y5. Accuracy (%) of Base Detectors Across Different Attack Types on the PHEME Dataset**

Index	Attack types	BERT	DistilBERT	RoBERTa	XLNet	ALBERT	Pearson correlation
1	Character-level attack (DeepWordBug)	86.67 (0.1993)	89.33 (0.2001)	90.67 (0.2042)	83.33 (0.1881)	<b>93.33</b> ( <b>0.2085</b> )	0.9688
2	Word-level attack (TFAdjusted)	87.33 (0.2036)	86.67 (0.1978)	<b>90.67</b> ( <b>0.2090</b> )	82.67 (0.1900)	88.00 (0.2001)	0.9609
3	Sentence-level attack (TREPAT)	84.67 (0.2027)	82.67 (0.1982)	84.00 (0.2013)	78.00 (0.1894)	<b>85.33</b> ( <b>0.2092</b> )	0.9551
4	Multi-level attack (ExplainDrive)	78.67 (0.1958)	81.33 (0.1919)	<b>85.00</b> ( <b>0.2107</b> )	79.33 (0.1916)	84.00 (0.2099)	0.8778

**Table Y6. Accuracy (%) of Base Detectors Across Different Attack Types on the White Supremacist Dataset**

Index	Attack types	BERT	DistilBERT	RoBERTa	XLNet	ALBERT	Pearson correlation
1	Character-level attack (DeepWordBug)	82.67 (0.2050)	82.00 (0.1946)	80.67 (0.1960)	81.20 (0.1959)	<b>86.00</b> ( <b>0.2089</b> )	0.8764
2	Word-level attack (TFAdjusted)	84.40 (0.2055)	80.40 (0.1985)	80.40 (0.1957)	81.60 (0.1931)	<b>88.67</b> ( <b>0.2072</b> )	0.8486
3	Sentence-level attack (TREPAT)	<b>74.00</b> ( <b>0.2110</b> )	64.67 (0.1904)	70.00 (0.2003)	68.00 (0.1950)	72.00 (0.2041)	0.9860
4	Multi-level attack (ExplainDrive)	<b>83.33</b> ( <b>0.2051</b> )	74.40 (0.1966)	74.67 (0.1982)	75.60 (0.1966)	81.33 (0.2042)	0.9726

### Y.3 Examine the Performance of Different Base Detectors on Different Topics

To further examine different base detectors' advantages in different cases, we examined them on different topics. Specifically, we extract topics from the ETHOS and White Supremacist datasets using Latent Dirichlet Allocation (LDA, (Blei et al. 2003)). LDA is a generative topic model that infers latent thematic structures by assuming that each text is generated from a mixture of topics, and each topic is represented as a probability distribution over words. By modeling the word co-occurrence patterns, LDA

produces a probabilistic topic distribution for each text. We use the Gensim (a python package) implementation of LDA to extract topic, assigning each test sample to the topic with the highest probability. Each topic is represented by its top eight words, and its semantic interpretation is derived from these representative words. For the PHEME dataset, since the data are already categorized into rumors and non-rumors corresponding to nine events (as described in Appendix O), we use its original event division as topic. Events with fewer than 30 test samples (Ebola-Essien, Gurlitt, and Putinmissing) are excluded from our analysis, as small sample sizes may fail to yield statistically reliable conclusions.

After obtaining the topic for each test sample, we evaluated the accuracy of each base detector in our ARHOCD using adversarial samples grouped by the selected topics. We also computed the average weight assigned to each detector by averaging its weights over all samples belonging to the same topic. The accuracies and their corresponding average weights for the five base detectors on each topic are presented in Tables Y7–Y9. For each topic, the detector achieving the highest accuracy is highlighted in bold, and the associated average weights are shown in brackets. Two conclusions can be drawn.

First, the base detectors exhibit strengths on different topics. For instance, in Table Y8 on the PHEME dataset, BERT is more effective at defending against adversarial samples related to the Germanwings Crash topic, achieving an accuracy of 95.35%, whereas XLNet performs better on adversarial samples associated with the Prince–Toronto topic, with an accuracy of 90.00%.

Second, across different topics, we can also observe that base detectors with higher accuracy tend to receive higher average weights. For example, on the ETHOS dataset, for the Gender and Sexism topic, RoBERTa attains the highest accuracy (81.36%) and correspondingly receives the highest average weight (0.2174). In contrast, the other four models (BERT, DistilBERT, XLNet, and ALBERT) obtain lower accuracies of 64.41%, 74.58%, 71.19%, and 69.49%, respectively, and are assigned lower average weights of 0.1935, 0.2013, 0.2040, and 0.1838. We also examine the Pearson correlation between accuracy and the assigned weight, and we find the values are consistently positive across all topics. For instance, on the ETHOS dataset, the Pearson correlation coefficients are 0.8434, 0.8061, 0.8413, and 0.8034 under the four topics. These results demonstrate the effectiveness of our Bayesian weight assignment method.

**Table Y7. Accuracy (%) of Base Detectors Across Different Topics on the ETHOS Dataset**

Index	Top words	Interpretation	BERT	DistilBERT	RoBERTa	XLNet	ALBERT	Pearson correlation
1	white, black, people, hate, fuck, back, shit, ass	Race-related Hate	<b>79.44</b> (0.2118)	71.75 (0.1941)	75.00 (0.2044)	76.67 (0.1966)	71.35 (0.1930)	0.8434
2	muslims, islam, god, religion, countries, kill, love, hate	Religion-related Hate	86.49 (0.1954)	<b>90.93</b> (0.2037)	90.80 (0.2036)	87.11 (0.1998)	82.47 (0.1976)	0.8061
3	women, men, girls, feminist, female, gender, bitch, kids	Gender and Sexism	70.15 (0.1893)	74.13 (0.2029)	<b>81.09</b> (0.2134)	79.10 (0.2055)	74.87 (0.1889)	0.8413
4	kill, shot, gun, war, drugs, death, proud, terrorist	Violence and Threats	64.41 (0.1935)	74.58 (0.2013)	<b>81.36</b> (0.2174)	71.19 (0.2040)	69.49 (0.1838)	0.8034

**Table Y8. Accuracy (%) of Base Detectors Across Different Topics on the PHEME Dataset**

Index	Event	BERT	DistilBERT	RoBERTa	XLNet	ALBERT	Pearson correlation
1	Sydney Siege	82.61 (0.2016)	83.70 (0.1989)	<b>88.57</b> (0.2071)	81.52 (0.1996)	75.00 (0.1927)	0.9587
2	Germanwings Crash	95.35 (0.2023)	91.70 (0.1936)	<b>95.85</b> (0.2066)	83.40 (0.1874)	97.67 (0.2101)	0.9479
3	Prince-Toronto	92.22 (0.2056)	87.78 (0.1750)	94.44 (0.2141)	90.00 (0.1803)	<b>97.78</b> (0.2250)	0.9689
4	Ferguson	<b>90.91</b> (0.2101)	87.80 (0.1961)	89.39 (0.2022)	83.09 (0.1902)	87.88 (0.2014)	0.9332
5	Charlie Hebdo	91.27 (0.1987)	91.57 (0.1996)	92.47 (0.2046)	83.73 (0.1961)	<b>92.91</b> (0.2010)	0.7695
6	Ottawa Shooting	81.09 (0.1984)	80.43 (0.1965)	<b>86.52</b> (0.2086)	80.87 (0.1884)	85.45 (0.2081)	0.8883

**Table Y9. Accuracy (%) of Base Detectors Across Different Topics on the White Supremacist Dataset**

Index	Top words	Interpretation	BERT	DistilBERT	RoBERTa	XLNet	ALBERT	Pearson correlation
1	europe, youth, soldiers, white, people, jews, race, european	European and White Identity	82.61 (0.2016)	83.70 (0.1989)	<b>88.57</b> (0.2071)	81.52 (0.1996)	75.00 (0.1927)	0.9587
2	hate, black, negro, jew, non-whites, japanese, asians, scum	Racial and Ethnic Hostility	95.35 (0.2023)	91.70 (0.1936)	95.85 (0.2066)	83.40 (0.1874)	<b>97.67</b> (0.2101)	0.9432
3	thread, group, link, message, news, site, read, welcome	Community and Forum Interaction	92.22 (0.2056)	87.78 (0.1750)	94.44 (0.2141)	90.00 (0.1803)	<b>97.78</b> (0.2250)	0.9689
4	town, school, home, kids, city, day, country, problem	Daily Life and Local Issues	<b>90.91</b> (0.2101)	87.80 (0.1961)	89.39 (0.2022)	83.09 (0.1902)	87.88 (0.2014)	0.9332
5	things, want, way, get, know, like, people, anyone	Personal Opinions and Advice	91.27 (0.1987)	91.57 (0.1996)	92.47 (0.2046)	83.73 (0.1961)	<b>92.91</b> (0.2010)	0.7695

6	video, youtube, music, band, watch, shows, teacher, student	Media and Entertainment	81.09 (0.1984)	80.43 (0.1965)	<b>86.52</b> <b>(0.2086)</b>	80.87 (0.1884)	85.45 (0.2081)	0.8883
---	---	-------------------------	-------------------	-------------------	---------------------------------	-------------------	-------------------	--------

#### Y.4 Analysis of Correctly and Incorrectly Predicted Samples on Different Attack Types

We further randomly selected 100 correctly predicted samples and 100 incorrectly predicted adversarial samples from our ARHOCD and examine their distribution across different attack types. The results are shown in Figure Y1.

The results show that, across different attack types, ARHOCD performs better under character-level attacks but shows relatively lower performance under sentence-level and multi-level attacks, a trend that is also reflected in Tables Y4–Y6. This pattern can be explained by the fact that character-level attacks are relatively easier to defend against, a finding that is also corroborated in Appendix W. In contrast, sentence-level and multi-level attacks produce more advanced and complex adversarial samples and make them more challenging to defend against. Importantly, despite such variability, our generalizability experiments show that the worst-case performance of our detector outperforms all baselines, confirming that the proposed framework provides stronger robustness.

In summary, while our ARHOCD achieves relatively higher performance across different types of attacks, the robustness against different attack types still differs. That is reasonable because some attacks such as character-level attacks are essentially easier to defend compared with others. Given the relatively more challenging task of defending against sentence-level and multi-level attacks, the future work can invest more efforts on those types of attacks.

**(a-1) ETHOS Dataset**

**(a-2) PHEME Dataset**

**(a-3) WHITE Supremacist Dataset**

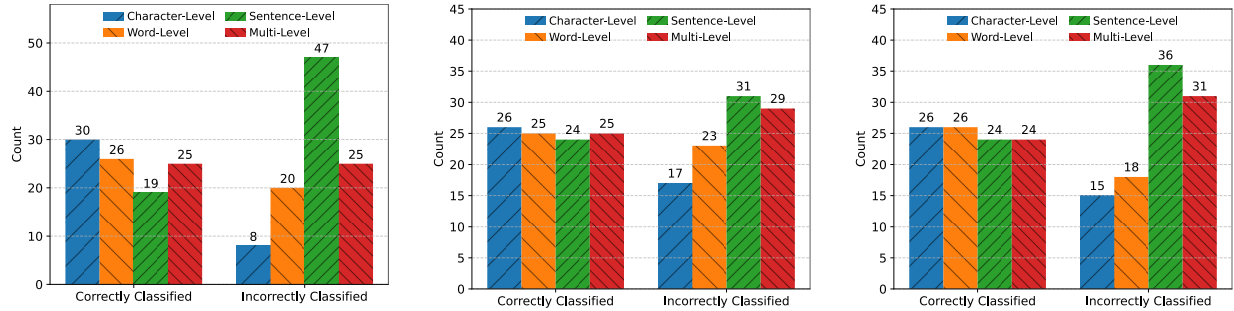


**Figure Y1. Distributions of Correctly and Incorrectly Predicted Samples across Different Attack Types**

### Y.5 Analysis of Correctly and Incorrectly Predicted Samples on Different Topics

We also examined the 200 samples previously randomly selected from our ARHOCD—100 correctly predicted and 100 incorrectly predicted adversarial samples—across different topics. The results are shown in Figure Y2.

The results show that, across different topics, ARHOCD shows substantial variation in the number of correctly and incorrectly predicted samples. For instance, on the ETHOS dataset, Topic 2 (Religion-related Hate; the mapping between indices and topics is provided in Tables Y7–Y9) is easier to defend than Topic 1 (Race-related Hate). This may be because some topics may exhibit specific linguistic characteristics that make them easier to defend compared with others. These observations highlight potential directions for future work, such as developing topic-aware defenses.

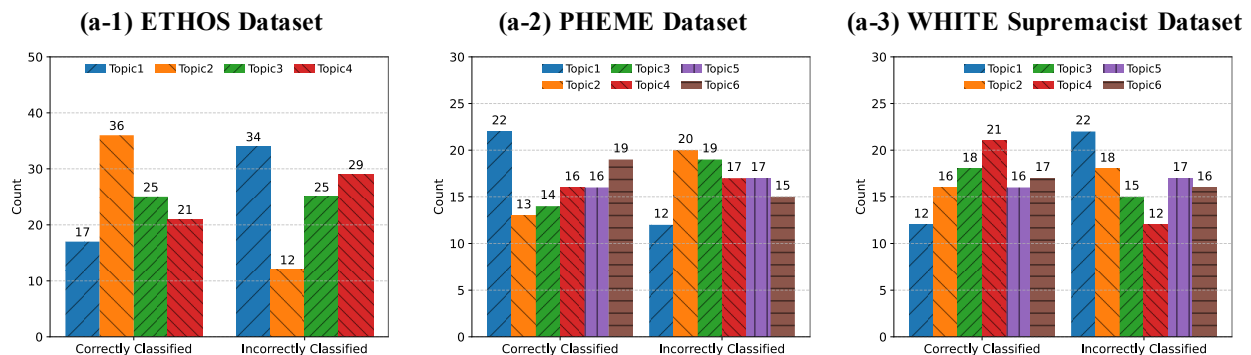


**Figure Y2. Distributions of Correctly and Incorrectly Predicted Samples across Different Topics**

## APPENDIX REFERENCE

Abbasi A, Parsons J, Pant G, Sheng ORL, Sarker S (2024) Pathways for design research on artificial intelligence. *Inf. Syst. Res.* 35(2):441–459.

Aggarwal S, Vishwakarma DK (2024) Exposing the Achilles' heel of textual hate speech classifiers using indistinguishable adversarial examples. *Expert Syst. Appl.* 254:124278.

Anguita D, Ghio A, Oneto L, Member S, Ridella S (2011) Selecting the Hypothesis Space for Improving the Generalization Ability of Support Vector Machines. *2011 Int. Jt. Conf. Neural Networks.* (IEEE), 1169–1176.

Arjovsky M, Gulrajani I, Lopez-paz D (2019) Invariant risk minimization. *arXiv Prepr. arXiv1907.02893*.

Ayetiran EF, Özgöbek Ö (2024) An inter-modal attention-based deep learning framework using unified modality for multimodal fake news, hate speech and offensive language detection. *Inf. Syst.* 123:102378.

Azumah SW, Elsayed N, Elsayed Z, Ozer M, Guardia A La (2024) Deep learning approaches for detecting adversarial cyberbullying and hate speech in social networks. *AIBThings 2024.* 1–10.

Bishop C, Lawrence N, Jaakkola T, Jordan M (1997) Approximating posterior distributions in belief networks using mixtures. *NeurIPS 1997*.

Bishop CM, Nasrabadi NM (2006) *Pattern recognition and machine learning* (Springer).

Blei DM, Kucukelbir A, McAuliffe JD (2017) Variational inference: A review for statisticians. *J. Am. Stat. Assoc.* 112(518):859–877.

Blei DM, Ng AY, Jordan MI (2003) Latent Dirichlet Allocation. *J. Mach. Learn. Res.* 3:993–1022.

Bozkir AS, Cankaya AO, Aydos M (2019) Utilization and comparision of convolutional neural networks in malware recognition. *Signal Process. Commun. Appl. Conf.* 1–4.

Carlini N, Wagner D (2017) Adversarial Examples Are Not Easily Detected : Bypassing Ten Detection Methods. *AISeC 2017.* 3–14.

Chai Y, Liang R, Samtani S, Zhu H, Wang M, Liu Y, Jiang Y (2023) Additive feature attribution explainable methods to craft adversarial attacks for text classification and text regression. *IEEE Trans. Knowl. Data Eng.* 35(12):12400–12414.

Chang G, Gao H, Yao Z, Xiong H (2023) TextGuise: Adaptive adversarial example attacks on text classification model. *Neurocomputing* 529:190–203.

Chen H, Ji Y (2022) Adversarial training for improving model robustness? Look at both prediction and interpretation. *AAAI 2022.* 10463–10472.

Chen KC, Chen CY, Li C Te (2023) Anti-disinformation: an adversarial attack and defense network towards improved robustness for disinformation detection on social media. *BigData 2023.* 5476–5484.

Cohn I, El-Hay T, Friedman N, Kupferman R (2010) Mean field variational approximation for continuous-time Bayesian networks. *J. Mach. Learn. Res.* 11:2745–2783.

Daunizeau J (2017) Semi-analytical approximations to statistical moments of sigmoid and softmax mappings of normal variables. *arXiv Prepr. arXiv1703.00091*.

Dong X, Luu AT, Ji R, Liu H (2021) Towards robustness against natural language word substitutions. *ICLR 2021*.

Dubey A, Maaten L Van Der, Yalniz Z, Li Y, Mahajan D (2019) Defense against adversarial images using web-scale nearest-neighbor search. *Proc. IEEE Comput. Soc. Conf. Comput. Vis. Pattern Recognit.* 8767–8776.

Etudo U, Yoon VY (2024) Ontology-based information extraction for labeling radical online content using distant supervision. *Inf. Syst. Res.* 35(1):203–225.

Fazlyab M, Entesari T, Roy A, Chellappa R (2023) Certified robustness via dynamic margin maximization and improved lipschitz regularization. *NeurIPS 2023.* 34451–34464.

Gao J, Lanchantin J, Soffa M Lou, Qi Y (2018) Black-box generation of adversarial text sequences to evade deep learning classifiers. *IEEE Secur. Priv. Work.* 50–56.

De Gibert O, Perez N, García-Pablos A, Cuadros M (2018) Hate speech dataset from a white supremacy forum. *Proc. 2nd Work. Abus. Lang. Online.* 11–20.

Glenn WB (1950) Verification of forecasts expressed in terms of probability. *Mon. Weather Rev.* 78(1):1–3.

Gloewkler M, Deistler M, Macke JH (2023) Adversarial robustness of amortized Bayesian inference. *ICML 2023*.

Godinić D, Obrenovic B (2020) Effects of economic uncertainty on mental health in the COVID-19 pandemic context: social identity disturbance, job uncertainty and psychological well-being model. *Int. J. Innov. Econ. Dev.* 6(1):61–74.

Goodfellow IJ, Shlens J, Szegedy C (2015) Explaining and harnessing adversarial examples. *ICLR 2015.* 1–11.

Hashmi E, Yayilgan SY, Yamin MM, Abomhara M, Ullah M (2025) Self-supervised hate speech detection in Norwegian texts with lexical and semantic augmentations. *Expert Syst. Appl.* 264:125843.

Herel D, Cisneros H, Mikolov T (2023) Preserving semantics in textual adversarial attacks. *ECAI 2023.* 1036–1043.

Hu Z, Yin JL, Chen B, Lin L, Chen BH, Liu X (2024) Meat: median-ensemble adversarial training for improving robustness and generalization. *ICASSP 2024.* 5600–5604.

Huang P, Yang Y, Jia F, Liu M, Ma F, Zhang J (2022) Word level robustness enhancement: Fight perturbation with perturbation. *AAAI 2022.* 10785–10793.

Huang T, Xu Z, Yu P, Yi J, Xu X (2025) A hybrid transformer model for fake news detection: Leveraging Bayesian optimization and bidirectional recurrent unit. *arXiv Prepr. arXiv2502.09097*.

Jensen JLWV (1906) Sur les fonctions convexes et les inégalités entre les valeurs moyennes. *Acta Math.* 30(1):175–193.

Jin D, Jin Z, Zhou JT, Szolovits P (2020) Is BERT really robust? A strong baseline for natural language attack on text classification and entailment. *AAAI 2020.* 8018–8025.

Kim Y, Park S, Namgoong Y, Han YS (2023) ConPrompt: Pre-training a language model with machine-generated data for implicit hate speech detection. *EMNLP 2023*. 10964–10980.

Kingma DP, Welling M (2014) Auto-encoding variational bayes. *ICLR 2014*. 1–14.

Kumbam PR, Syed SU, Thamminedi P, Harish S, Perera I, Dorr BJ (2025) Exploiting explainability to design adversarial attacks and evaluate attack resilience in hate-Speech detection models. *ICWSM 2025*. 1038–1050.

Kurakin A, Goodfellow I, Bengio S (2017) Adversarial machine learning at scale. *ICLR 2017*.

Lecuyer M, Atlidakis V, Geambasu R, Hsu D, Jana S (2019) Certified robustness to adversarial examples with differential privacy. *IEEE Symp. Secur. Priv.* 656–672.

Lee K, Ram S (2024) Explainable deep learning for false information identification: An argumentation theory approach. *Inf. Syst. Res.* 35(2):890–907.

Leshno M, Lin VY, Pinkus A, Schocken S (1993) Multilayer feedforward networks with a nonpolynomial activation function can approximate any function. *Neural networks* 6(6):861–867.

Li L, Song D, Qiu X (2023) Text adversarial purification as defense against adversarial attacks. *ACL 2023*. 338–350.

Li W, Chai Y (2022) Assessing and enhancing adversarial robustness of predictive analytics: An empirically tested design framework. *J. Manag. Inf. Syst.* 39(2):542–572.

Liu Y, Yang C, Li D, Ding J, Jiang T (2024) Defense against adversarial attacks on no-reference image quality models with gradient norm regularization. *CVPR 2024*. 25554–25563.

Madry A, Makelov A, Schmidt L, Tsipras D, Vladu A (2018) Towards deep learning models resistant to adversarial attacks. *ICLR 2018*.

Miller GA (1995) WordNet: A lexical database for English. *Commun. ACM* 38(11):39–41.

Mollas I, Chrysopoulou Z, Karlos S, Tsoumacas G (2022) ETHOS: a multi-label hate speech detection dataset. *Complex Intell. Syst.* 8(6):4663–4678.

Moraffah R, Khandelwal S, Bhattacharjee A, Liu H (2024) Adversarial text purification: A large language model approach for defense. *PAKDD 2024*. 65–77.

Morris John X., Lifland E, Lanchantin J, Ji Y, Qi Y (2020) Reevaluating adversarial examples in natural language. *EMNLP 2020*. 3829–3839.

Morris John X, Lifland E, Yoo JY, Grigsby J, Jin D, Qi Y (2020) Textattack: A framework for adversarial attacks, data augmentation, and adversarial training in nlp. *EMNLP 2020*. 119–126.

Mozes M, Stenetorp P, Kleinberg B, Griffin LD (2021) Frequency-guided word substitutions for detecting textual adversarial examples. *Proc. 16th Conf. Eur. chapter Assoc. Comput. Linguist.* 171–186.

Nguyen DM, Tuan LA (2022) Textual manifold-based defense against natural language adversarial examples. *EMNLP 2022*:6612–6625.

Oak R (2019) Poster: Adversarial examples for hate speech classifiers. *Proc. 2019 ACM SIGSAC Conf. Comput. Commun. Secur.* 2621–2623.

Ocampo NB, Cabrio E, Villata S (2023) Playing the part of the sharp bully: Generating adversarial examples for implicit hate speech detection. *ACL 2023*. 2758–2772.

Oswald C, Simon SE, Bhattacharya A (2022) SpotSpam: Intention analysis-driven sms spam detection using bert embeddings. *ACM Trans. Web* 16(3):1–27.

Padmanabhan B, Fang X, Sahoo N, Burton-jones A (2022) Editor’s comments: Machine learning in information systems research. *MIS Q.* 46(1):iii–xix.

Papernot N, McDaniel P, Swami A, Harang R (2016) Crafting adversarial input sequences for recurrent neural networks. *MILCOM 2016*. (IEEE), 49–54.

Pennycook G, Bear A, Collins ET, Rand DG (2020) The implied truth effect: Attaching warnings to a subset of fake news headlines increases perceived accuracy of headlines without warnings. *Manage. Sci.* 66(11):4944–4957.

Pereira M, Dodhia R, Anderson H, Brown R (2024) Metadata-based detection of child sexual abuse material. *IEEE Trans. Dependable Secur. Comput.* 21(4):3153–3164.

Pruthi D, Dhingra B, Lipton ZC (2019) Combating adversarial misspellings with robust word recognition. *ACL 2019*. 5582–5591.

Przybyła P, McGill E, Saggion H (2025) Attacking misinformation detection using adversarial examples generated by language models. *EMNLP 2025*. 27614–27630.

Qin R, Wang L, Du X, Chen X, Yan B (2023) Dynamic ensemble selection based on deep neural network uncertainty estimation for adversarial robustness. *arXiv Prepr. arXiv2308.00346*.

Qiu S, Liu Q, Zhou S, Huang W (2022) Adversarial attack and defense technologies in natural language processing: A survey. *Neurocomputing* 492:278–307.

Rath A, Mishra D, Panda G, Satapathy SC, Xia K (2022) Improved heart disease detection from ECG signal using deep learning based ensemble model. *Sustain. Comput. Informatics Syst.* 35:100732.

Ribeiro MT, Singh S, Guestrin C (2016) “Why should i trust you?” Explaining the predictions of any classifier. *SIGKDD 2016*. 1135–1144.

Sen S, Ravindran B, Raghunathan A (2020) EMPIR: Ensembles of mixed precision deep networks for increased robustness against adversarial attacks. *ICLR 2020*.

Shokri R, Stronati M, Song C, Shmatikov V (2017) Membership inference attacks against machine learning models. *IEEE Symp. Secur. Priv.* 3–18.

Ting KM (2002) An instance-weighting method to induce cost-sensitive trees. *IEEE Trans. Knowl. Data Eng.* 14(3):659–665.

Vishwamitra N, Guo K, Romit FT, Ondracek I, Cheng L, Zhao Z, Hu H (2024) Moderating new waves of online hate with chain-of-thought reasoning in large language models. *IEEE Symp. Secur. Priv.* (IEEE), 788–806.

Waghela H, Sen J, Rakshit S, Dasgupta S (2024) Adversarial robustness through dynamic ensemble learning. *SILCON 2024*. 1–6.

Wang J, Bao R, Zhang Z, Zhao H (2022) Rethinking textual adversarial defense for pre-trained language models. *IEEE/ACM Trans. Audio Speech Lang. Process.* 30:2526–2540.

Wang Z, Liu Z, Zheng X, Su Q, Wang J (2023) RMLM: A Flexible Defense Framework for Proactively Mitigating Word-level Adversarial Attacks. *Proc. Annu. Meet. Assoc. Comput. Linguist.* 1(1):2757–2774.

Waseda F, Chang C chun, Echizen I (2025) Rethinking invariance regularization in adversarial training to improve robustness-accuracy trade-off. *ICLR 2025*.

Wei X, Zhang Z, Zhang M, Chen W, Zeng DD (2022) Combining crowd and machine intelligence to detect false news on social media. *MIS Q.* 46(2):977–1008.

Wu J, Zheng Z, Zhao JL (2021) FairPlay: Detecting and deterring online customer misbehavior. *Inf. Syst. Res.* 32(4):1323–1346.

Yan S, Ren J, Wang W, Sun L, Zhang W, Yu Q (2023) A Survey of Adversarial Attack and Defense Methods for Malware Classification in Cyber Security. *IEEE Commun. Surv. Tutorials* 25(1):467–496.

Yang Y, Liu X, He K (2025) Synonym-unaware fast adversarial training against textual adversarial attacks. *NAACL 2025*. 727–739.

Yang Y, Wang X, He K (2022) Robust textual embedding against word-level adversarial attacks. *UAI 2022*. 2214–2224.

Ye M, Gong C, Liu Q (2020) SAFER: A structure-free approach for certified robustness to adversarial word substitutions. *ACL 2020*. 3465–3475.

Yin W, Agarwal V, Jiang A, Zubiaga A, Sastry N (2023) Annobert: Effectively representing multiple annotators' label choices to improve hate speech detection. *ICWSM 2023*. 902–913.

Yoo JY, Qi Y (2021) Towards improving adversarial training of NLP models. *EMNLP 2021*. 945–956.

Zeng J, Xu J, Zheng X, Huang X (2023) Certified robustness to text adversarial attacks by randomized [MASK]. *Comput. Linguist.* 49(2):395–427.

Zhang C, Zhou X, Wan Y, Zheng X, Chang KW, Hsieh CJ (2022) Improving the adversarial robustness of NLP models by information bottleneck. *ACL 2022*. 3588–3598.

Zhang J, Li C (2020) Adversarial examples: opportunities and challenges. *IEEE Trans. Neural Networks Learn. Syst.* 31(7):2578–2593.

Zhang S, Gao H, Rao Q (2021) Defense against adversarial attacks by reconstructing images. *IEEE Trans. Image Process.* 30:6117–6129.

Zhang X, Hong H, Hong Y, Huang P, Wang B, Ba Z, Ren K (2024) Text-crs: A generalized certified robustness framework against textual adversarial attacks. *Proc. - Secur. Priv.* 2920–2938.

Zhang Y, Yang Q (2018) An overview of multi-task learning. *Natl. Sci. Rev.* 5(1):30–43.

Zhao J, Wei P, Mao W (2021) Robust neural text classification and entailment via mixup regularized adversarial training. *SIGIR 2021*. 1778–1782.

Zhou Y, He B, Sun L (2024) Humanizing machine-generated content: evading AI-text detection through adversarial attack. *Lr. 2024*. 8427–8437.

Zhou Y, Zheng X, Hsieh CJ, Chang KW, Huang X (2021) Defense against synonym substitution-based adversarial attacks via dirichlet neighborhood ensemble. *ACL-IJCNLP 2021*. 5482–5492.